Galaxy Clustering:
Observables & Theoretical Modelling
Part 2

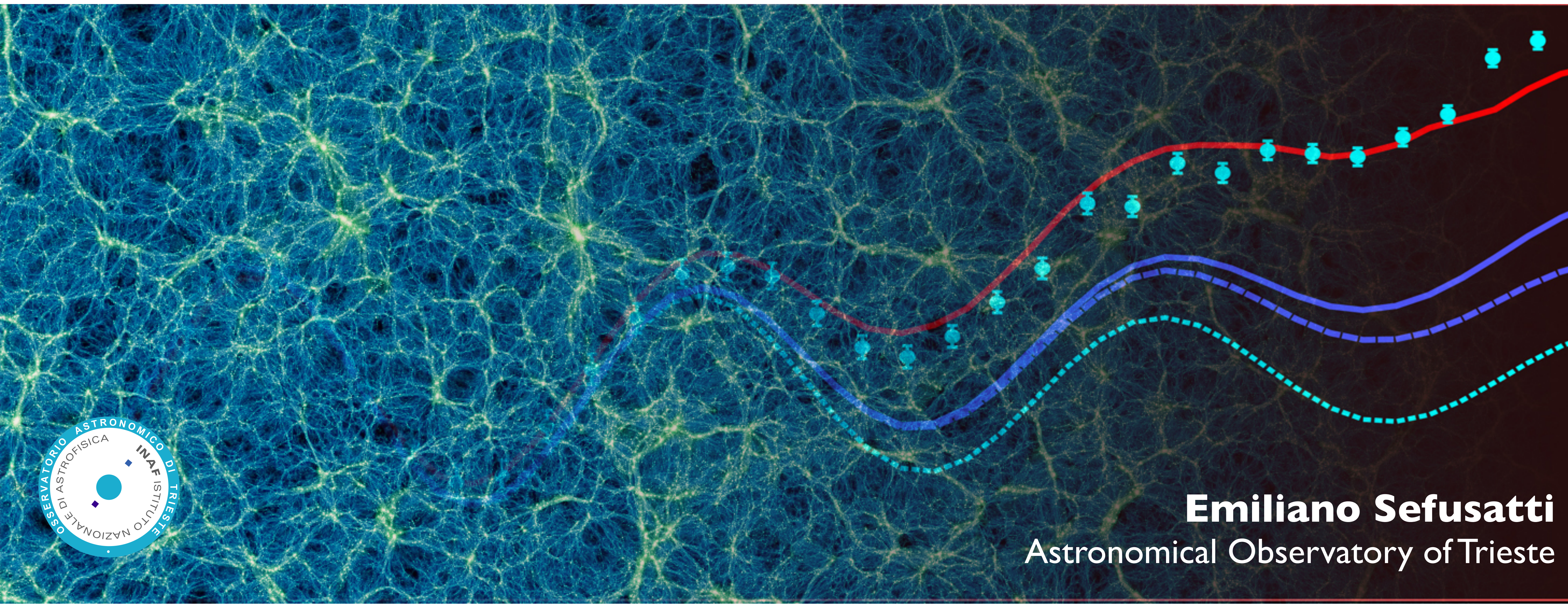

Emiliano Sefusatti
Astronomical Observatory of Trieste

Future Cosmology
Ecole thématique du CNRS
April 23-29, 2023 - Institute d'Études Scientifiques de Cargèse

Lecture 2

- Galaxy bias
- Baryonic Acoustic Oscillations & Infrared Resummation
- Redshift-Space Distortions
- Stochastic contributions
- Recent analyses of the BOSS survey
- *Neutrinos*
- *Non-Gaussianity & Higher-Order Statistics*
- *Primordial non-Gaussianity*

Galaxy Bias

Galaxies

Galaxy bias review: Desjacques, Jeong & Schmidt (2018)

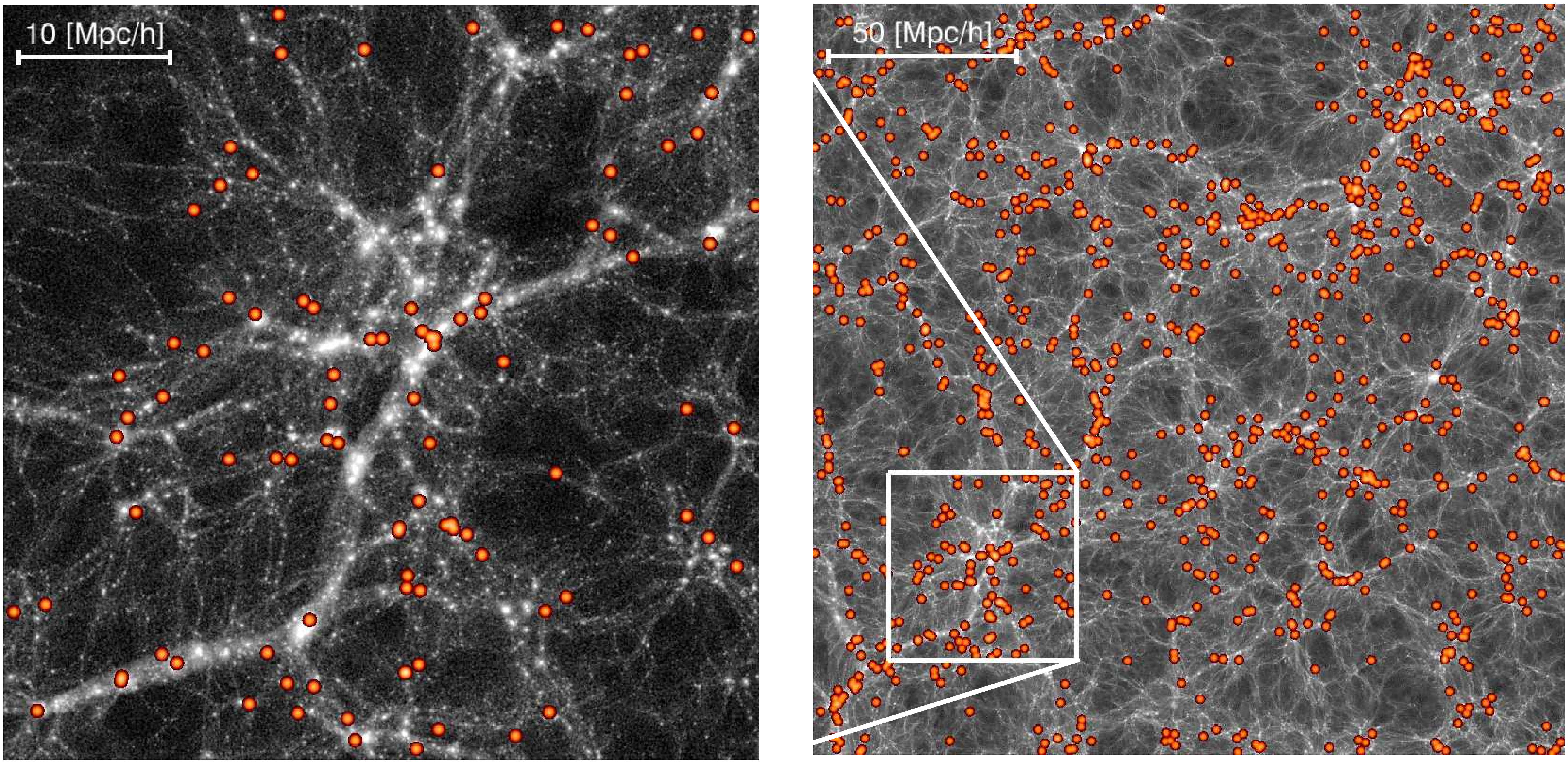

from Orsi *et al.* (2009)

Local galaxy bias

A very simple assumption …

local galaxy bias

$$\delta_g(x) \equiv \frac{n_g(x) - \bar{n}_g}{\bar{n}_g} = f\left[\delta(x)\right]$$

If galaxies form in regions of large dark matter density, we can expect a direct dependence of the **galaxy overdensity** on the **matter overdensity**

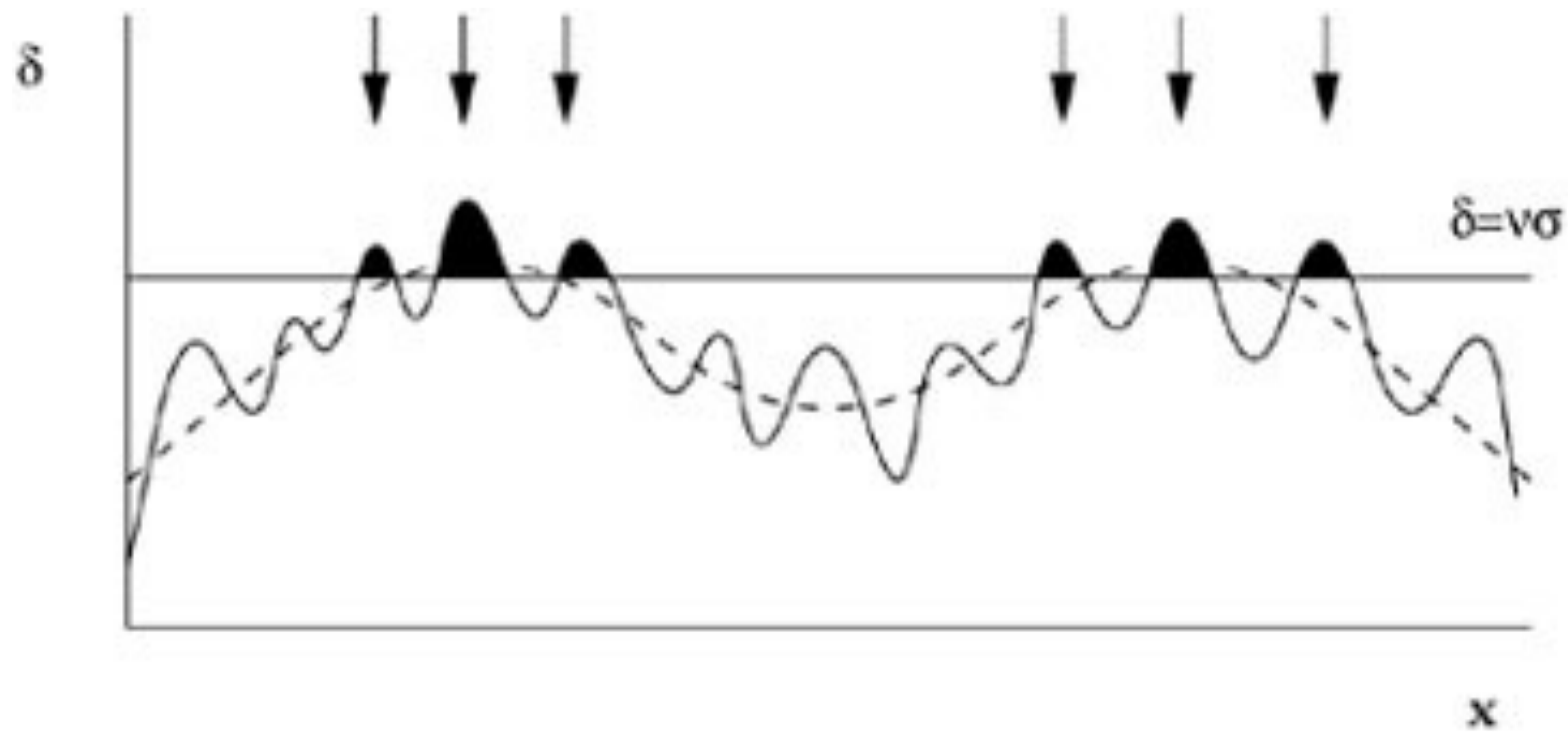

Local galaxy bias

A very simple assumption …

local galaxy bias
$$\delta_g(x) \equiv \frac{n_g(x) - \bar{n}_g}{\bar{n}_g} = f\,[\delta(x)]$$

we can expand it in a Taylor series
$$\delta_g(x) = b\,\delta(x) + \frac{1}{2}\,b_2\,\delta^2(x) + \ldots$$

linear bias   nonlinear bias corrections

At *large* scales, we expect a very **simple, linear relation between galaxy and matter correlation functions**

$$\langle \delta_g \delta_g \rangle = b^2\,\langle \delta\delta \rangle \rightarrow$$

$$\xi_g(x) \simeq b^2 \xi(x)$$

$$P_g(k) \simeq b^2 P(k)$$

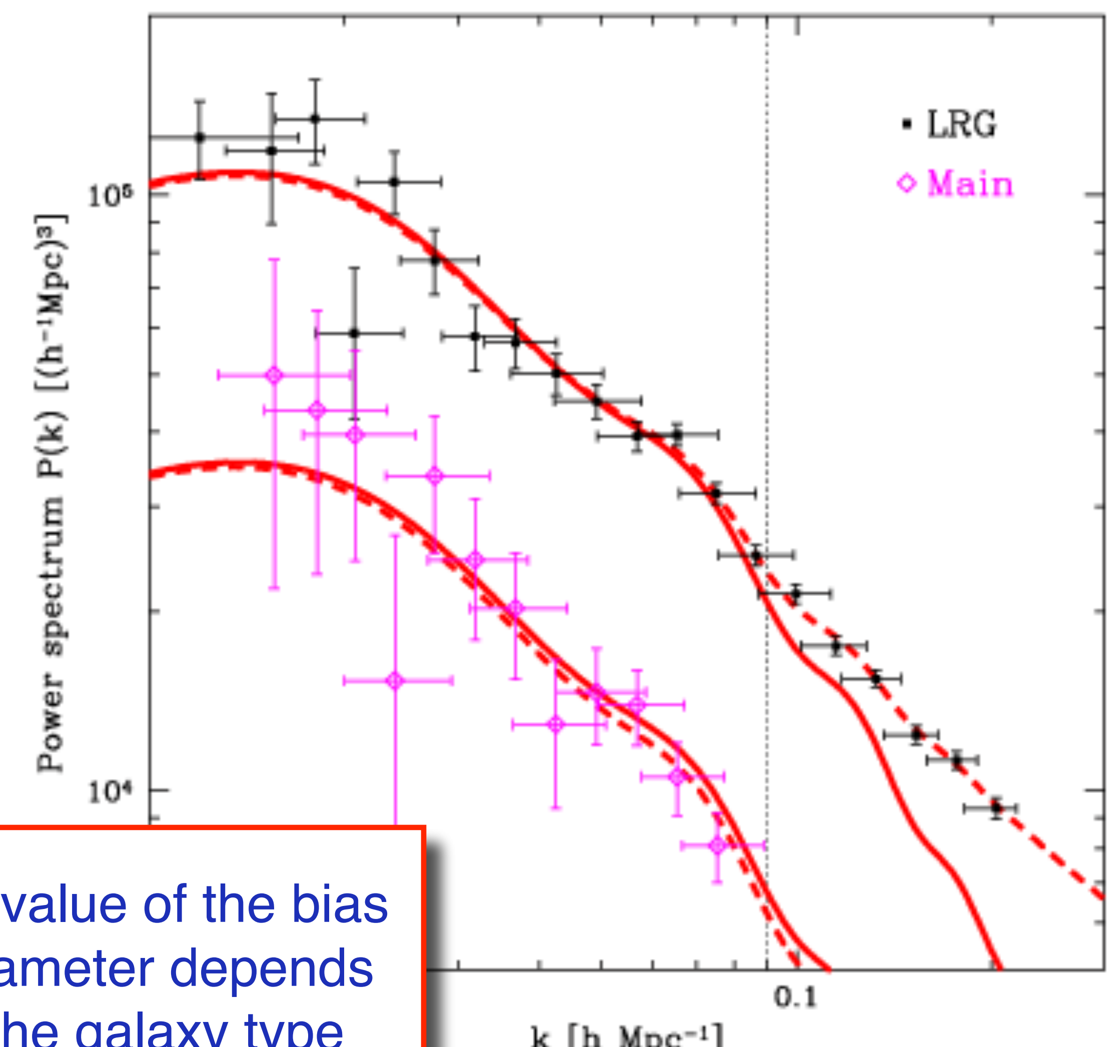

the value of the bias parameter depends on the galaxy type

The galaxy bispectrum

Nonlinear bias is also a source of non-Gaussianity

$$\langle \delta_g \delta_g \delta_g \rangle = b_1^3 \langle \delta\delta\delta \rangle + b_1^2\, b_2 \langle \delta\delta\delta^2 \rangle + \ldots$$

$$B_g(k_1,k_2,k_3) = b_1^3\, B(k_1,k_2,k_3) + b_1^2\, b_2\, P(k_1)\, P(k_2) + 2 \text{ perm.} + \ldots$$

matter contribution nonlinear bias corrections

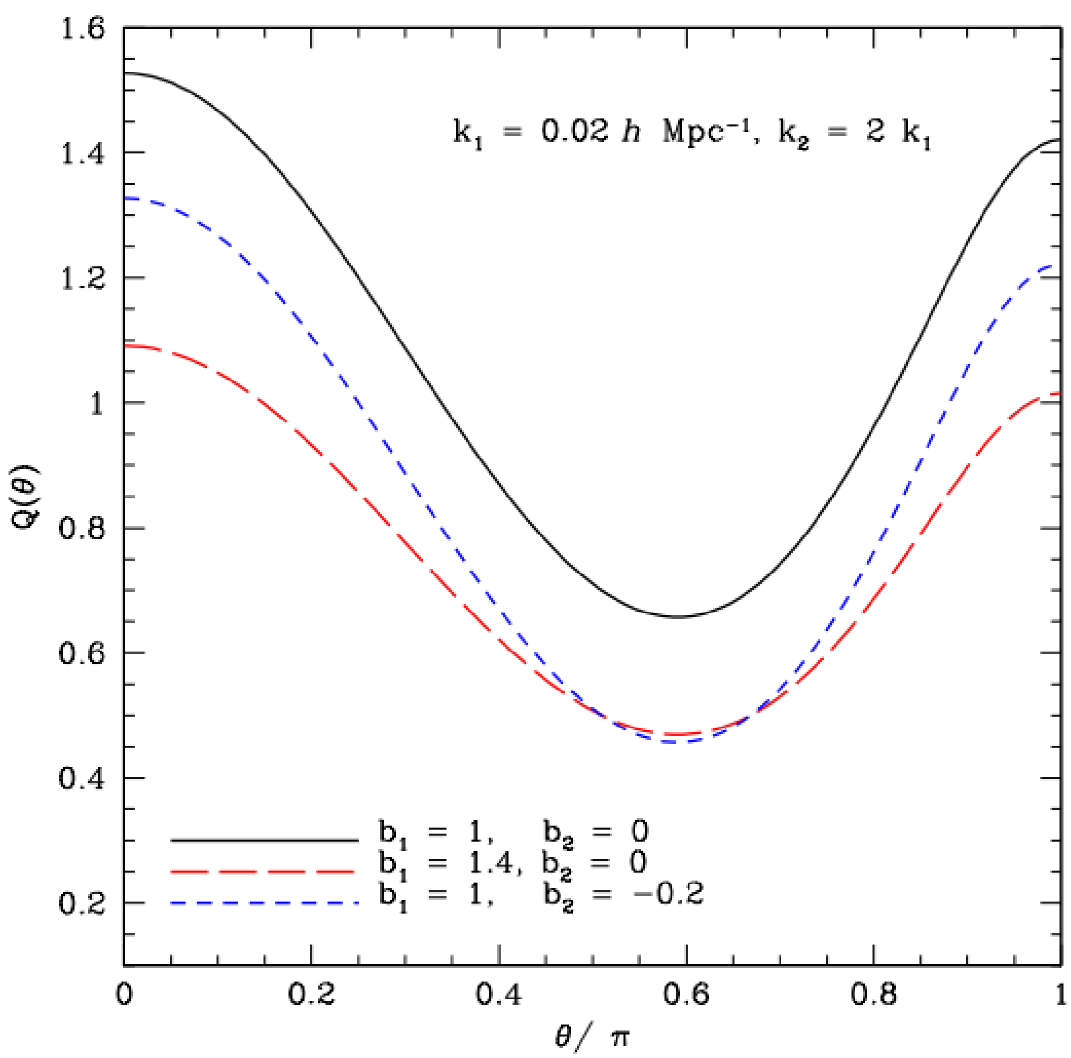

$$Q_g(k_1,k_2,k_3) = \frac{1}{b_1} Q(k_1,k_2,k_3) + \frac{b_2}{b_1^2}$$

This allows to break the degeneracy between b_1 and A_s …

but also determine b_2

Non-linear bias *and* non-linear gravitational instability

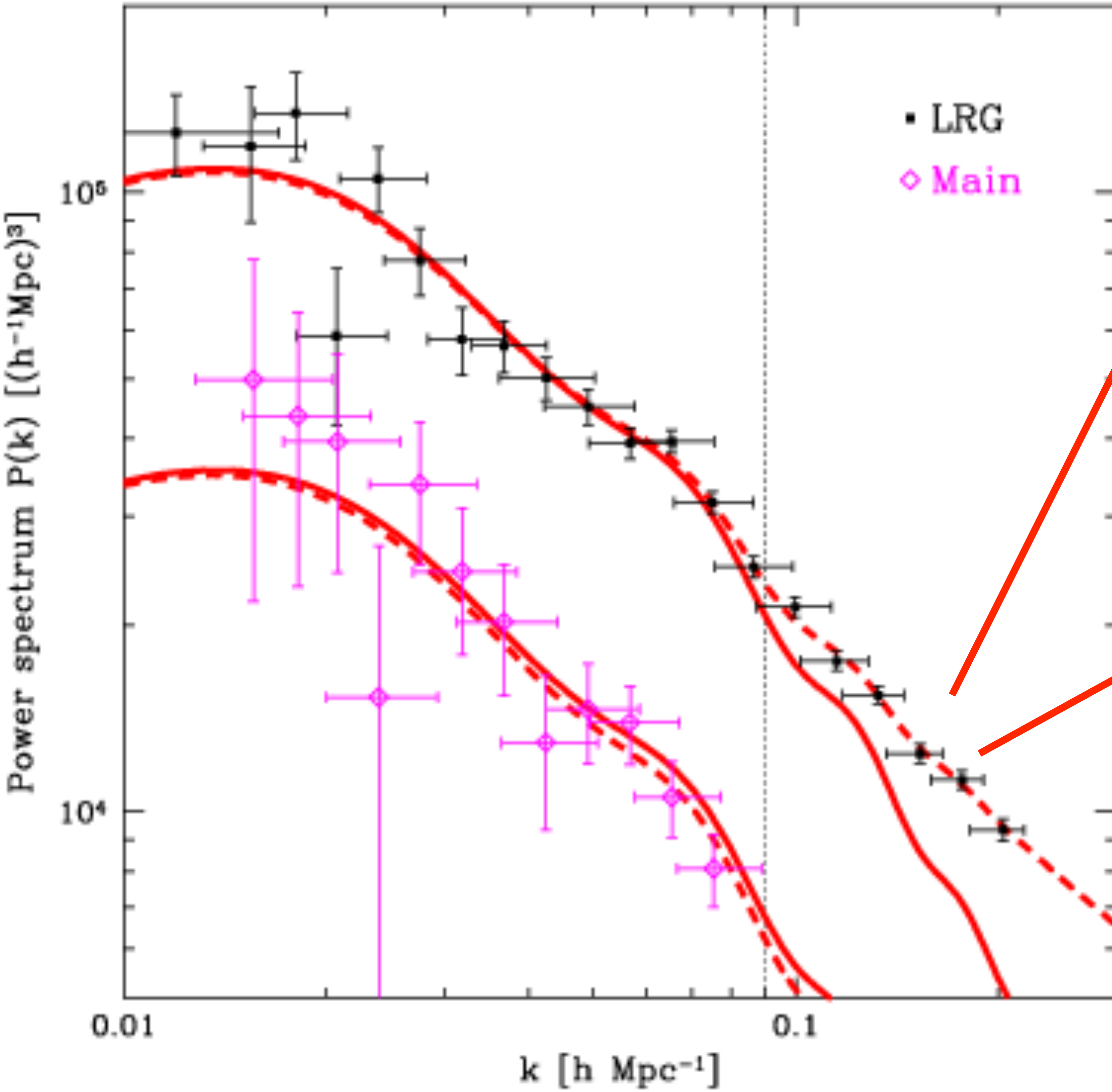

at small scales, non-linear bias is degenerate with non-linear corrections to the matter power spectrum!

at small scales we also have better statistics (smaller error bars)

Non-*local* galaxy bias

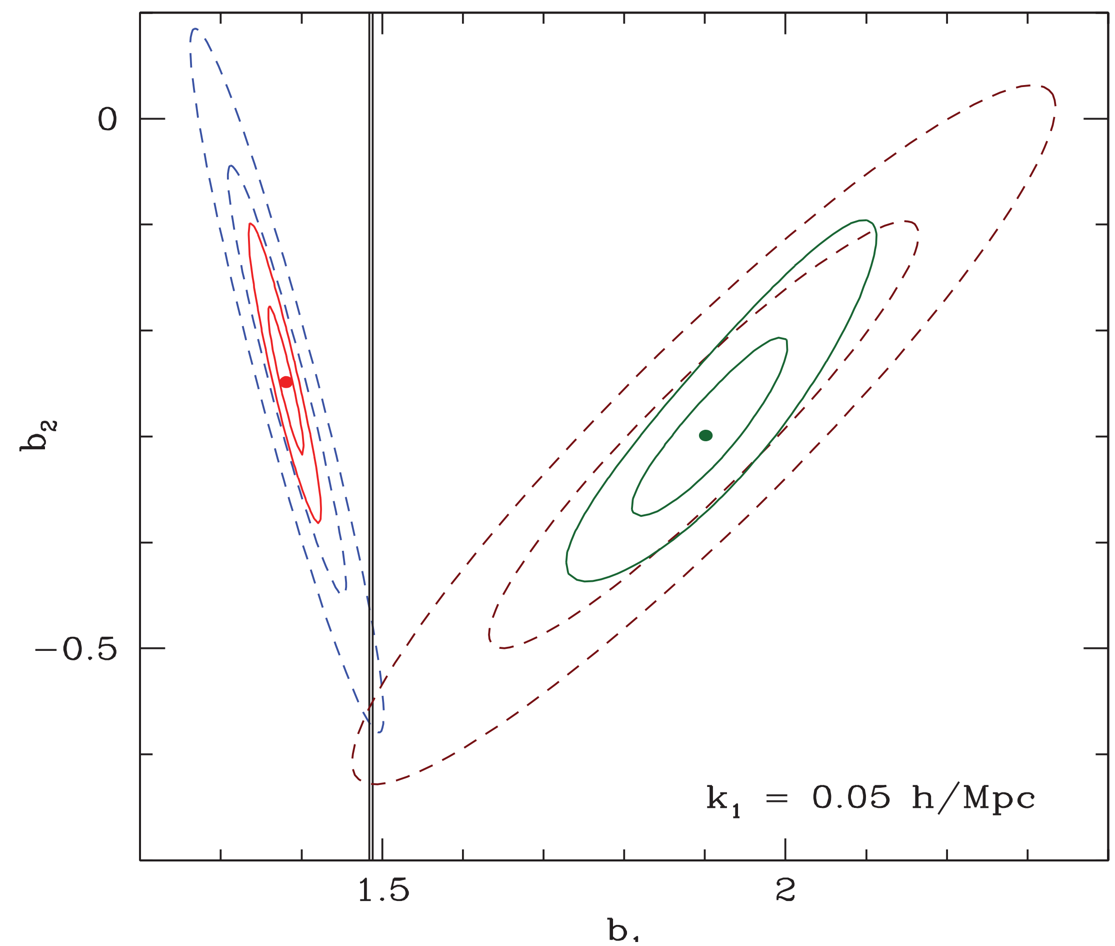

Pollack, Smith & Porciani (2012)

If we assume local bias then power spectrum and bispectrum provide (in simulations) different values for the bias parameters …

The solution is to assume a more general model for galaxy bias, allowing for **non-local operators**

$$\delta_g(\vec{x}) = f[\nabla_i \nabla_j \Phi(\vec{x}),\, \nabla_i \nabla_j \Phi_v(\vec{x})]$$

$$\nabla^2 \Phi = \delta \qquad \nabla^2 \Phi_v = \vec{\nabla} \cdot \vec{u} = \theta$$

with Φ and Φ_v are the (normalised) gravitational and velocity potentials

Non-*local* galaxy bias

$$\delta_g(\vec{x}) = f[\nabla_i \nabla_j \Phi(\vec{x}),\ \nabla_i \nabla_j \Phi_v(\vec{x})]$$

Chan, Scoccimarro & Sheth (2012)
Baldauf *et al.* (2012)

We just write down all operators invariant under Galilean transformations:

$$\mathcal{G}_1(\Phi) = \nabla^2 \Phi = \delta$$ local bias

$$\mathcal{G}_2(\Phi) = (\nabla_i \nabla_j \Phi)^2 - (\nabla^2 \Phi)^2$$ *tidal* bias

$\dots$

And so on … plus the same for the velocity potential $\mathscr{G}_n(\Phi_v)$ (the are the same at linear level, but not at second order). Then we have powers, as $\mathscr{G}_1^2(\Phi) = \delta^2$, etc …

At second order the bias expansion is now

$$\delta_g = b_1\,\delta + \frac{b_2}{2}\,\delta^2 + \gamma_2\,\mathcal{G}_2[\Phi] + \mathcal{O}(\Phi_L^3)$$

a lot of new terms and new (free?) parameters!

The galaxy bispectrum - take 2

The galaxy bispectrum model (at tree-level) now reads

$$B_g(k_1,k_2,k_3) = b_1^3\, B(k_1,k_2,k_3) + b_1^2\, b_2\, P_L(k_1)\, P_L(k_2) + \text{perm.}$$

local, linear bias local, nonlinear bias

$$+2\, b_1^2\, \gamma\, \Sigma(\mathbf{k_1},\mathbf{k_2})\, P_L(k_1)\, P_L(k_2) + \text{perm.} + \ldots$$

nonlocal (tidal) bias

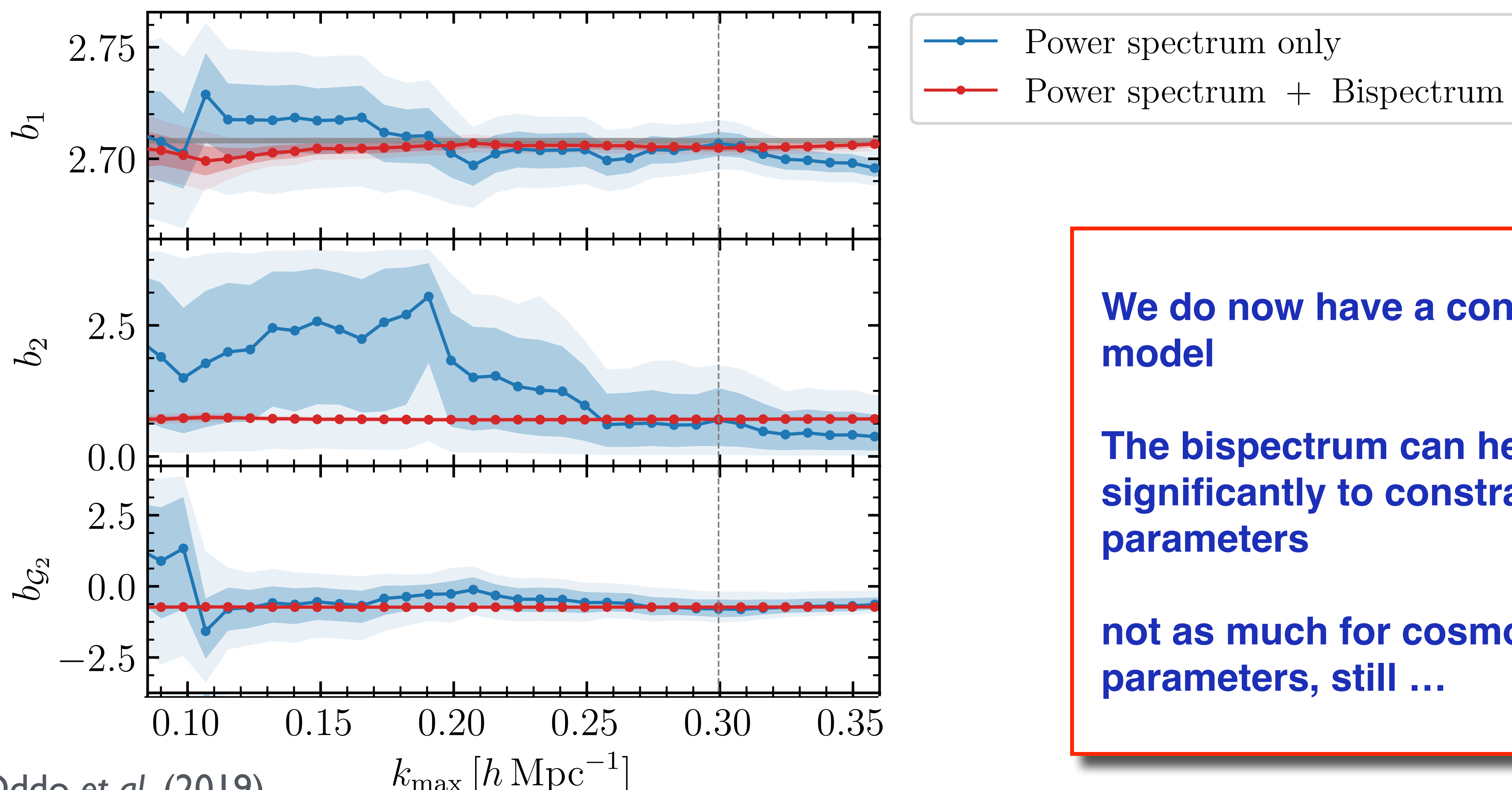

Oddo *et al.* (2019)

We do now have a consistent model

The bispectrum can help significantly to constrain bias parameters

not as much for cosmological parameters, still …

Higher-derivatives galaxy bias

Suppose we now want to account galaxy formation happening on an region of finite size R …

$$b_1\,\delta(\vec{x}) \rightarrow \int d^3y\,F_R(\vec{y})\,\delta(\vec{x}-\vec{y})$$

$$\simeq \left[\int d^3y\,F_R(\vec{y})\right]\,\delta(\vec{x}) + \left[\frac{1}{6}\int d^3y\,y^2\,F_R(\vec{y})\right]\,\nabla^2\delta(\vec{x}) + \ldots$$

The (linear, local) bias relation now becomes

$$\delta_b = b_1\,\delta - \beta_1\,k^2\,\delta + \mathcal{O}[(k\,R)^4]$$

but this is then totally degenerate with the matter power spectrum counter term at one-loop …

$$\delta_l = \delta_l^{(1)} + \delta_l^{(2)} + \delta_l^{(3)} + c_0\,k^2\,\delta_l^{(1)} + \ldots$$

$$P_g(k) \supset b_1^2\,c_0\,k^2\,P_L(k) - \beta_1\,b_1\,k^2\,P_L(k)$$

For all bias parameters we should consider in principle possible scale-dependent corrections …

For the one-loop power spectrum this is not adding anything, in practice

Bias Loop Corrections & Renormalization

McDonald (2006)
Assassi *et al.* (2014)
Eggemeier *et al.* (2019)

Let's assume, for simplicity, a local bias expansion

$$\delta_g = \bar{b}_1\,\delta + \frac{1}{2}\,\bar{b}_2\,\delta^2 + \frac{1}{6}\,\bar{b}_3\,\delta^3 + \dots$$

and look at the 2-point function beyond the linear approximation

$$\langle \delta_g(\vec{x}_1)\delta_g(\vec{x}_2)\rangle \supset \bar{b}_1^2\langle\delta_1\delta_2\rangle + \frac{1}{4}\bar{b}_2^2\langle\delta_1^2\delta_2^2\rangle + \frac{1}{6}\bar{b}_1\bar{b}_3\langle\delta_1\delta_2^3\rangle + \mathrm{perm.}$$

The galaxy power spectrum becomes then

$$P_g(k) \supset \bar{b}_1^2 P(k) + \frac{1}{2}\bar{b}_2^2\int d^3\,P_L(q)\,P_L(|\vec{q}-\vec{k}|) + \bar{b}_1\bar{b}_3 P_L(k)\int d^3q\,P_L(q)$$

this is a constant σ^2!

$$= \left(\bar{b}_1^2 + \bar{b}_1\bar{b}_3\sigma^2\right)P_L(k) + \frac{1}{4}\bar{b}_2^2\int d^3\,P_L(q)\,P_L(|\vec{q}-\vec{k}|)$$

Observable (renormalized) linear bias

$$b_1 = \bar{b}_1 + \bar{b}_3\sigma^2/2$$

Bias loop correction

To sum up (in real space, we are not done yet)

$$P_g(k) = b_1^2\left[P_0(k) + P_m^{1-\mathrm{loop}}(k)\right] + b_1 b_2 \mathcal{I}_{\delta^2}(k) + 2 b_1 b_{\mathcal{G}_2}\mathcal{I}_{\mathcal{G}_2}(k)$$
$$+\frac{1}{4}b_2^2\mathcal{I}_{\delta^2\delta^2}(k) + b_{\mathcal{G}_2}^2\,\mathcal{I}_{\mathcal{G}_2\mathcal{G}_2}(k) + b_2 b_{\mathcal{G}_2}\mathcal{I}_{\delta^2\mathcal{G}_2}(k) + 2b_1\left(b_{\mathcal{G}_2} + \frac{2}{5}b_{\Gamma_3}\right)\mathcal{F}_{\mathcal{G}_2}(k)$$

$$\mathcal{I}_{\delta^2}(k) = 2\int_{\mathbf{q}} F_2(\mathbf{q},\mathbf{k}-\mathbf{q})P_0(|\mathbf{k}-\mathbf{q}|)P_0(q),$$
$$\mathcal{I}_{\mathcal{G}_2}(k) = 2\int_{\mathbf{q}} S^2(\mathbf{q},\mathbf{k}-\mathbf{q})F_2(\mathbf{q},\mathbf{k}-\mathbf{q})P_0(|\mathbf{k}-\mathbf{q}|)P_0(q),$$
$$\mathcal{I}_{\delta^2\delta^2}(k) = 2\int_{\mathbf{q}} \left[P_0(|\mathbf{k}-\mathbf{q}|)P_0(q) - P_0^2(q)\right],$$
$$\mathcal{I}_{\mathcal{G}_2\mathcal{G}_2}(k) = 2\int_{\mathbf{q}} \left[S^2(\mathbf{q},\mathbf{k}-\mathbf{q})\right]^2 P_0(|\mathbf{k}-\mathbf{q}|)P_0(q),$$
$$\mathcal{I}_{\delta^2\mathcal{G}_2}(k) = 2\int_{\mathbf{q}} S^2(\mathbf{q},\mathbf{k}-\mathbf{q})P_0(|\mathbf{k}-\mathbf{q}|)P_0(q),$$
$$\mathcal{F}_{\mathcal{G}_2}(k) = 4P_0(k)\int_{\mathbf{q}} S^2(\mathbf{q},\mathbf{k}-\mathbf{q})F_2(\mathbf{q},-\mathbf{k})P_0(q),$$

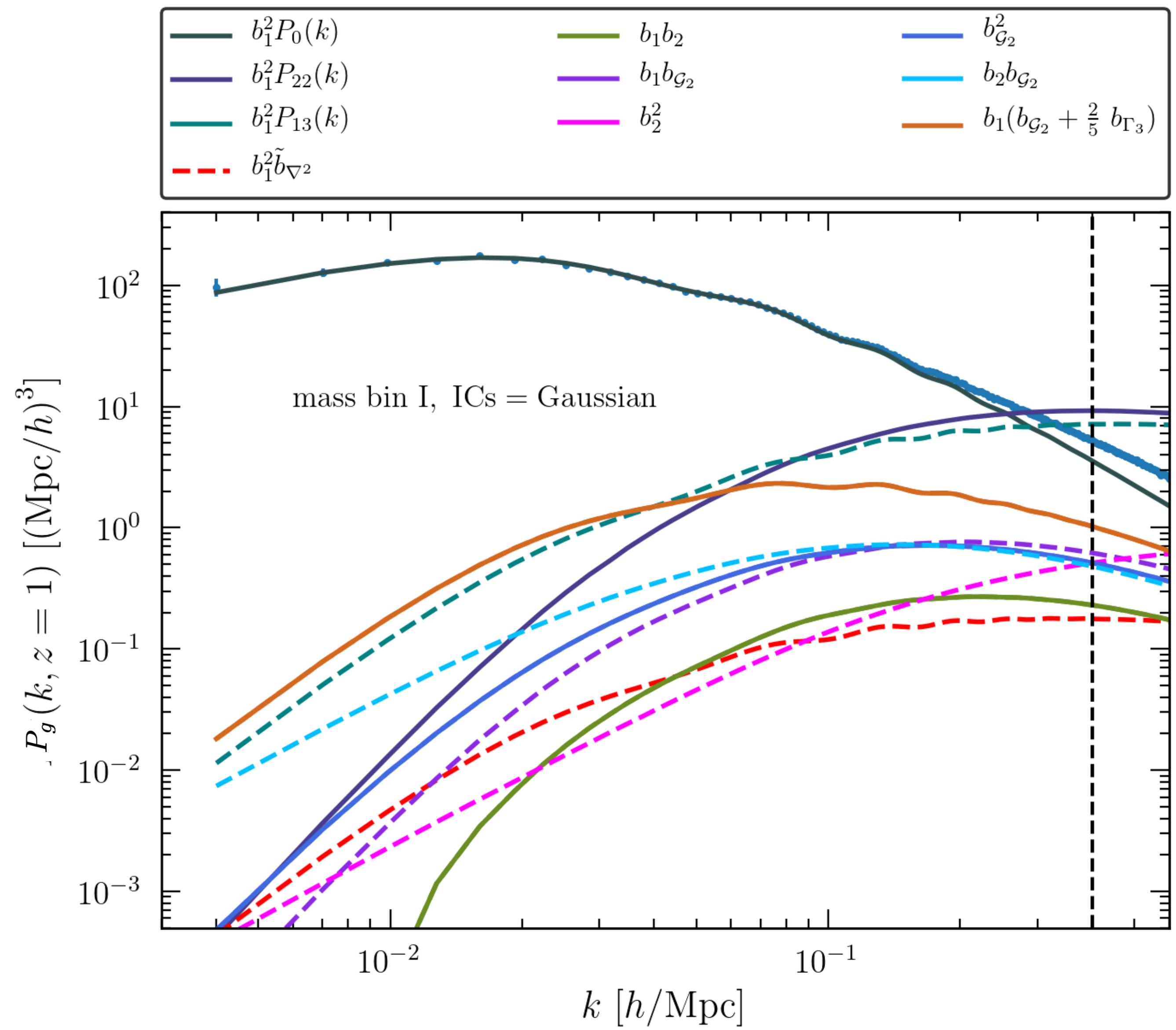

4 bias parameters

many non-linear, bias corrections to some extent degenerate

from Moradinezhad *et al.* (2021)

Baryonic Acoustic Oscillations
& Infrared Resummation

Baryonic Acoustic Oscillations

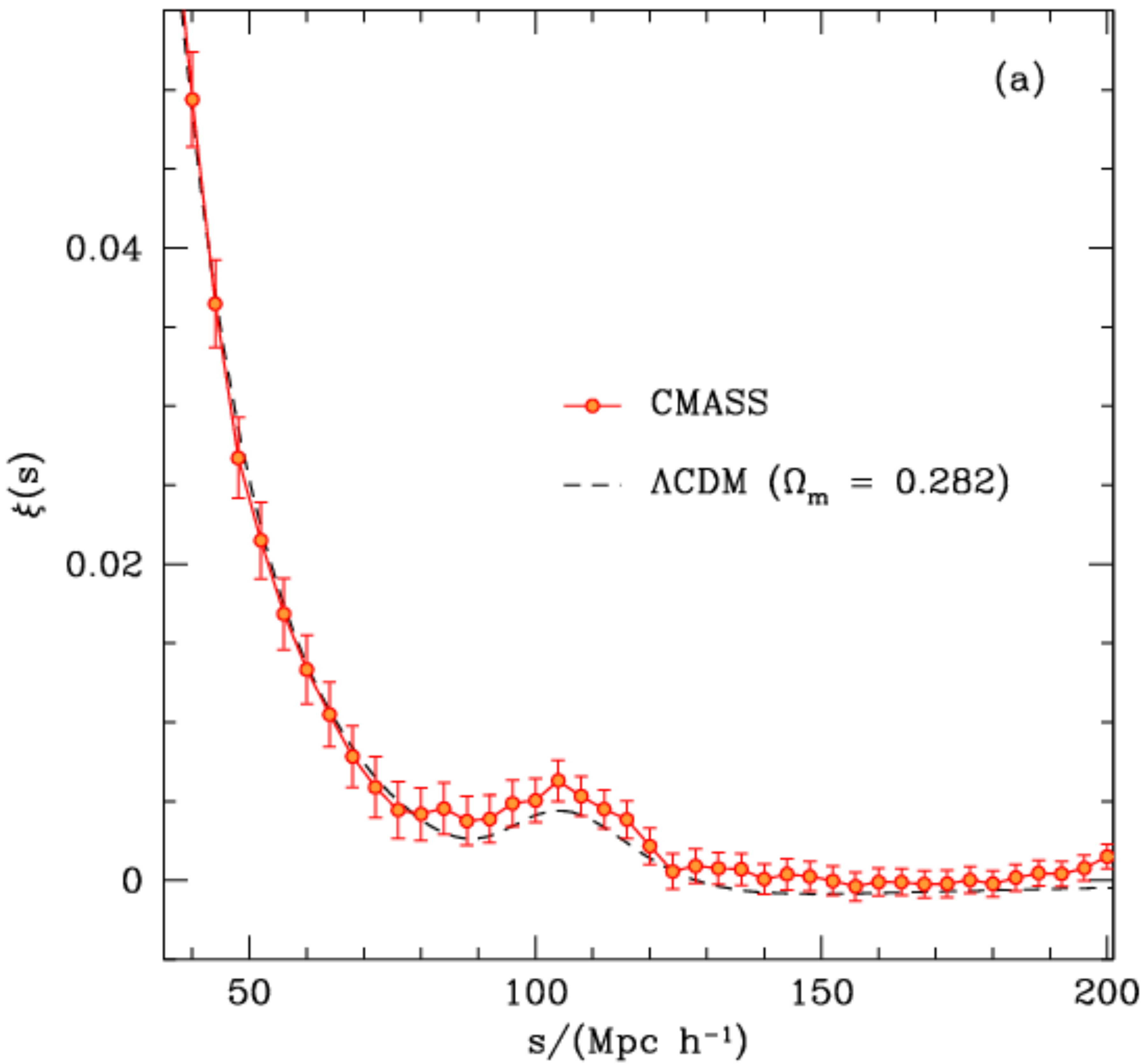

A standard ruler

We know the size of the "oscillation ring" very well from CMB observations

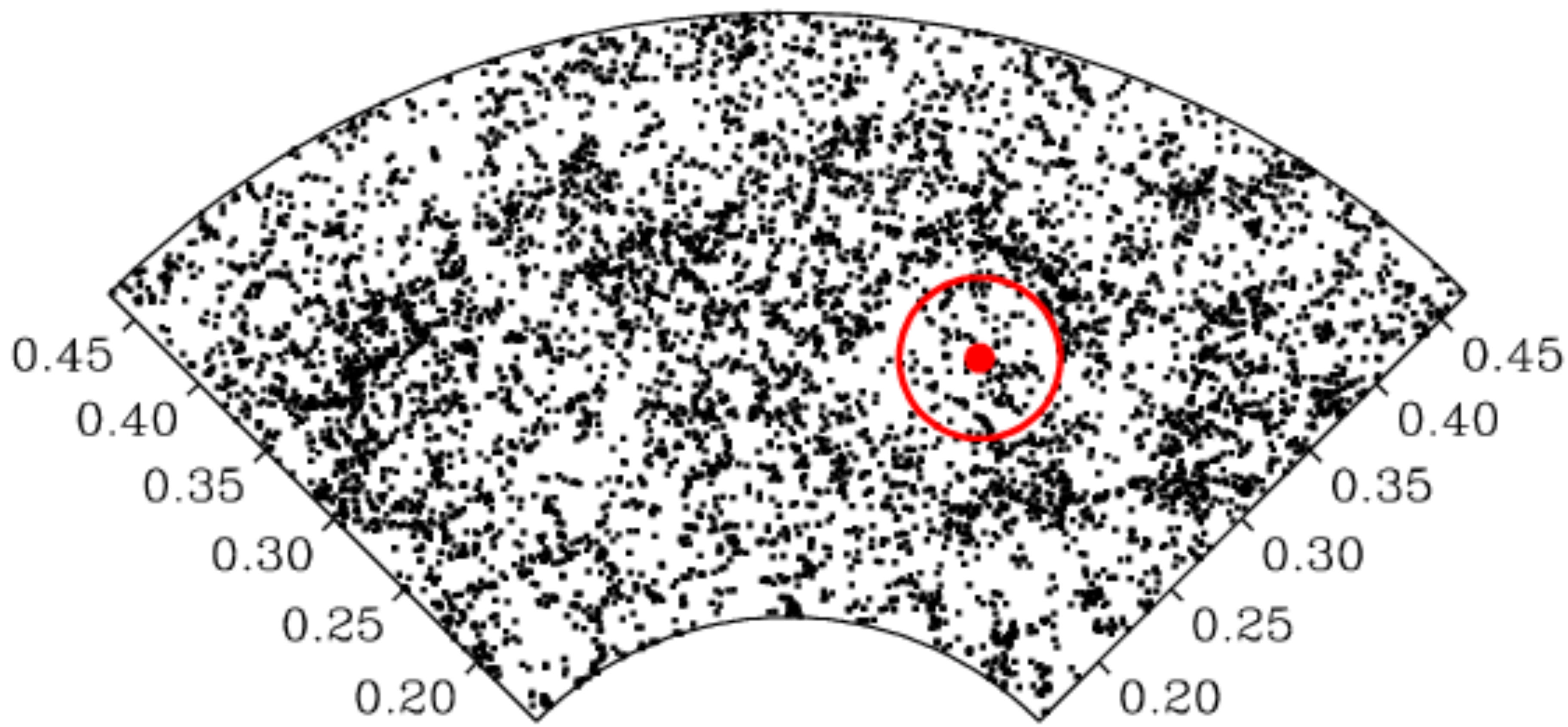

A standard ruler

We know the size of the "oscillation ring" very well from CMB observations

We can use it measurement in the galaxy 2-point function to constrain Cosmic expansion

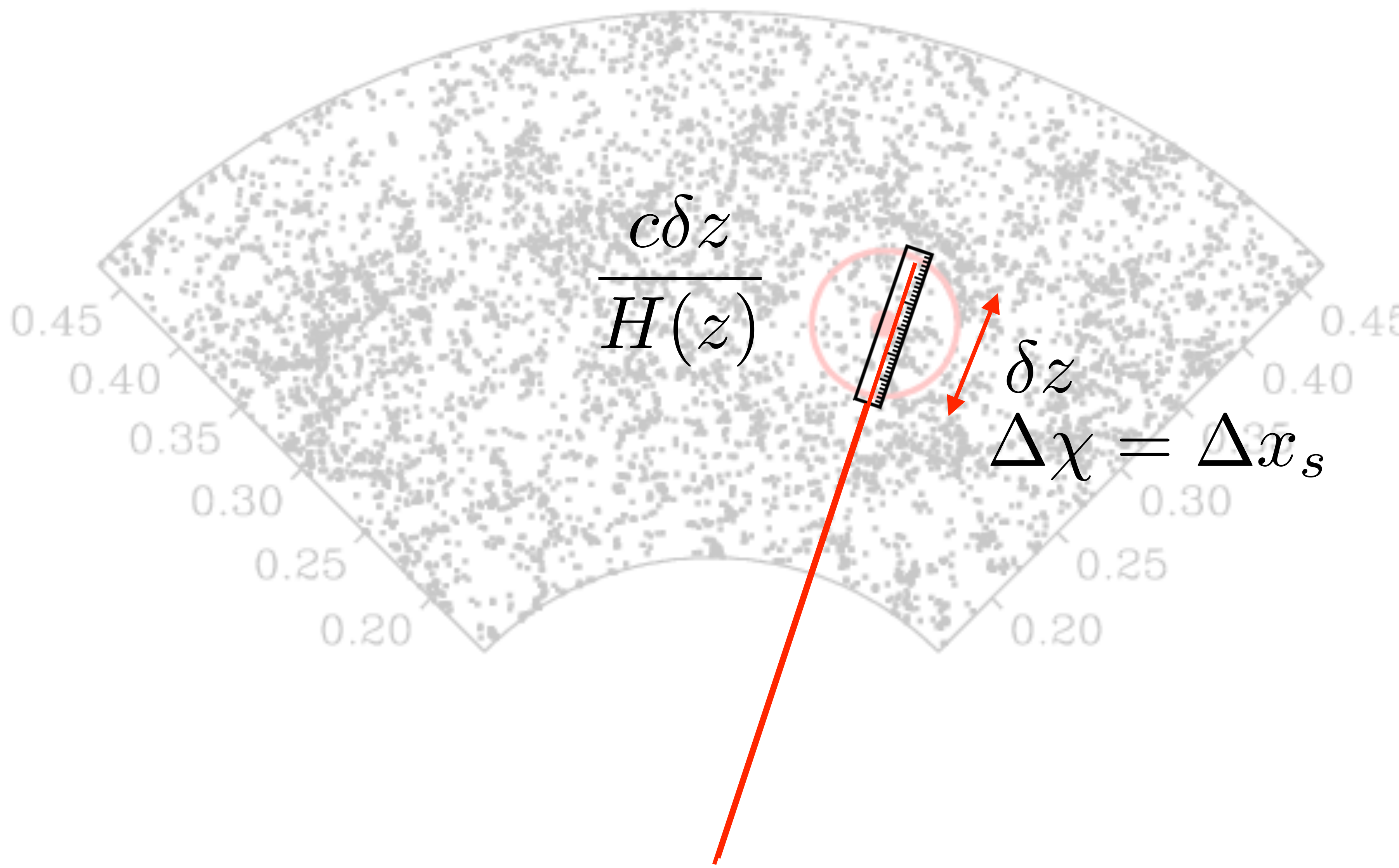

comoving distance along the line-of-sight

$$\chi = \int_{t_e}^{t_o} \frac{dt'}{a(t')} = \int_{a_e}^{a_o} \frac{da'}{H(a')} = \int_0^z \frac{dz'}{H(z')}$$

A standard ruler

We know the size of the "oscillation ring" very well from CMB observations

We can use it measurement in the galaxy 2-point function to constrain Cosmic expansion

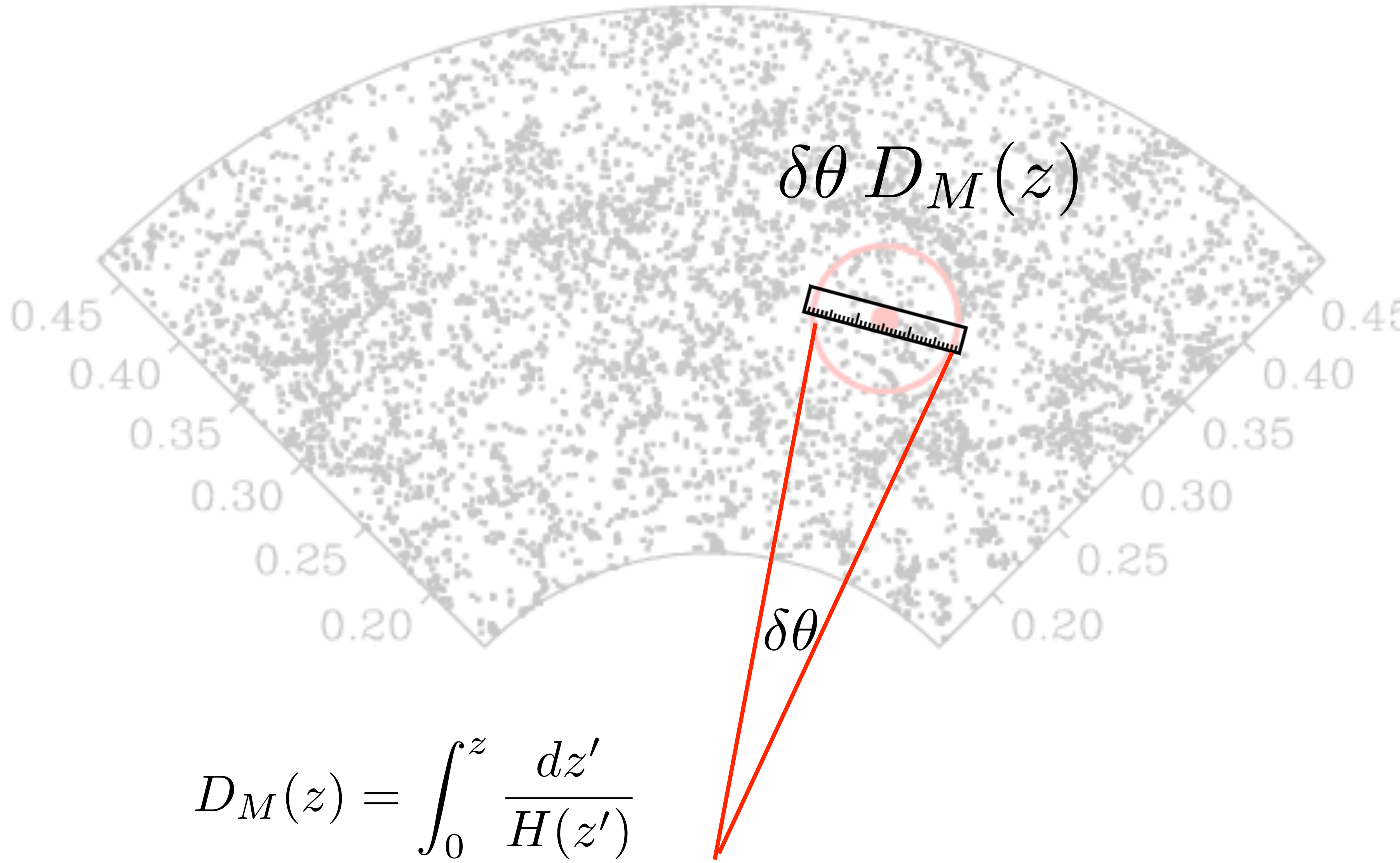

$$D_M(z) = \int_0^z \frac{dz'}{H(z')}$$

comoving angular diameter distance

BAO: how well do we measure them?

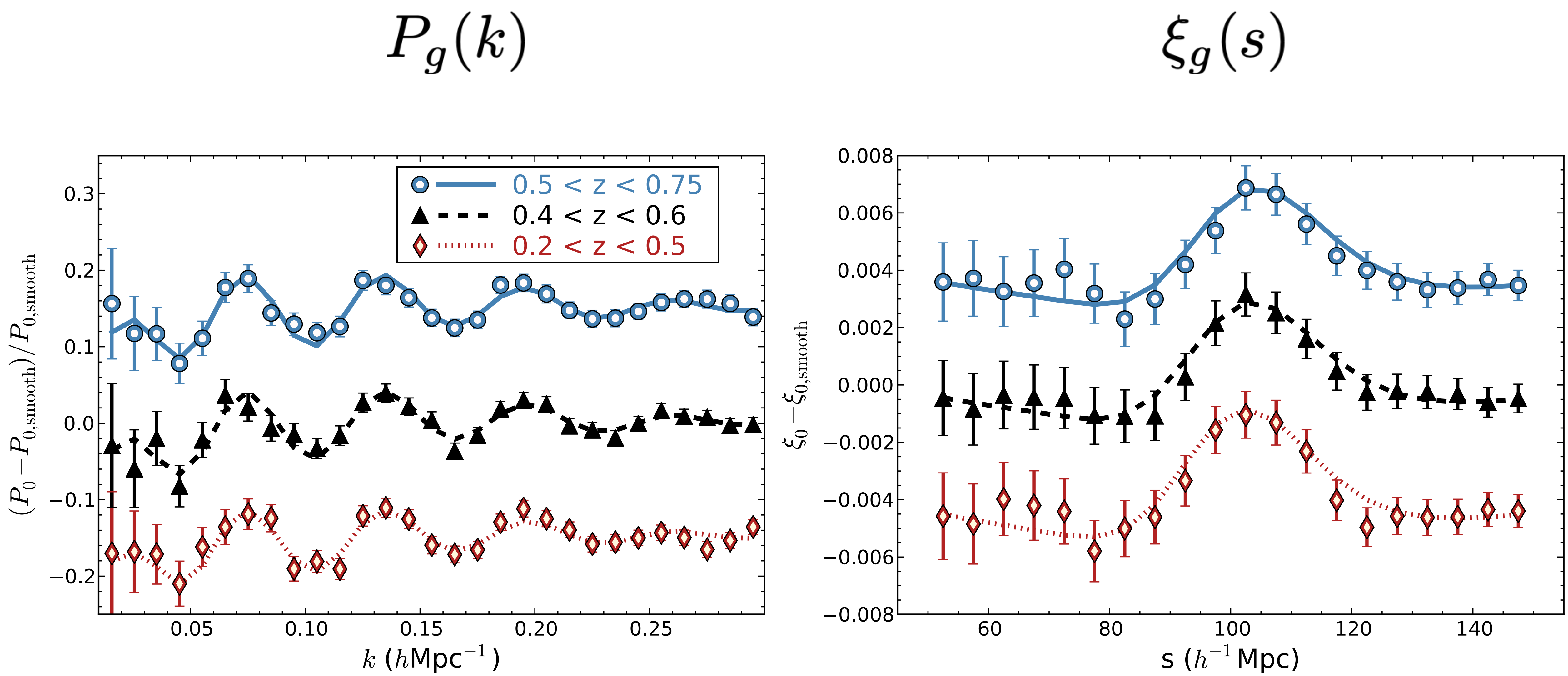

Baryon Oscillation Spectroscopic Survey (BOSS) - DR12 (final)

Alam *et al.* (2017)

Nonlinear evolution of BAO

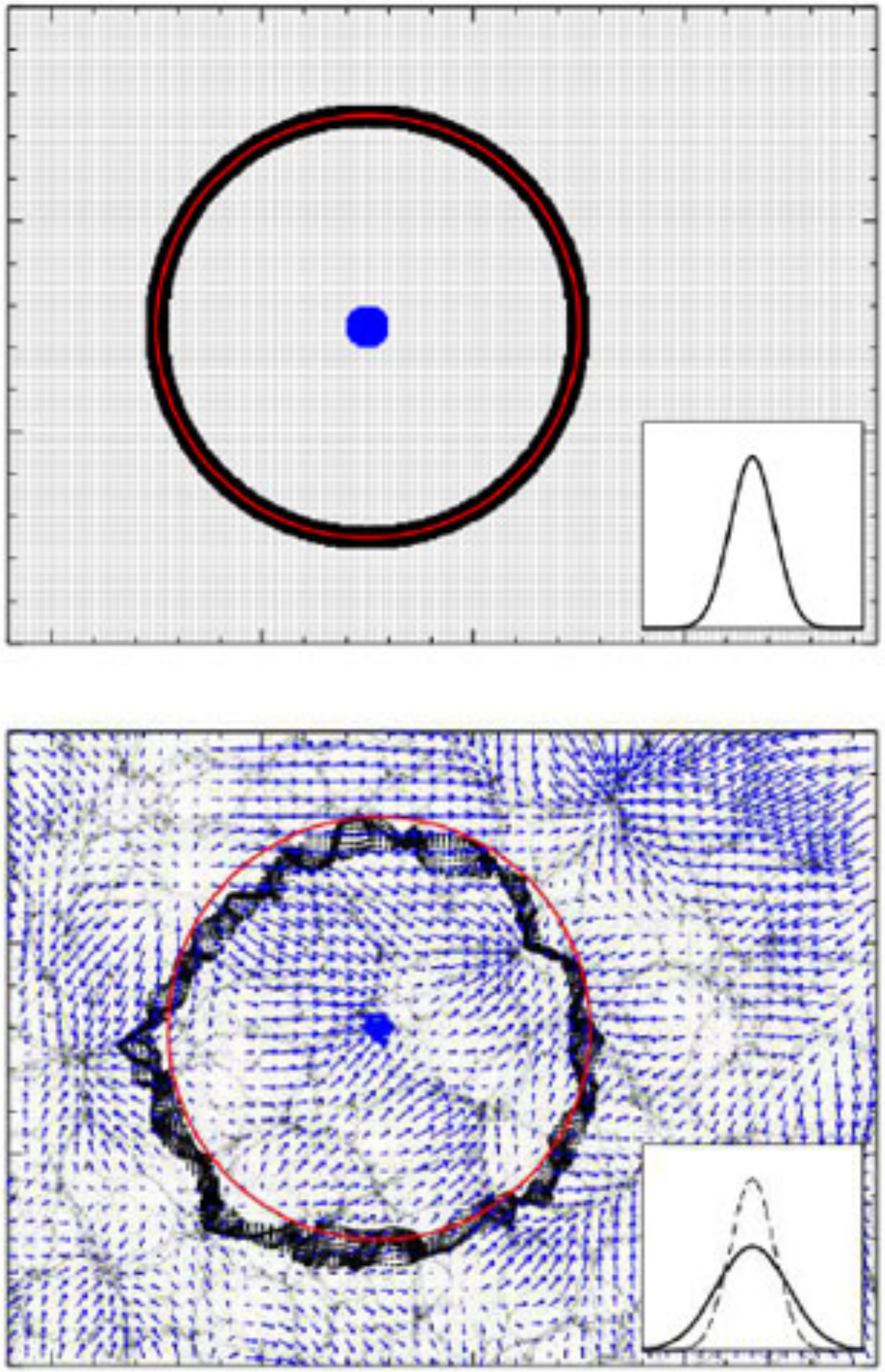

Nonlinear evolution induces a broadening of the BAO peak, mainly due to bulk flows

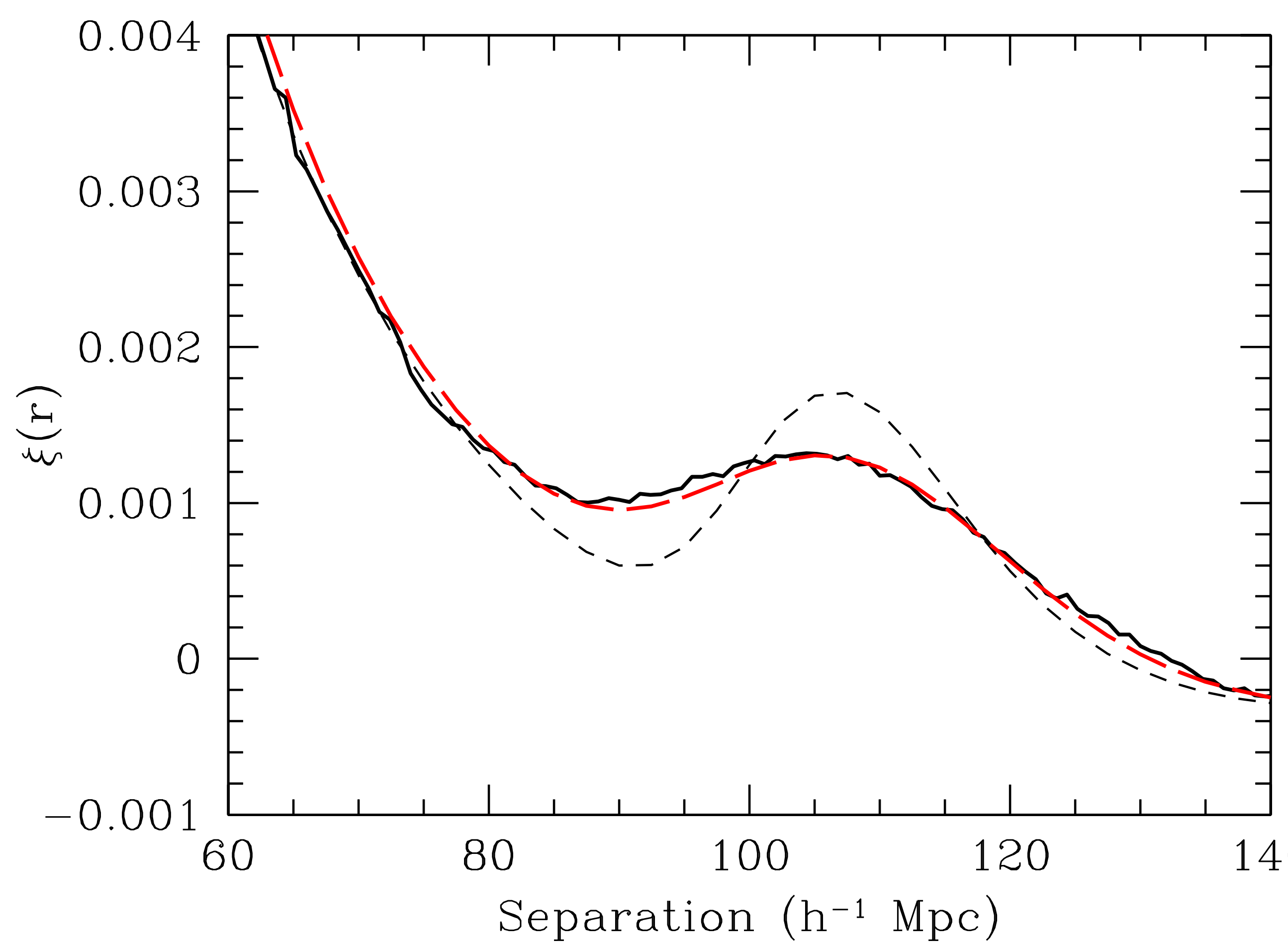

Padmanabhan *et al.* (2012)

Seo, Eisenstein, Seo & White (2006)

Nonlinear evolution of BAO

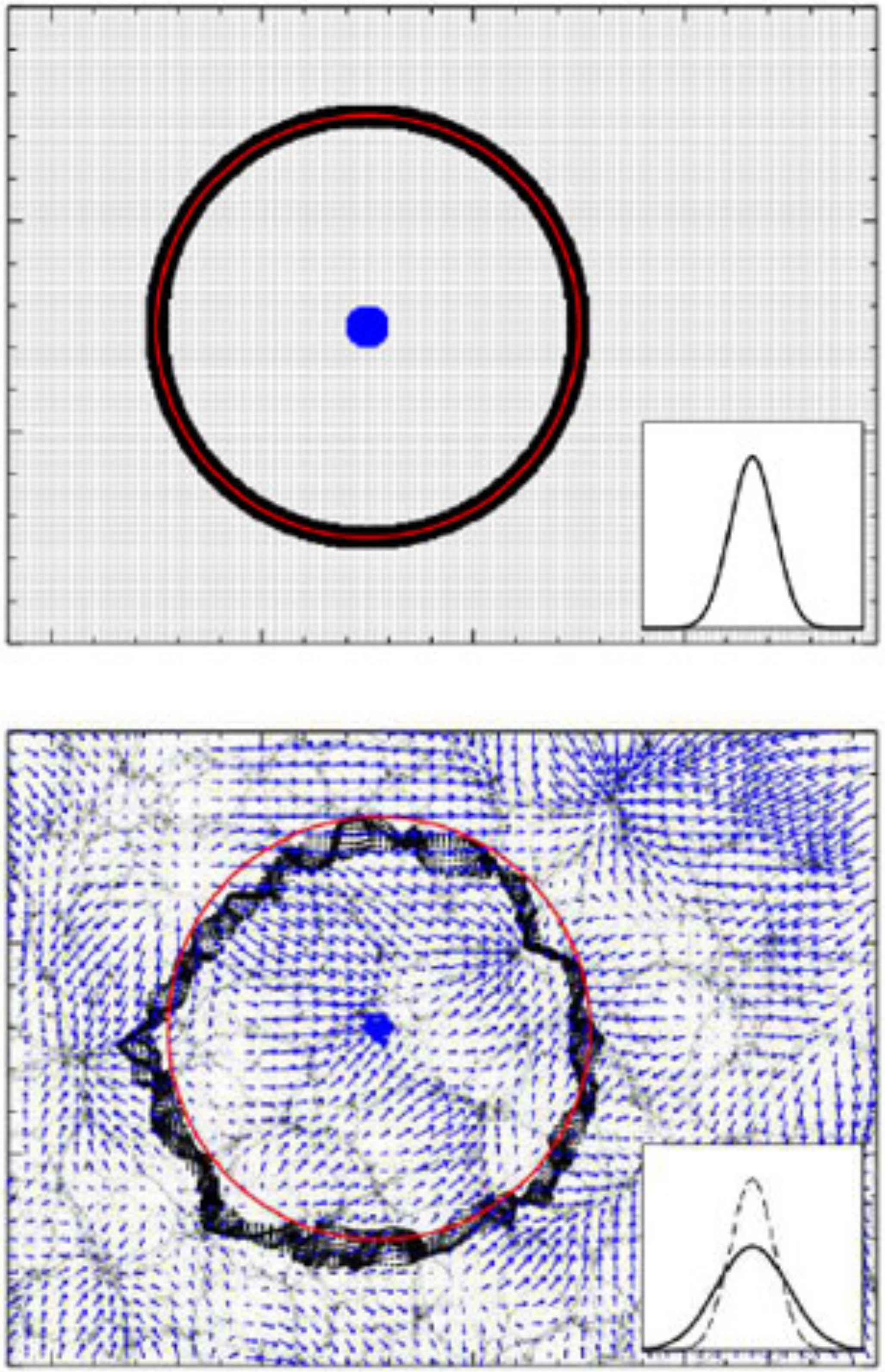

In template fitting this is typically described as

$$P(k) = P^{\rm nw}(k) + P^{\rm w}(k)$$

$$P(k) = P^{\rm nw}(k)\left(1 + \frac{P_L^{\rm w}}{P_L^{\rm nw}} e^{-k^2\Sigma^2/2}\right)$$

where Σ is a free parameter to fit

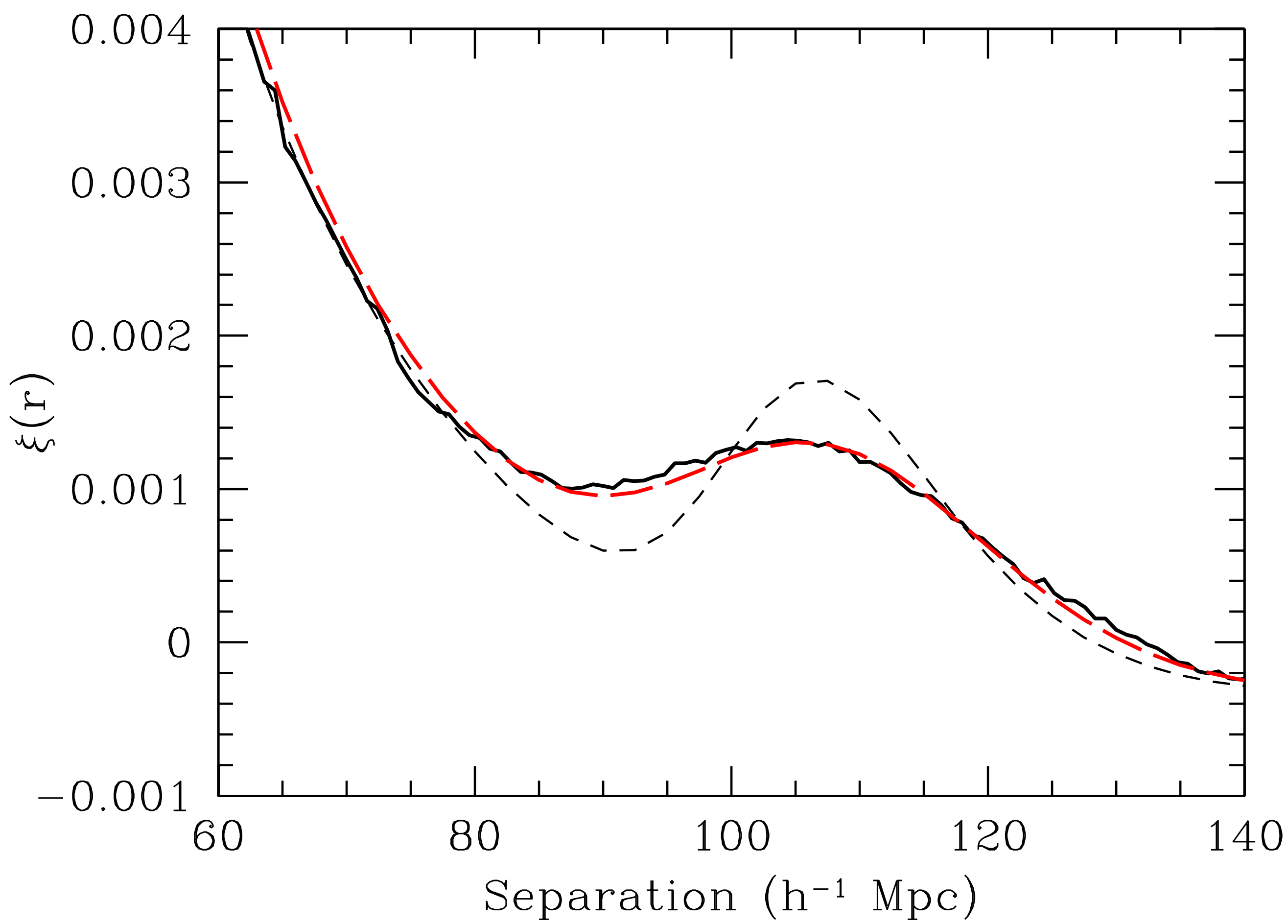

Padmanabhan *et al.* (2012)

Seo, Eisenstein, Seo & White (2006)

Nonlinear modelling of BAO

Theoretical arguments based on the equivalence principle motivated a parameter-free model consistent with the EFT at one-loop

$$P(k) = P_L^{\rm nw}(k) + P_{1-{\rm loop}}^{\rm nw}(k) + e^{-k^2\Sigma_\Lambda^2}\left(1 + k^2\Sigma_\Lambda^2\right) P_L^{\rm w} + e^{-k^2\Sigma_\Lambda^2} P_{1-{\rm loop}}^{\rm w}$$

$$\Sigma_\Lambda^2 \simeq \frac{1}{6\pi^2}\int P_L^{\rm nw}(q)[1 - j_0(q\ell_{BAO}) + 2j_2(q\ell_{BAO})]$$

Infrared Resummation

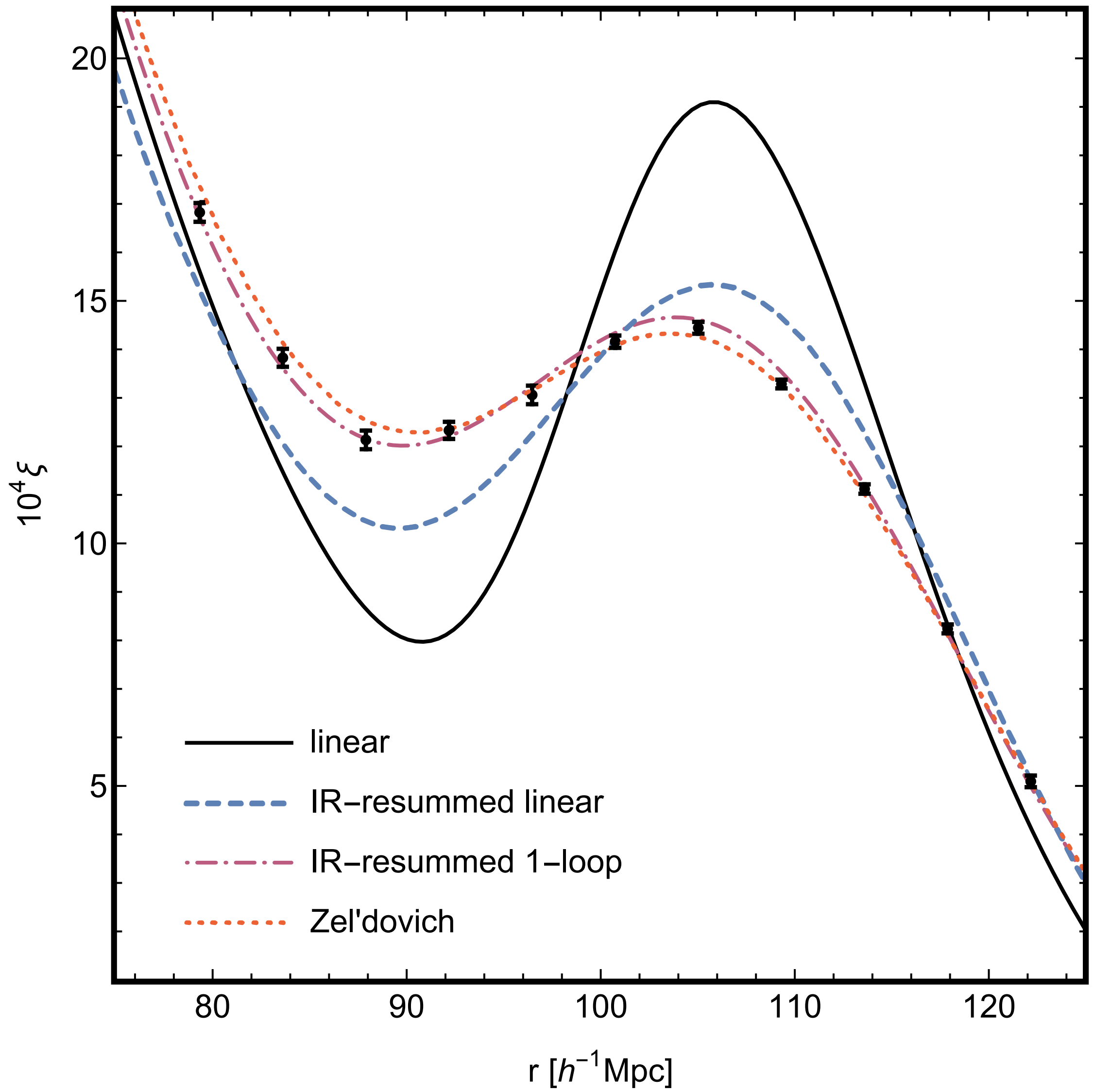

Baldauf *et al.* (2015)
Vlah et al. (2015)
Blas et al. (2016)

see also Senatore & Zaldarriaga (2014)

Redshift-space distortions

Redshift-space

Galaxies are observed in **redshift space** *not* in real space

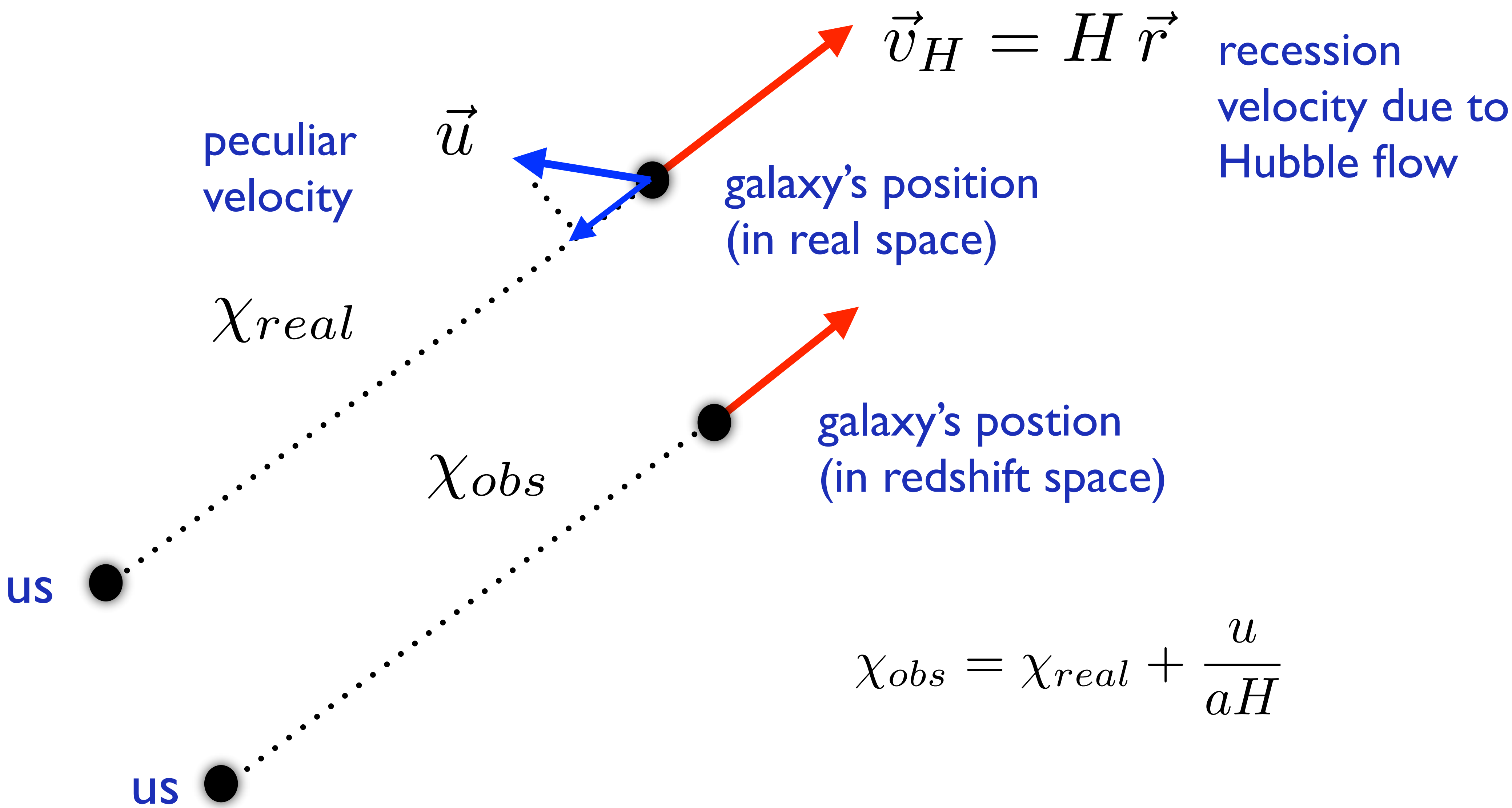

$$\chi_{obs} = \chi_{real} + \frac{u}{aH}$$

Two main effects:

- **Kaiser effect at large scales**
- **Finger-of-God effect at small scales**

Kaiser effect

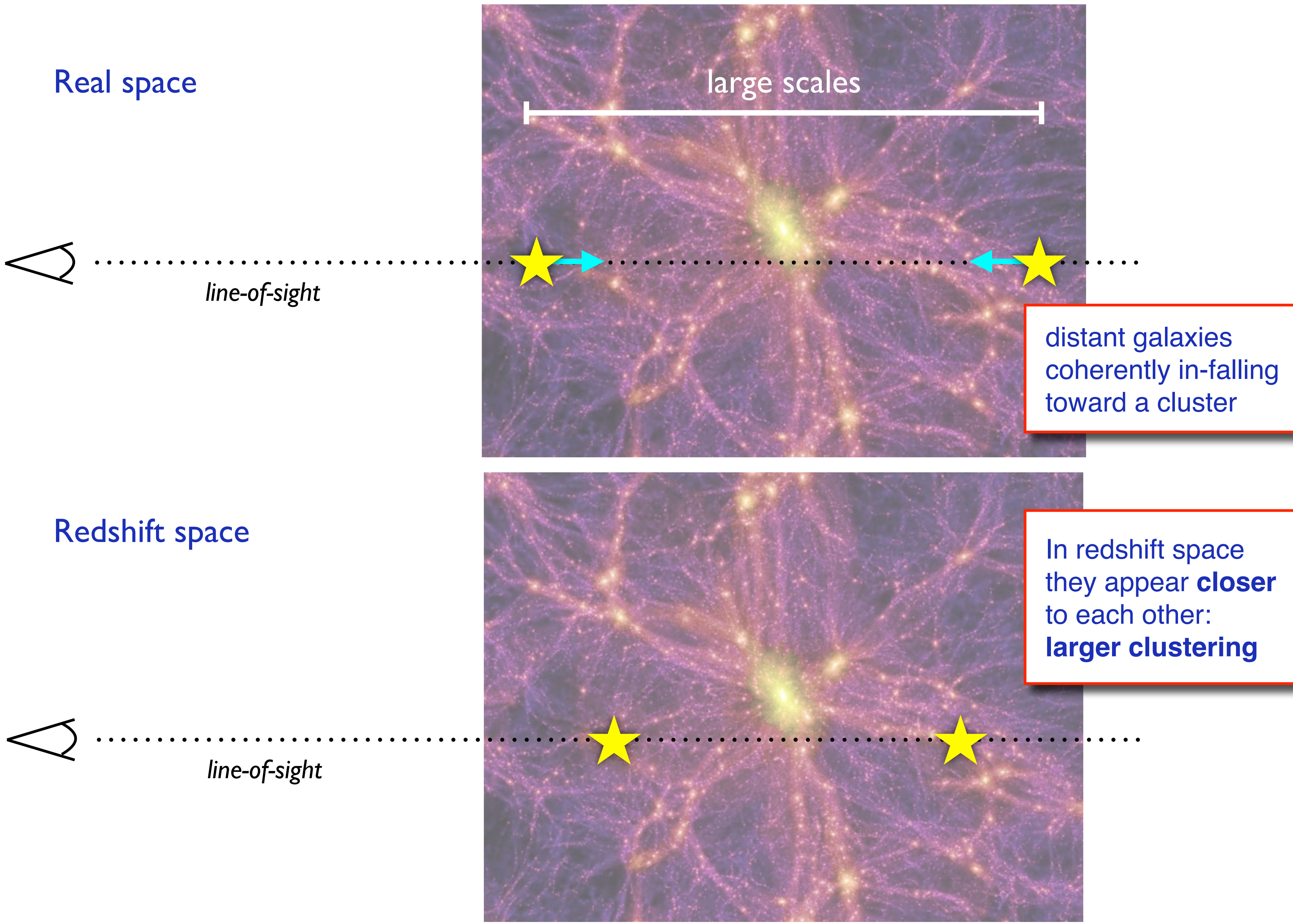

Kaiser effect

Kaiser (1987)

We look at the coordinate transformation between real ($\vec{x}$) and redshift space ($\vec{s}$)

$$\vec{s} = \vec{x} + \frac{u_z(\vec{x})}{\mathcal{H}}\hat{z}$$

Then the density in redshift-space is obtained from mass conservation:

$$\bar{\rho}[1+\delta_s(\vec{s})]d^3s = \bar{\rho}[1+\delta(\vec{x})]d^3x$$

$$\delta_s(\vec{k}) = \int \frac{d^3s}{(2\pi)^3}\, e^{-i\vec{k}\cdot\vec{s}}\delta_s(\vec{s}) = \int \frac{d^3x}{(2\pi)^3}\, e^{-i\vec{k}\cdot[\vec{x}-u_z(\vec{x})\hat{z}/\mathcal{H}]}[\delta(\vec{x}) - \nabla_z u_z(\vec{x})/\mathcal{H}]$$

At linear level, this boils down to

$$\delta_{s,L}(\vec{k}) = \delta_L(\vec{k}) - \mu^2\frac{\theta_L(\vec{k})}{\mathcal{H}} = (1+f\,\mu^2)\,\delta_L(\vec{k})$$

For galaxies

$$\delta_{s,L}(\vec{k}) = (b_1 + f\,\mu^2)\,\delta_L(\vec{k}) \equiv Z_1(\vec{k})\delta_L(\vec{k})$$

Kaiser effect

Kaiser (1987)

The linear power spectrum is now

$$\boxed{P_s(\vec{k}) = P_s(k,\mu) = (b_1 + f\,\mu^2)^2\,P_L(k)}$$

Enhancement along the line-of-sight proportional to the growth rate

$$f \equiv \frac{d\ln D(a)}{d\ln a} = \Omega_m^\gamma(z)$$

The **redshift-space power spectrum** is **anisotropic**
we consider an expansion in Legendre polynomials

$$P_s(\vec{k}) = \sum_\ell P_\ell(k)\mathcal{L}_\ell(\mu)$$

(The multipoles $P_\ell(k)$ are the observables of the first slide!)

Standard **PT** results can be rewritten in terms of **kernels** accounting for **matter evolution**, **bias** and **redshift-space distortions**

$$\delta_s(\vec{k}) = Z_1(\vec{k})\delta_L(\vec{k}) + \int d^3q\,Z_2(\vec{q},\vec{k}-\vec{q})\delta_L(\vec{q})\delta_L(\vec{k}-\vec{q}) + \dots$$

$$Z_2(\vec{k}_1,\vec{k}_2) = b_1\,F_2(\vec{k}_1,\vec{k}_2) + \frac{b_2}{2} + \gamma\,\Sigma(\vec{k}_1,\vec{k}_2) + f\,\mu_{12}\,G_2(\vec{k}_1,\vec{k}_2) + \frac{f\mu_{12}k_{12}}{2}\left[\frac{\mu_1}{k_1}Z_1(\vec{k}_2) + \frac{\mu_2}{k_2}Z_1(\vec{k}_1)\right]$$

Finger-of-God effect

Real space

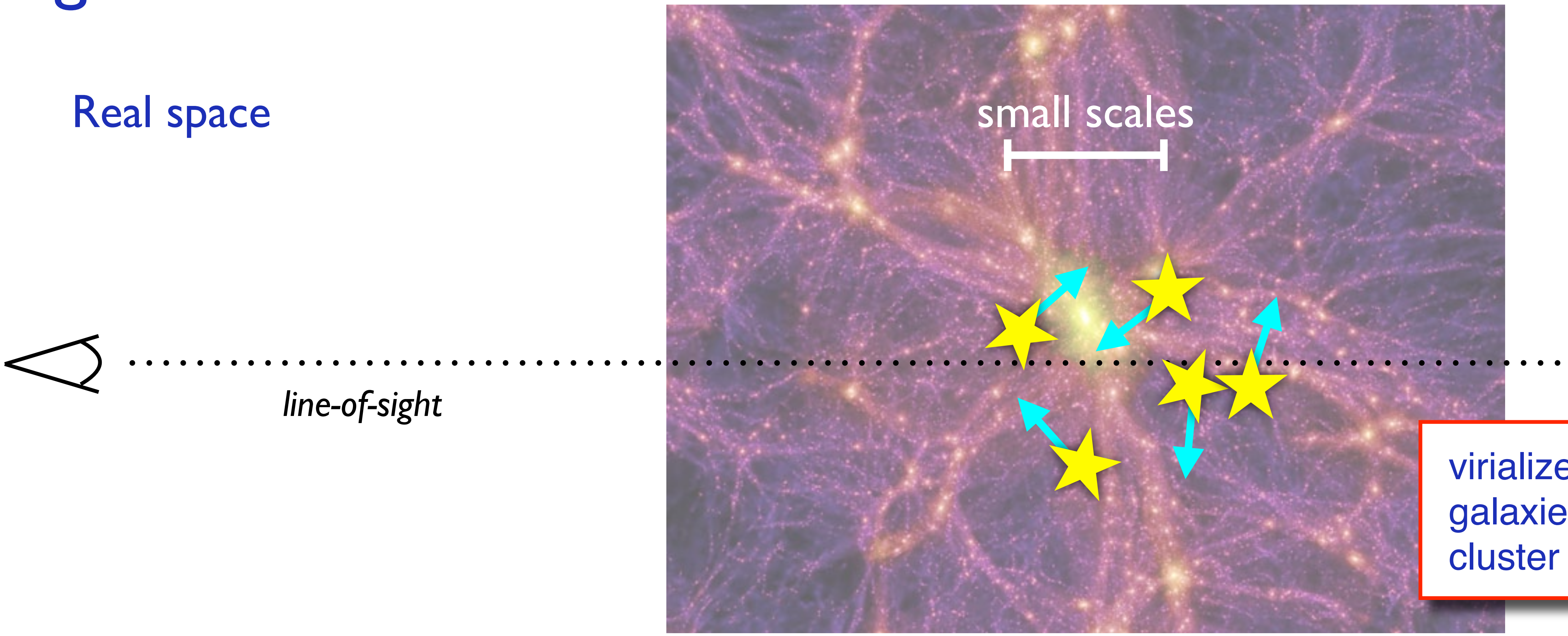

virialized motion of galaxies *within* a cluster

Redshift space

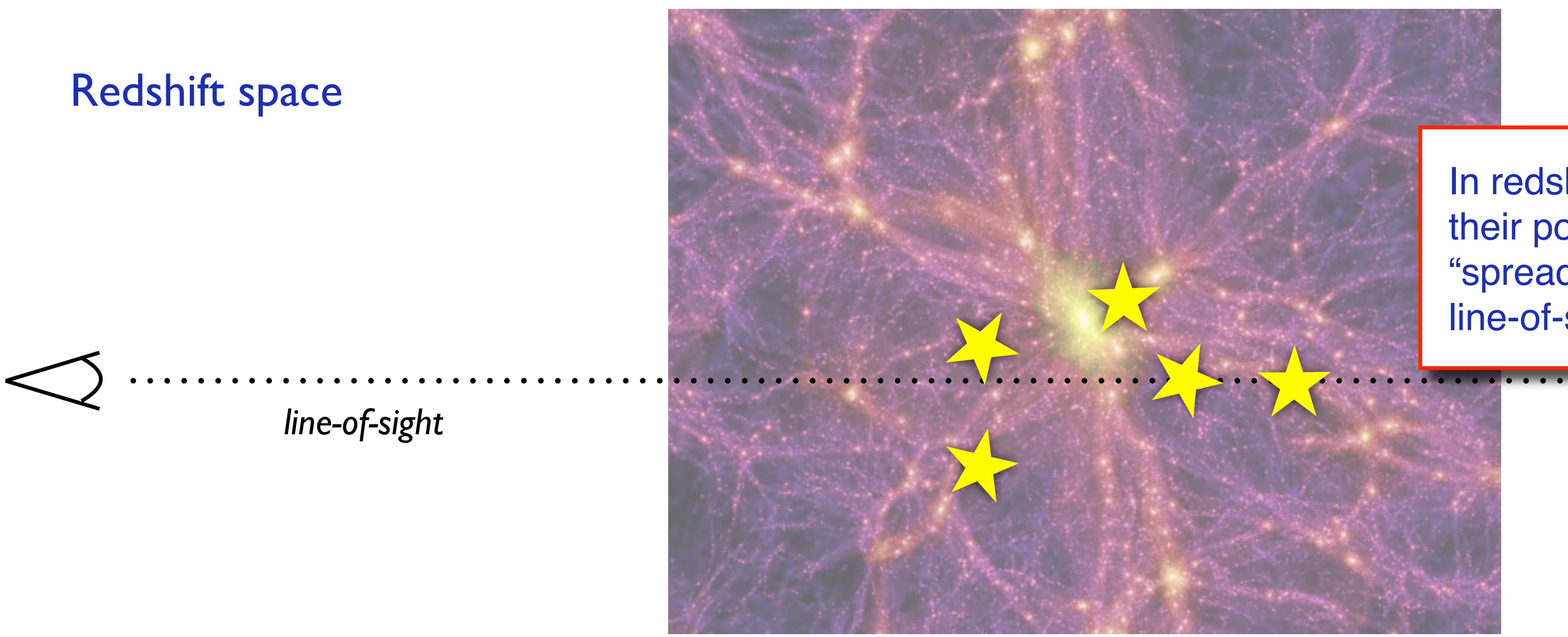

In redshift space their positions are “spread” along the line-of-sight

Finger-of-God modelling

Several phenomenological model have been proposed over the years

$$P_s(k,\mu) = D[k\mu f\sigma_v] P_{\text{Kaiser}}(k,\mu) \qquad D_{\text{FoG}}[x] = \begin{cases} \exp(-x^2) & \text{Gaussian,} \\ 1/(1+x^2) & \text{Lorentzian} \end{cases}$$

1D velocity dispersion $\sigma_v^2 \equiv \frac{1}{6\pi^2}\int \mathrm{d}k\, P_{\rm L}(k)$

Peacock & Dodds (1996)
Scoccimarro (2004)
Taruya, Nishimichi & Saito (2010)

A recent proposal:

$$D_{\text{FoG}} = \frac{1}{\sqrt{1-\lambda^2 a_{\text{vir}}^2}} \exp\left(\frac{\lambda^2\sigma_v^2}{1-\lambda^2 a_{\text{vir}}^2}\right)$$

Sanchez *et al.* (2017)

a_{vir} free parameter related to the kurtosis of the velocity distribution

Orthodox implementation of the EFTofLSS prescription describe FoG with counterterms

$$P_0^{\text{ctr}} = -2\, c_0^2\, k^2\, P_L(k)$$ monopole

$$P_2^{\text{ctr}} = -\frac{4}{3}\, f\, c_2^2\, k^2\, P_L(k)$$ quadrupole

+ next-to-leading order $$P^{\nabla_z^4 \delta ctr} = -c(\mu k f)^4 (b_1 + f\,\mu)^2\, P_L(k)$$

Maybe on FoG there is still some possible improvement …

Stochastic Contributions

(almost there now)

Shot-noise in power spectrum measurements

Our original observable is the galaxy catalog.
A simple expression for galaxy number density can be

$$n_g(\vec{x}) = \sum_{i=1}^{N_g} \delta_D(\vec{x} - \vec{x}_i) \qquad \delta_g(\vec{k}) = \frac{1}{\bar{n}_g} \int \frac{d^3x}{(2\pi)^3} e^{-i\vec{k}\cdot\vec{x}} n_g(\vec{x}) = \frac{1}{\bar{n}_g} \sum_i^{N_g} e^{-i\vec{k}\cdot\vec{x}_i}$$

(here $k \neq 0$)

A simple estimator for the power spectrum can be

$$\hat{P}(k) = \frac{(2\pi)^3}{V} \frac{1}{N_k} \sum_{\vec{q}\in k} \delta(\vec{q})\delta(-\vec{q})$$

where

$$N_k = \sum_{\vec{q}\in k}$$

is the number of modes $\vec{q}$ in a shell of radius k

For our catalog we have

$$\hat{P}(k) = \frac{(2\pi)^3}{V} \frac{1}{N_k} \sum_{\vec{q}\in k} \frac{1}{\bar{n}_g^2} \sum_{i,j} e^{-i\vec{k}\cdot(\vec{x}_i - \vec{x}_j)}$$

$$\sum_{i,j} = \sum_{i\neq j} + \sum_{i=j}$$

→

$$\boxed{\hat{P}(k) \supset \frac{(2\pi)^3}{V} \frac{1}{N_k} \sum_{\vec{q}\in k} \frac{1}{\bar{n}_g^2} \sum_{i=j} = \frac{(2\pi)^3}{\bar{n}_g}}$$

shot-noise contribution

Shot-noise: 2 considerations

1. The signal we are after is often limited by shot-noise at small scale

In current spectroscopic surveys this is by design: we need for the sufficient density to detect BAOs (measuring spectra is expensive)

2. The Poisson $1/\bar{n}_g$ value is only expected in the large k limit

At small k we expect corrections to to halo exclusion and nonlinear clustering

Hence: *more free parameters*

$$\frac{1}{\bar{n}_g} \to N_0 + N_2\, k^2 + \ldots$$

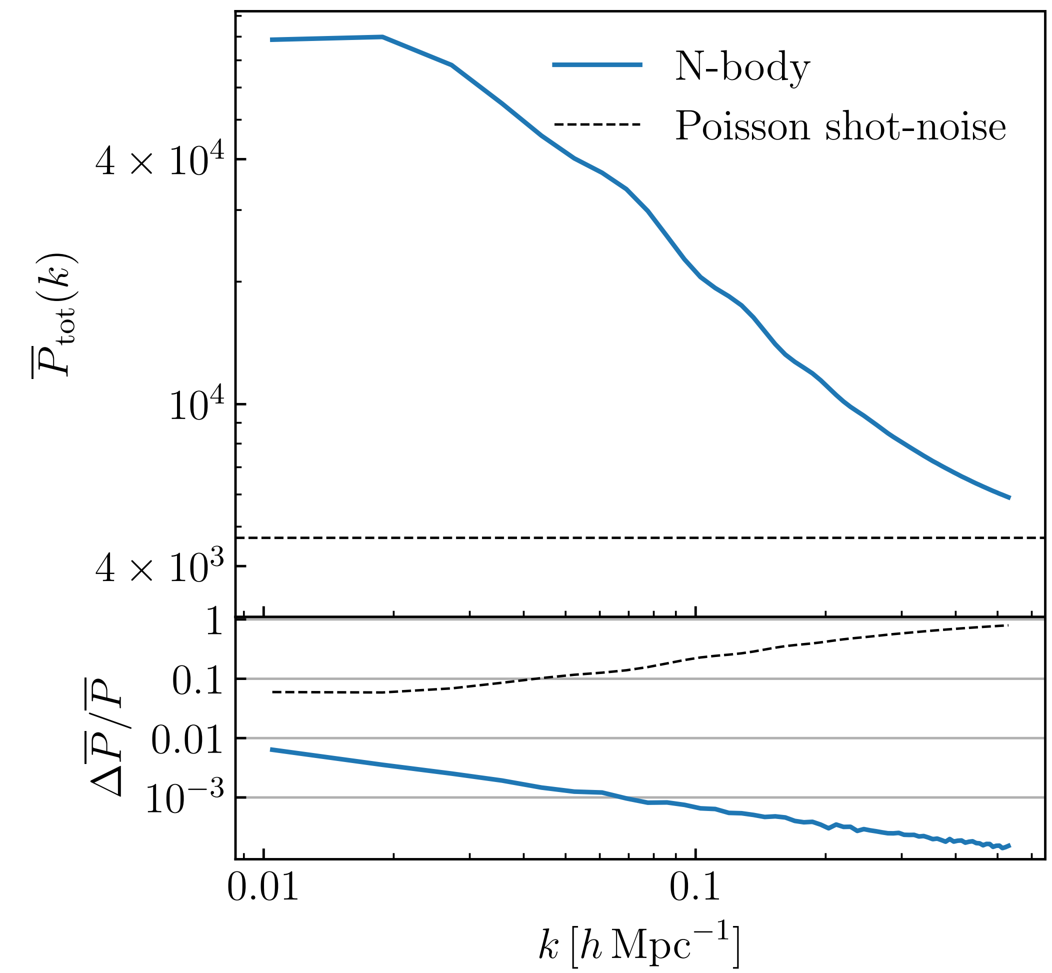

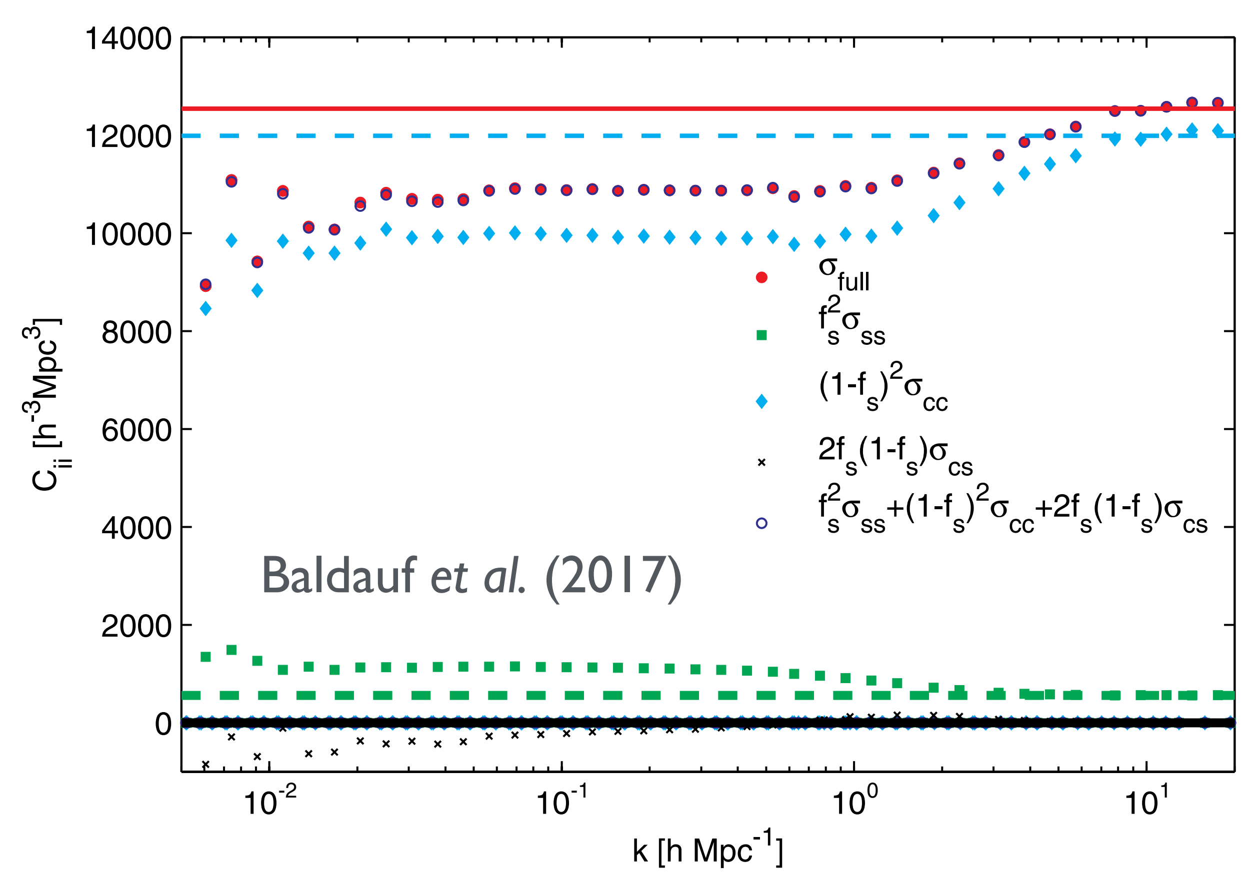

To Sum Up

(for real now)

PT Blind Challenge on 600 Gpc^3/h^3-volume simulations

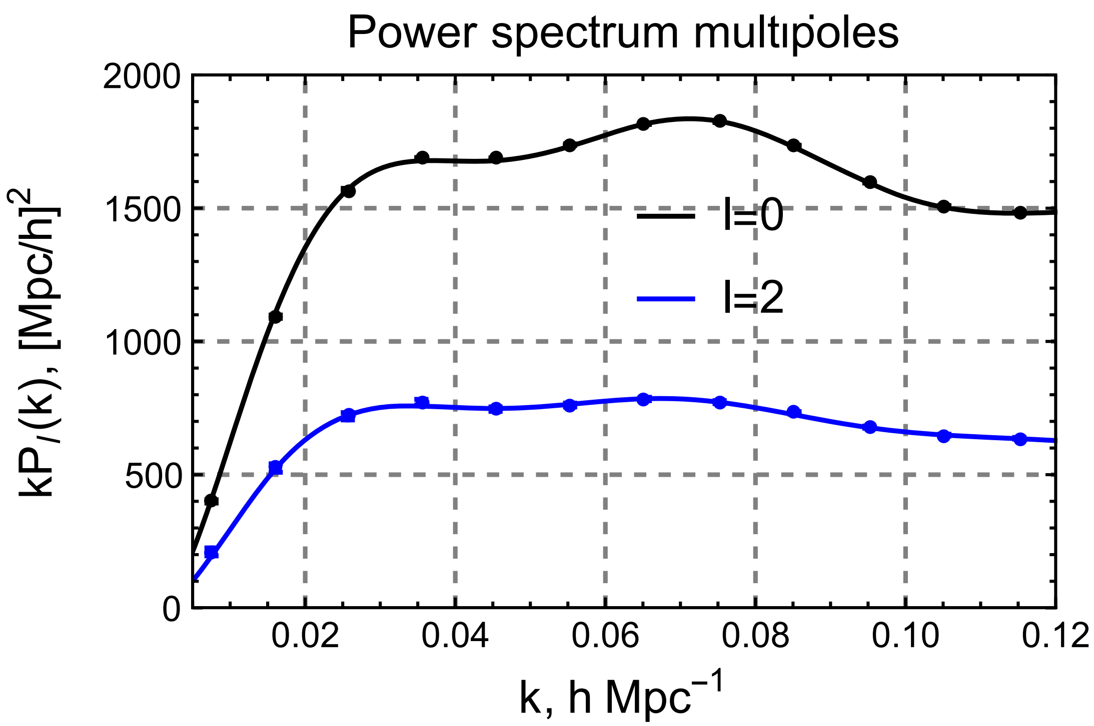

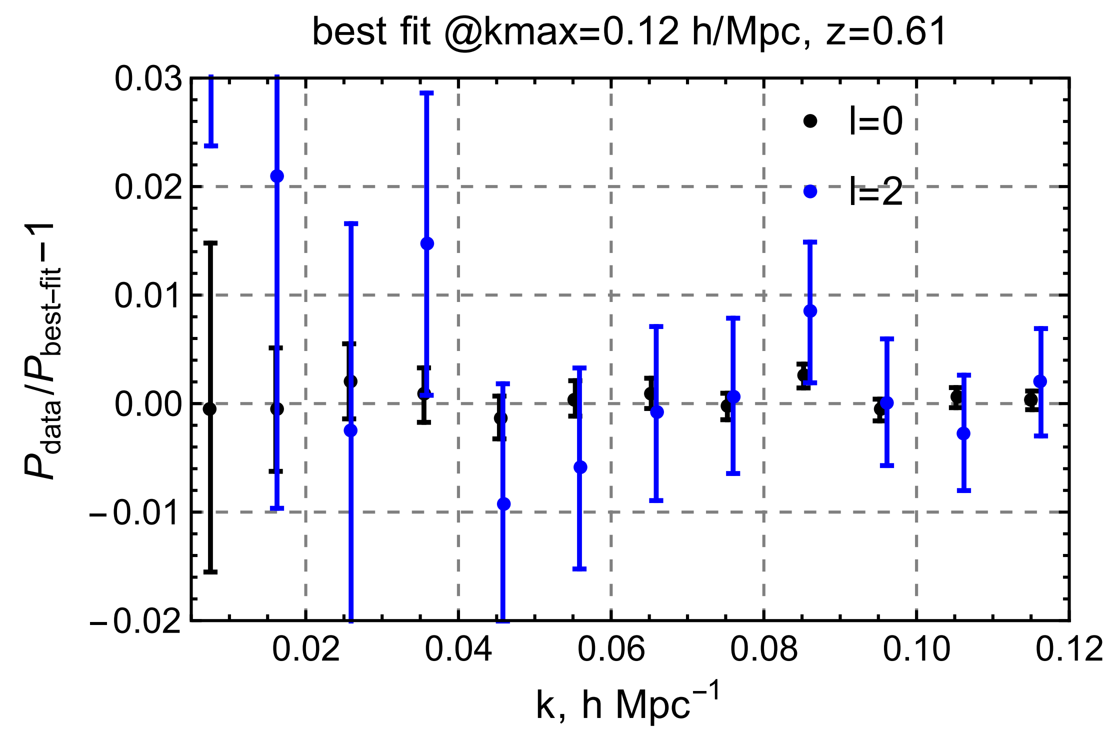

$$P_g(k,\mu) = Z_1(\mu)^2 P_{11}(k)$$ linear Kaiser effect

$$+2\int \frac{d^3q}{(2\pi)^3} Z_2(\boldsymbol{q},\boldsymbol{k}-\boldsymbol{q},\mu)^2 P_{11}(|\boldsymbol{k}-\boldsymbol{q}|)P_{11}(q)$$ P_{22} one-loop correction (matter, bias, RSDs)

$$+6Z_1(\mu)P_{11}(k)\int \frac{d^3q}{(2\pi)^3} Z_3(\boldsymbol{q},-\boldsymbol{q},\boldsymbol{k},\mu)P_{11}(q)$$ P_{13} one-loop correction (matter, bias, RSDs)

$$+2Z_1(\mu)P_{11}(k)\left(c_{\rm ct}\frac{k^2}{k_{\rm M}^2} + c_{r,1}\mu^2\frac{k^2}{k_{\rm M}^2} + c_{r,2}\mu^4\frac{k^2}{k_{\rm M}^2}\right)$$ one-loop counterterms (matter, bias, RSDs)

$$+\frac{1}{\bar{n}_g}\left(c_{\epsilon,1} + c_{\epsilon,2}\frac{k^2}{k_{\rm M}^2} + c_{\epsilon,3} f\mu^2\frac{k^2}{k_{\rm M}^2}\right).$$ shot-noise

Nishimichi *et al* (2006)

PT Blind Challenge on 600 Gpc^3/h^3-volume simulations

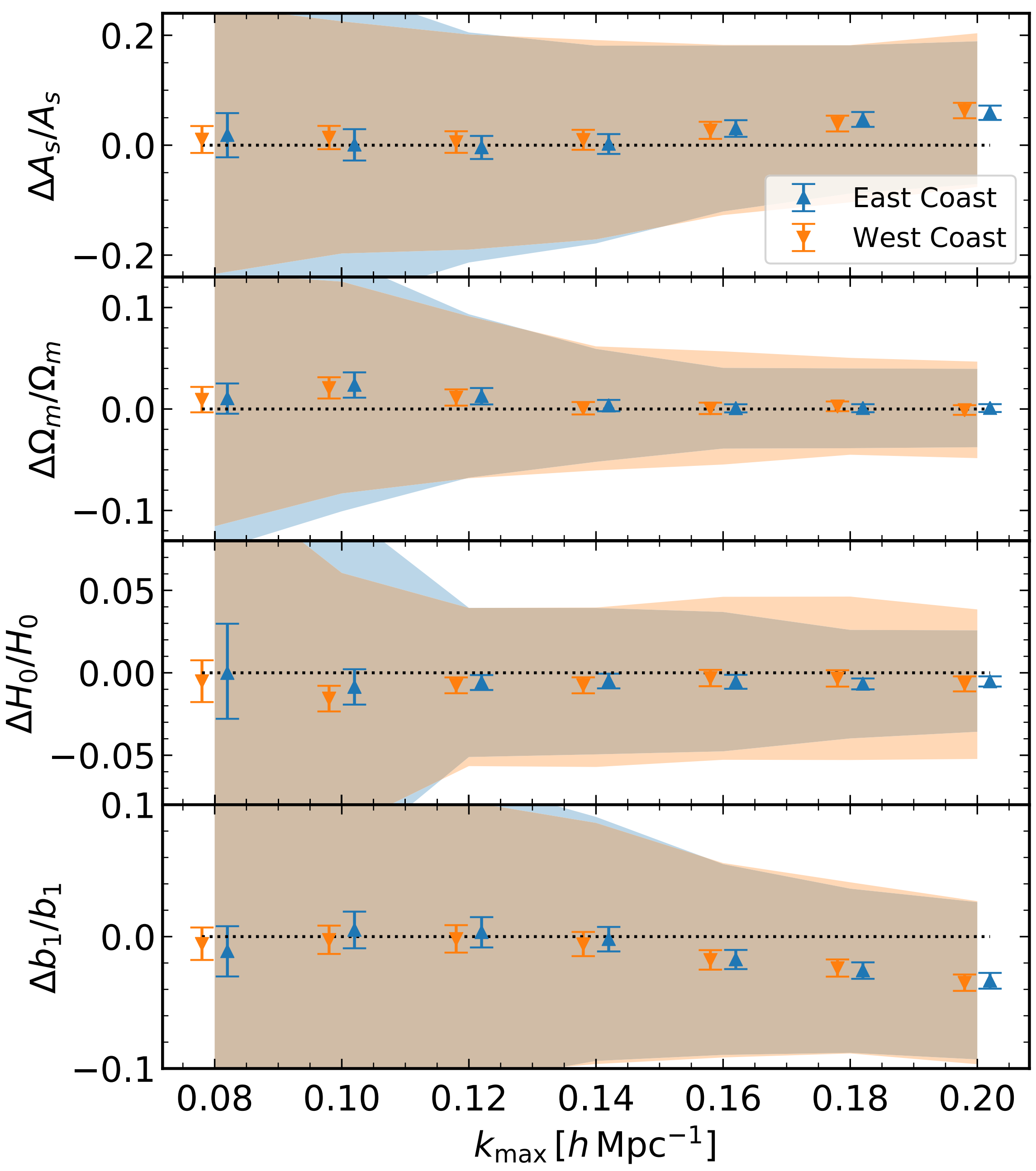

Recovered cosmological parameters as a function of the largest k included

6 nuisance parameters for the East Coast team

8 for the West Coast team

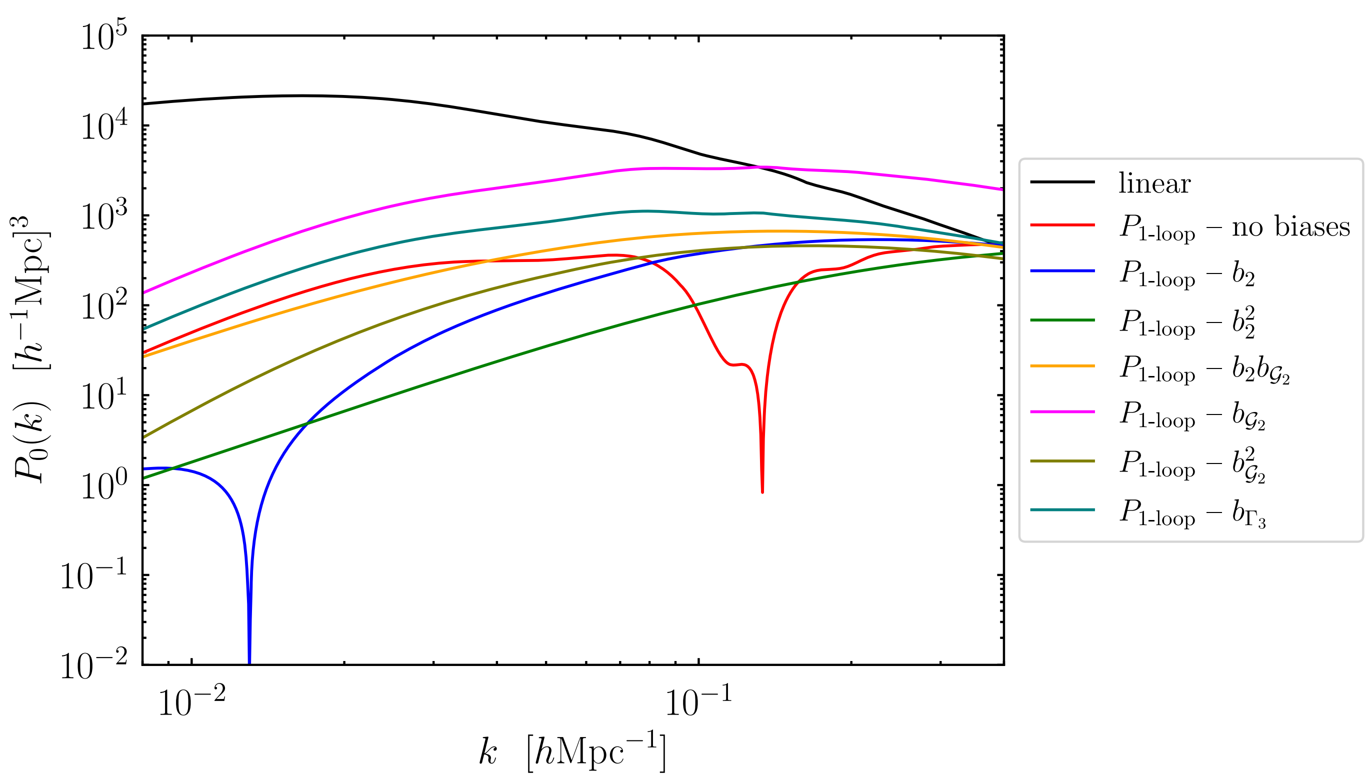

Nishimichi *et al* (2006)

Cabass *et al.* (2022)

All these free bias parameters?

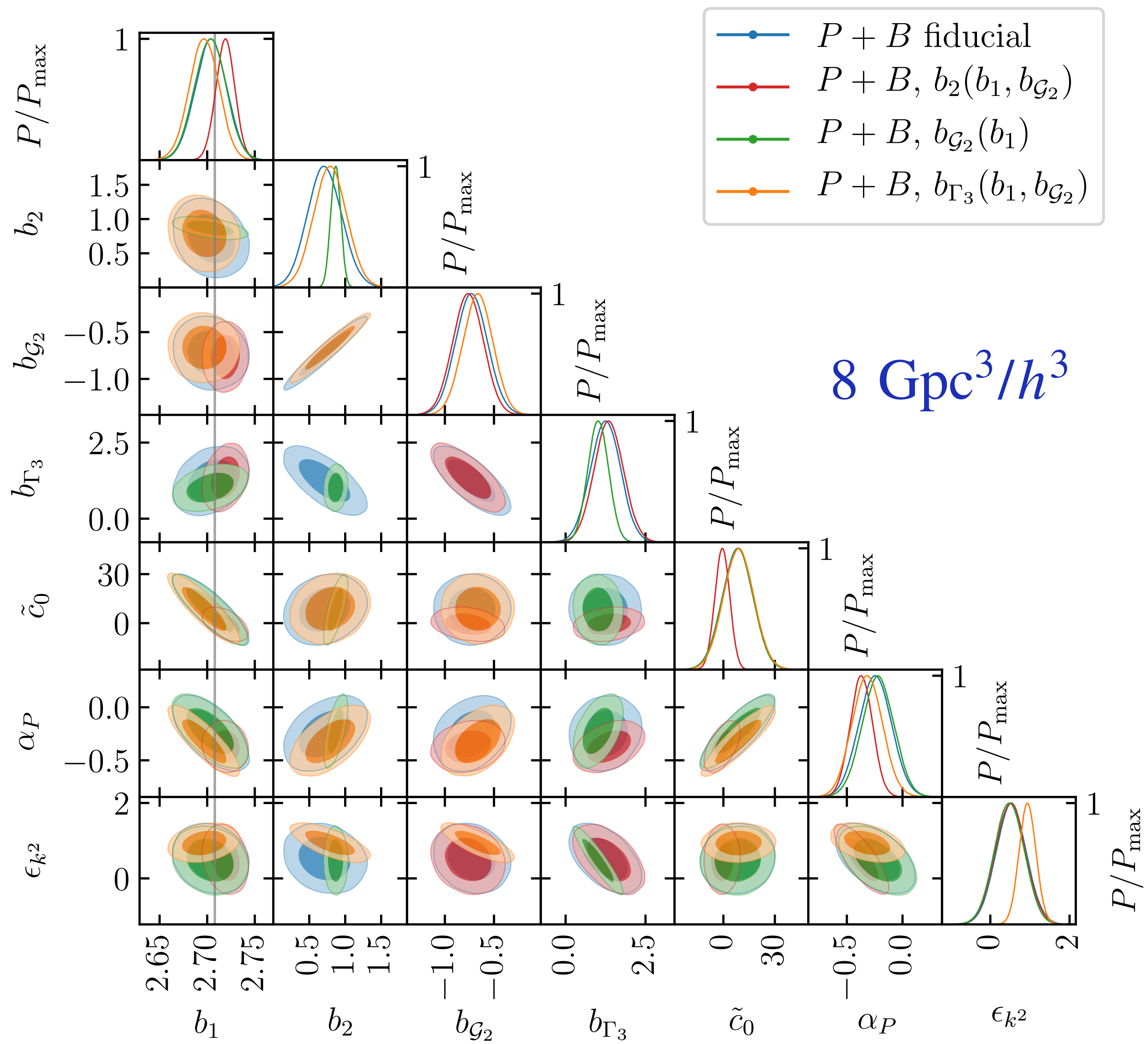

Oddo *et al* (2021)

We can introduce relations among bias parameters from simulations or the Halo Model

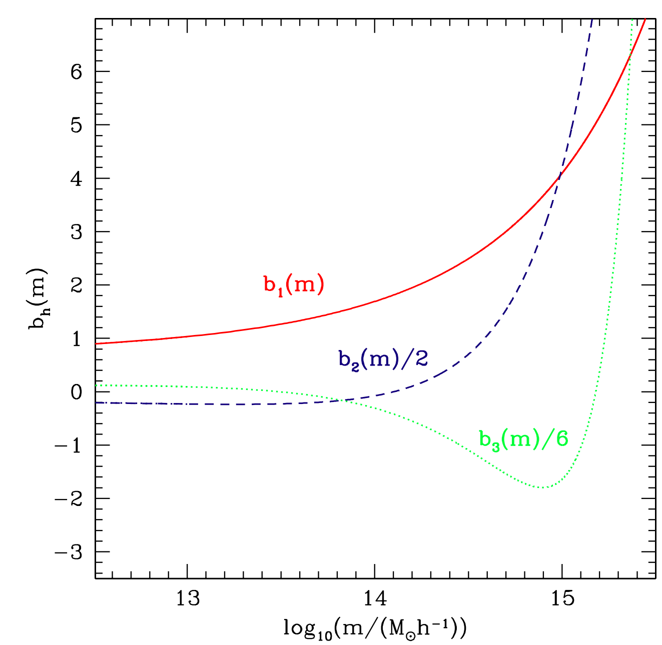

$$b_i = \frac{1}{\bar{n}_g} \int dm n(m) b_i(m) \langle N_{\rm gal}(m) \rangle,$$

The gain is not great on cosmological parameters

All these free bias parameters?

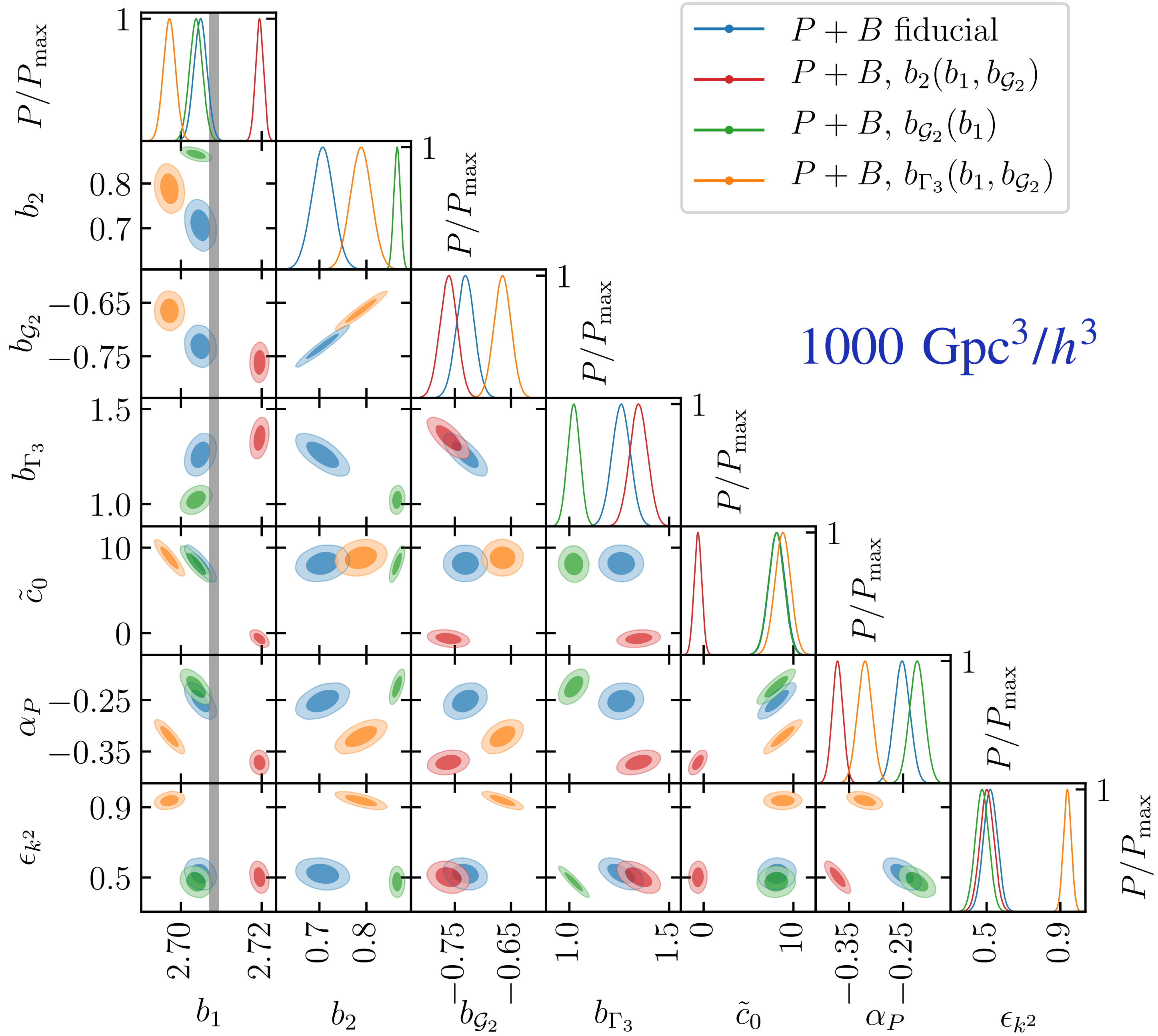

Oddo *et al* (2021)

And we must avoid to introduce systematics

We can introduce relations among bias parameters from simulations or the Halo Model

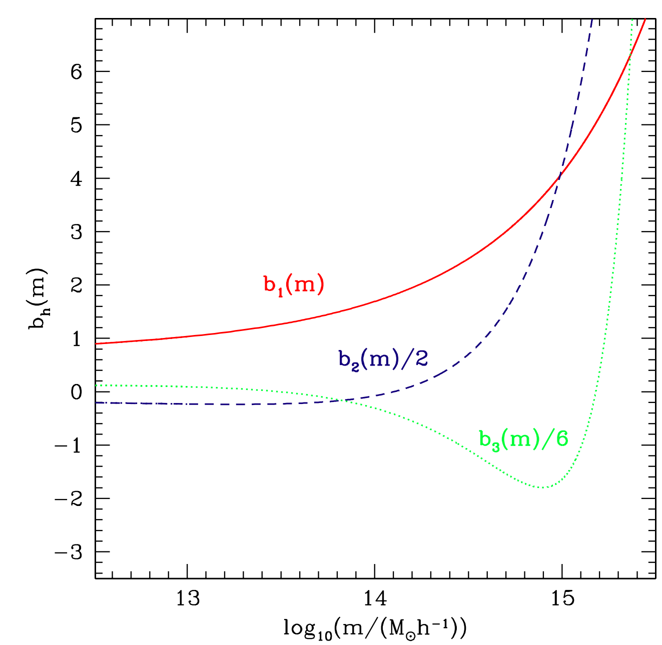

$$b_i = \frac{1}{\bar{n}_g} \int dm n(m) b_i(m) \langle N_{\rm gal}(m) \rangle,$$

The gain is not great on cosmological parameters

Higher-order Statistics

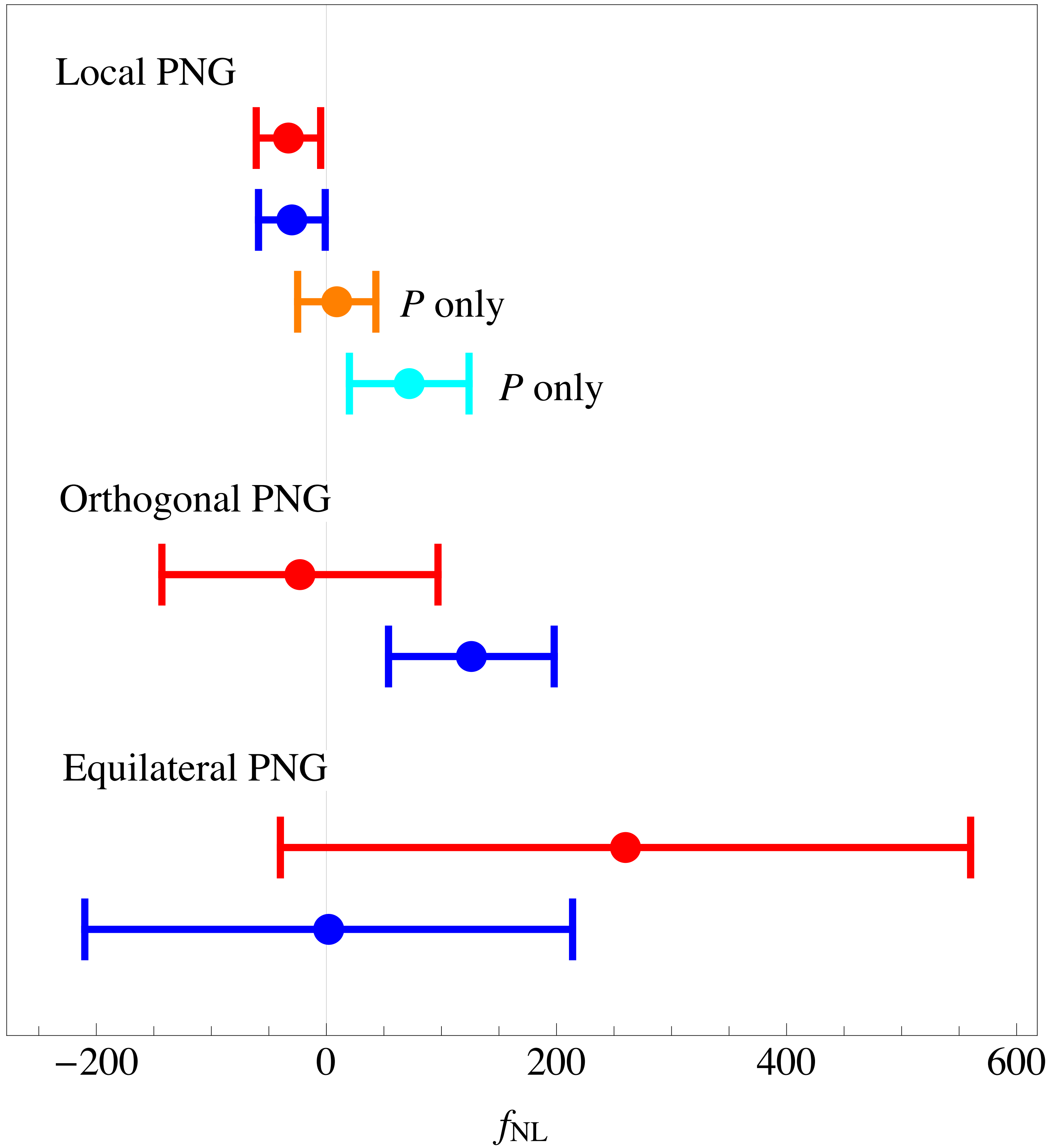

Recent constraints on Primordial non-Gaussianity from the joint analysis of **power spectrum and bispectrum**

D'Amico *et al.* (2022)
Cabass *et al.* (2022A, 2022B)

Some general and personal considerations

The EFTofLSS (and some common sense) provided a fairly complete parametrisation of our ignorance on the galaxy power spectrum modelling, at least under a strictly theoretical point of view

The model is implemented now efficiently (FFTlog) and we have several emulators

We know more, on bias at least, from the Halo Model, or simulations … but with some systematic uncertainty that could be a limiting factor, sooner or later

More can be done for higher-order statistics, at the level of estimators, modelling & emulators

Full-shape analysis of BOSS data

Combining Full-Shape with BAOs (reconstructed)

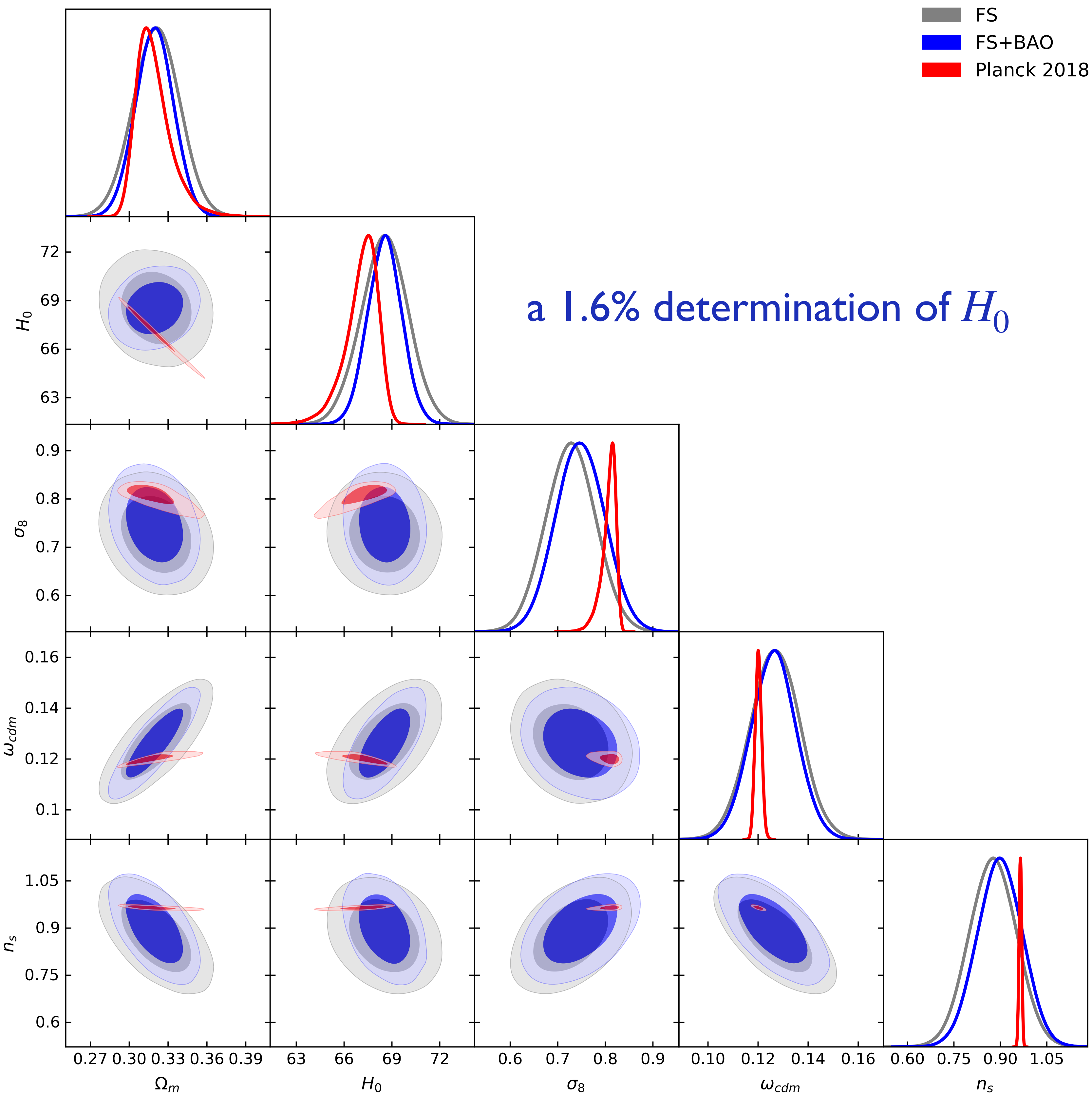

a 1.6% determination of H_0

Philcox *et al.* (2020)

Similar results from D'Amico *et al.* (2020)

BOSS + eBOSS

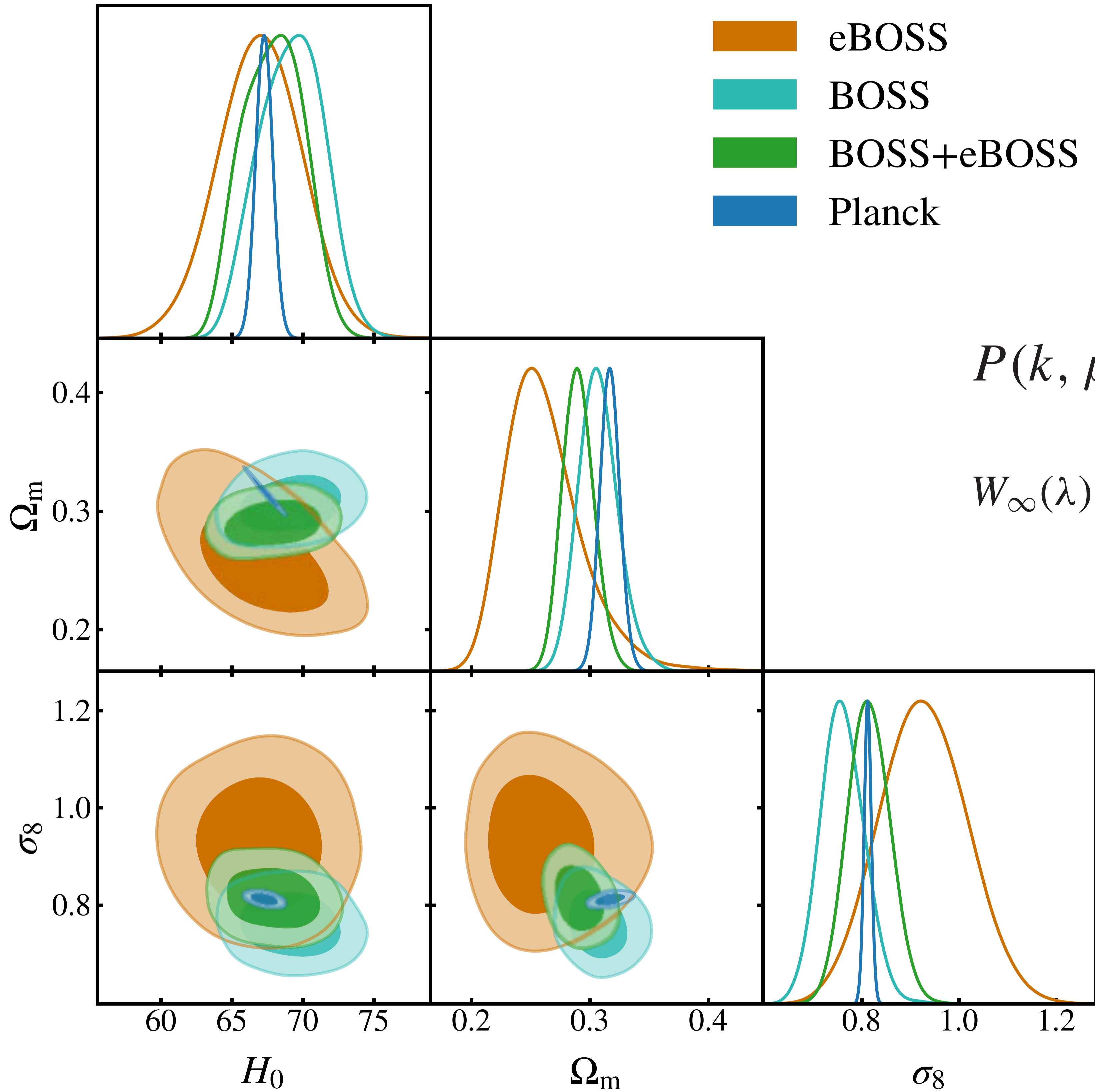

$$P(k,\mu) = W_\infty(ifk\mu)\,P_{\rm novir}(k,\mu)$$

$$W_\infty(\lambda) = \frac{1}{\sqrt{1-\lambda^2 a_{\rm vir}^2}} \exp\left(\frac{\lambda^2\sigma_v^2}{1-\lambda^2 a_{\rm vir}^2}\right)$$

Semenaite *et al.* (2022)
BOSS + eBOSS data

Neutrinos

Neutrinos in the Universe

Neutrinos in the early Universe (at high temperature) are kept in equilibrium with other species by weak interactions

$$f_{\rm eq}(p) = \left[\exp\left(\frac{p}{T}\right) + 1\right]^{-1}$$

Fermi-Dirac distribution

They decouple when the temperature drops below $T \sim 1\,\mathrm{MeV}$

Therefore they decouple when ultra relativistic!

Two regimes:

- At **high redshift** they (mostly) contribute to the **radiation** energy density
- At **low redshift** they (mostly) contribute to the **matter** energy density

$$1 + z_{nr} \simeq 1890 \frac{m_{\nu,i}}{1\ \mathrm{eV}} \qquad \Omega_{\nu,0} h^2 = \frac{M_\nu}{93.14\,\mathrm{eV}}.$$

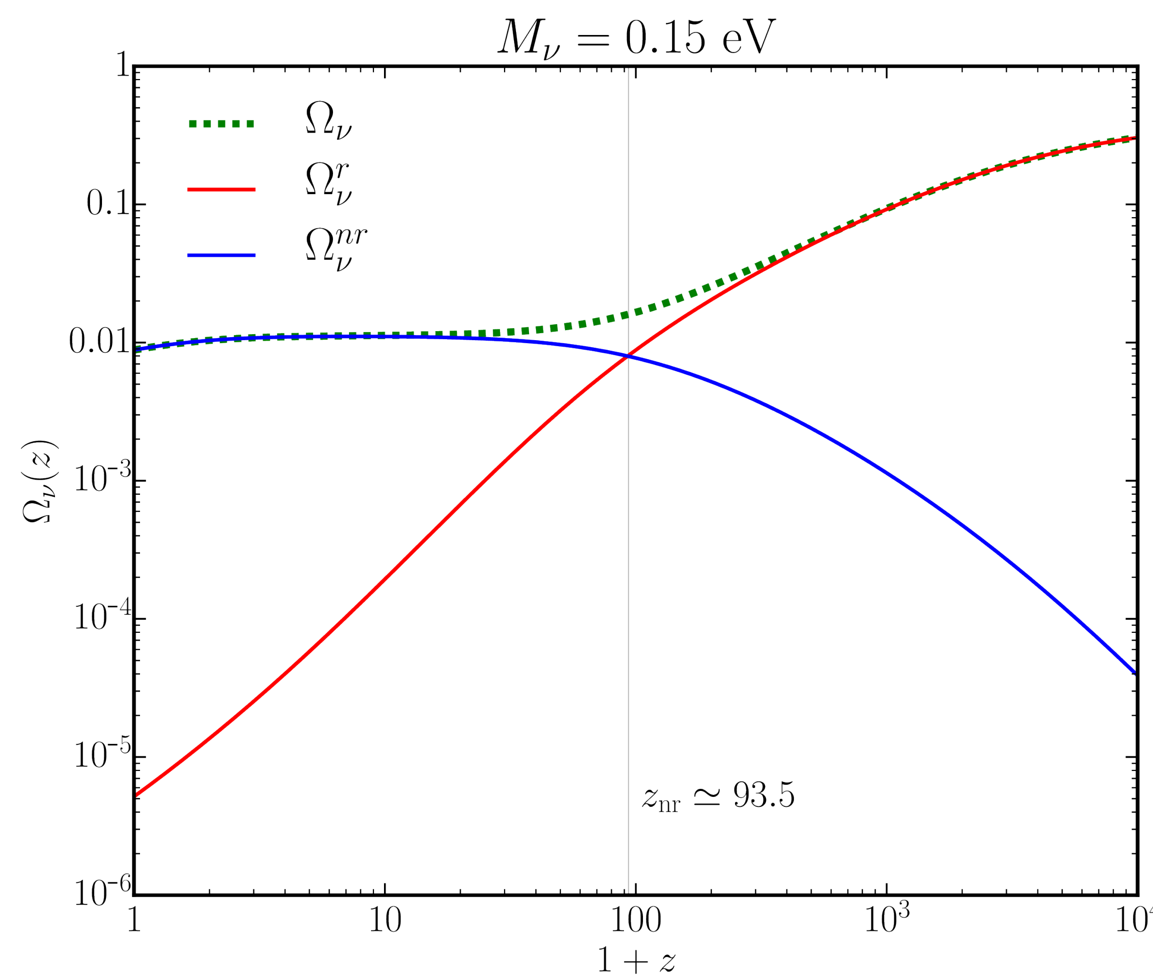

The free-streaming scale

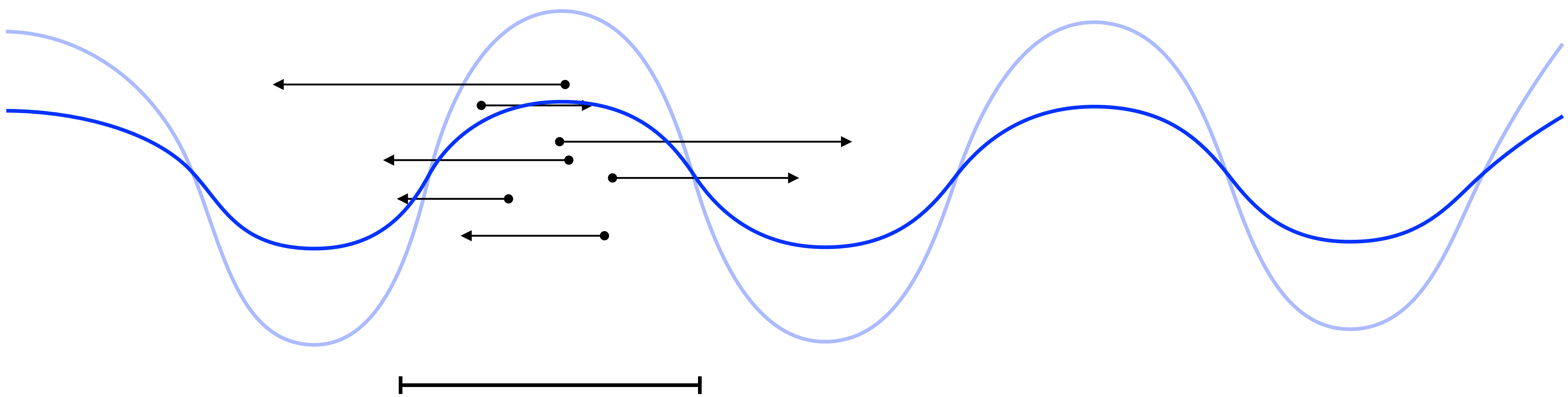

$$\lambda_{\rm FS} \sim 1/k_{\rm FS}$$

$$\sigma^2_{\nu,{\rm i}}(z) \;\equiv\; \frac{\int d^3p\; p^2/m^2_{\nu,{\rm i}}(\exp[p/T_\nu(z)]+1)^{-1}}{\int d^3p\;(\exp[p/T_\nu(z)]+1)^{-1}}$$

Velocity dispersion

$$k_{\rm FS,i} \sim \frac{aH(a)}{\sigma_{\nu,i}}$$

$$k_{\rm FS,i} \simeq \frac{0.677}{(1+z)^2}\left(\frac{m_{\nu,{\rm i}}}{1\ {\rm eV}}\right)\left[\Omega_m(1+z)^3+\Omega_\Lambda\right]^{\frac{1}{2}}\ h\ {\rm Mpc}^{-1}.$$

$$k_{\rm FS,i} \lesssim 0.1h{\rm Mpc}^{-1}$$

$$(m_{\nu,i} \lesssim 0.1eV)$$

the free-streaming scale is fairly large (almost linear scales) for viable values of the neutrino mass

The matter power spectrum

from Castorina *et al.* (2015)

The *total* matter overdensity

$$\delta_m = (1 - f_\nu)\,\delta_c + f_\nu\,\delta_\nu\,,$$

Neutrino fraction:

$$f_\nu \equiv \frac{\Omega_\nu}{\Omega_m} = \frac{\bar{\rho}_\nu}{\bar{\rho}_m}$$

The *total* matter power spectrum

$$P_{mm} = (1 - f_\nu)^2\,P_{cc} + 2 f_\nu\,(1 - f_\nu)\,P_{c\nu} + f_\nu^2\,P_{\nu\nu}$$

$$\frac{P_{mm}(k; f_\nu)}{P_{mm}(k; f_\nu = 0)} \simeq 1 - 8 f_\nu$$

the suppression of the power spectrum due to neutrinos is proportional to the (total) neutrino mass

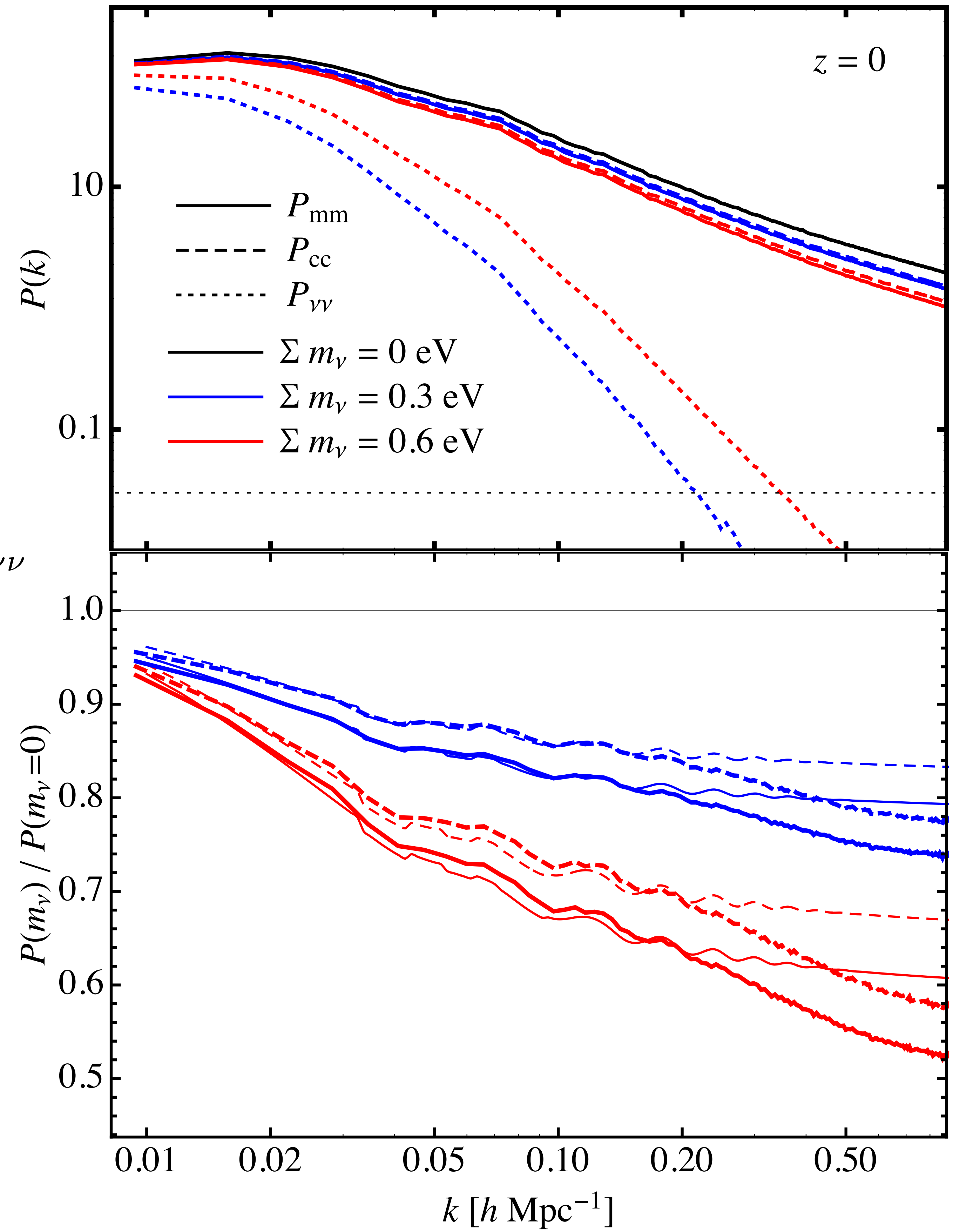

BOSS: DR12 consensus paper

95 per cent upper limit of 0.16 eV c^{-2} on the neutrino mass sum.

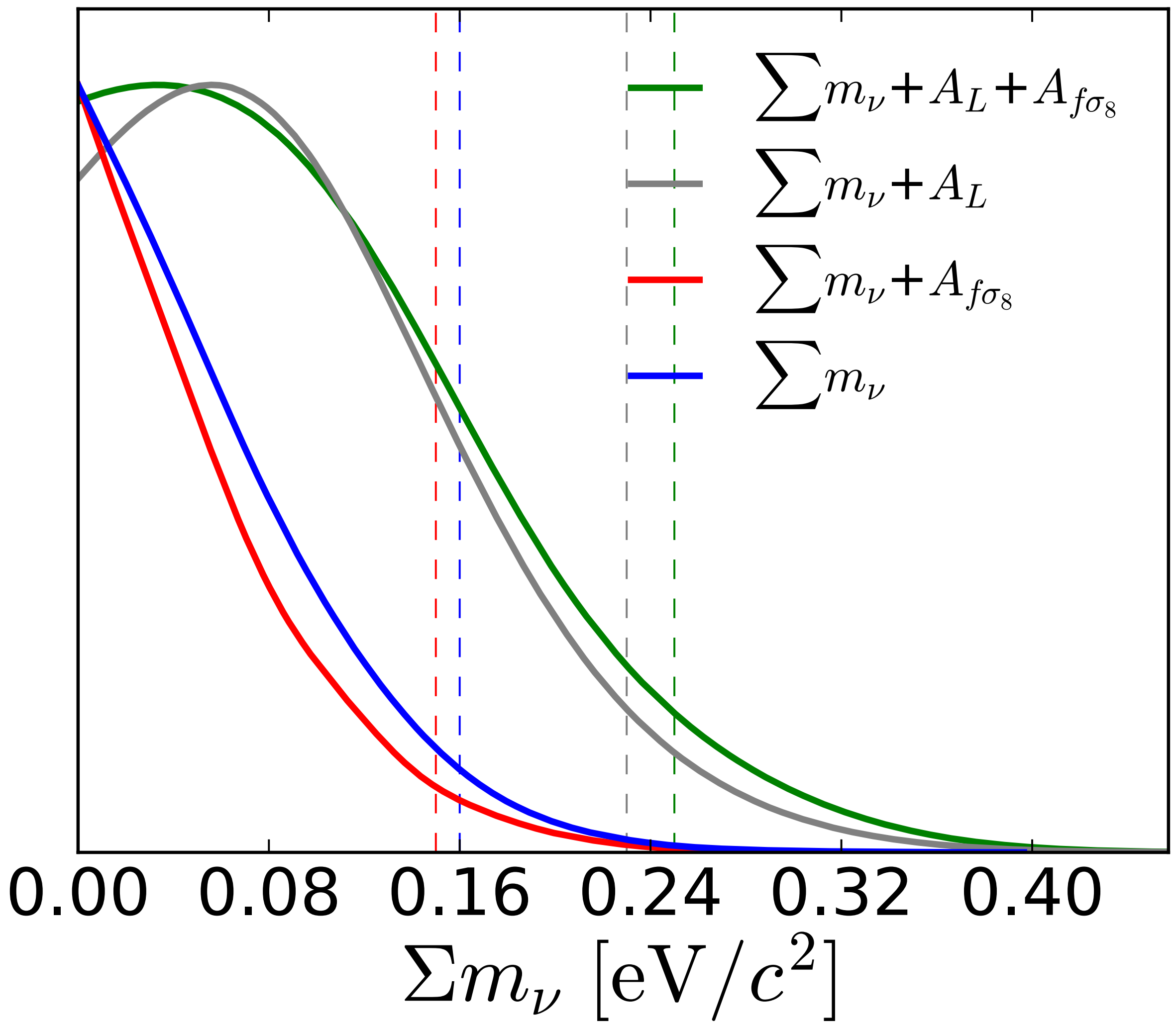

Figure 19. Posterior distribution for the sum of the mass of neutrinos in the ΛCDM cosmological model. The blue curve includes the growth measurement from the lensing impacts on the CMB power spectrum and from the BOSS RSD measurement of $f\sigma_8$. The green curve excludes both of these constraints; one still gets constraint on the neutrino mass from the impact on the distance scale. Red and grey curves relax one of the growth measurements at a time; showing that most of the extra information comes from the CMB lensing. The vertical dashed lines indicate the 95 per cent upper limits corresponding to each distribution.

Alam *et al.* (2021)
BOSS collab.

BOSS: Full-Shape + BAOs

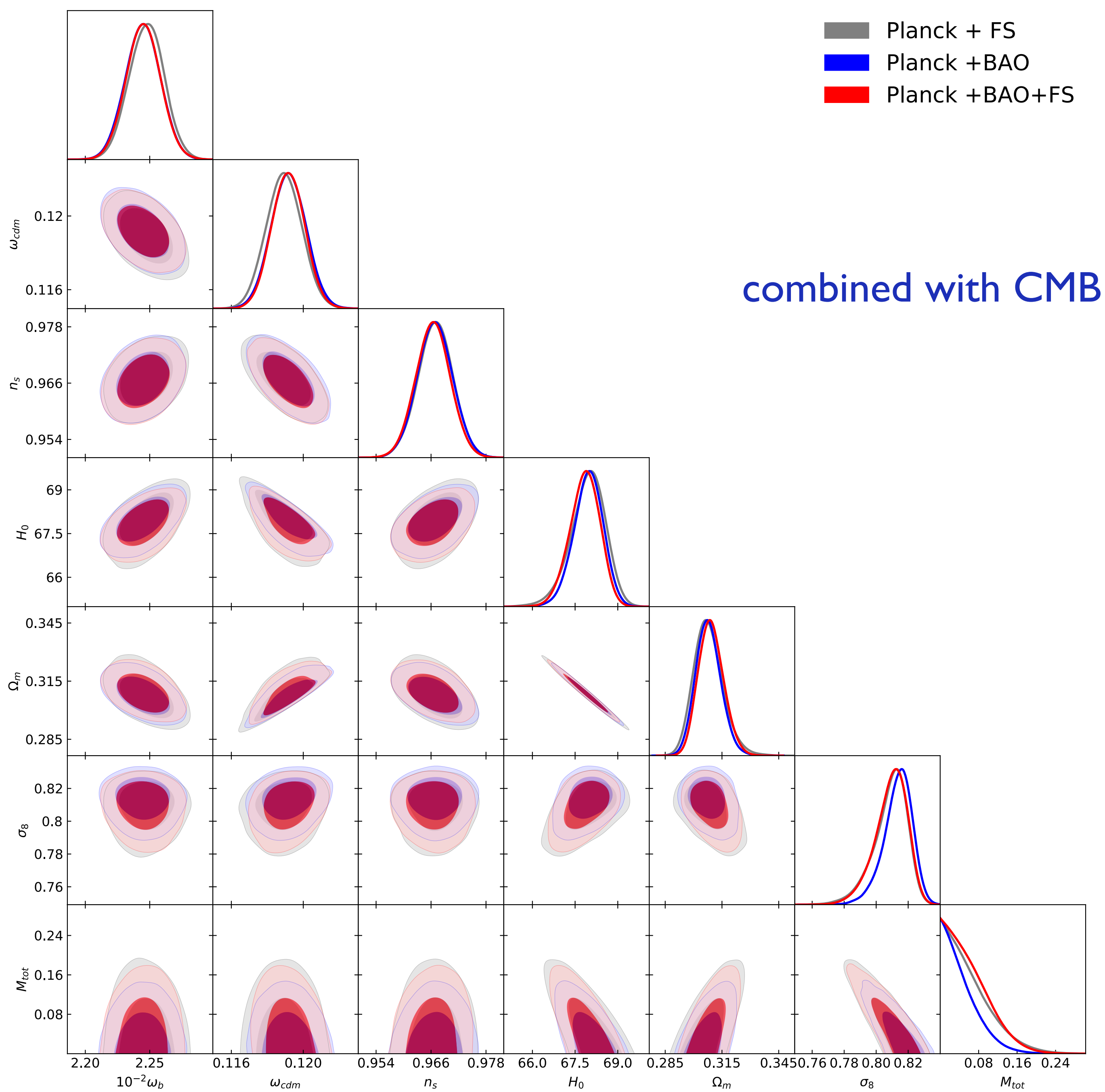

Figure 8. Marginalized one-dimensional posterior distribution and two-dimensional probability contours (at the 68% and 95% CL) for the parameters of the $\nu\Lambda$CDM model, including varied neutrino masses, as obtained from analyses of the Planck likelihood in combination with BAO and FS information from BOSS. $N_{\rm eff}$ is fixed to the standard model value 3.046 and we quote H_0 in $\rm km\,s^{-1}Mpc^{-1}$, with $M_{\rm tot}$ given in eV.

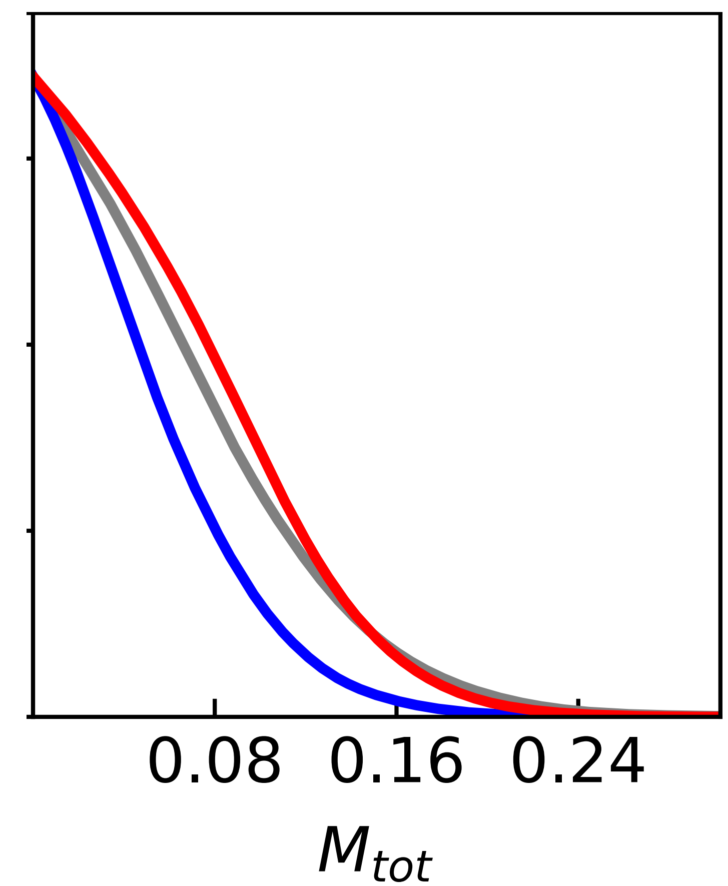

$$\sum m_\nu < 0.14\,\text{eV (at 95\% confidence)}$$

Philcox *et al.* (2022)
BOSS data

Non-Gaussianity &
Higher-Order Correlation Functions

The Model: galaxy bias (tree-level)

P at 1-loop, B tree-level
Halos
test on $1000\,h^{-3}\text{Gpc}^3$ of cumulative volume

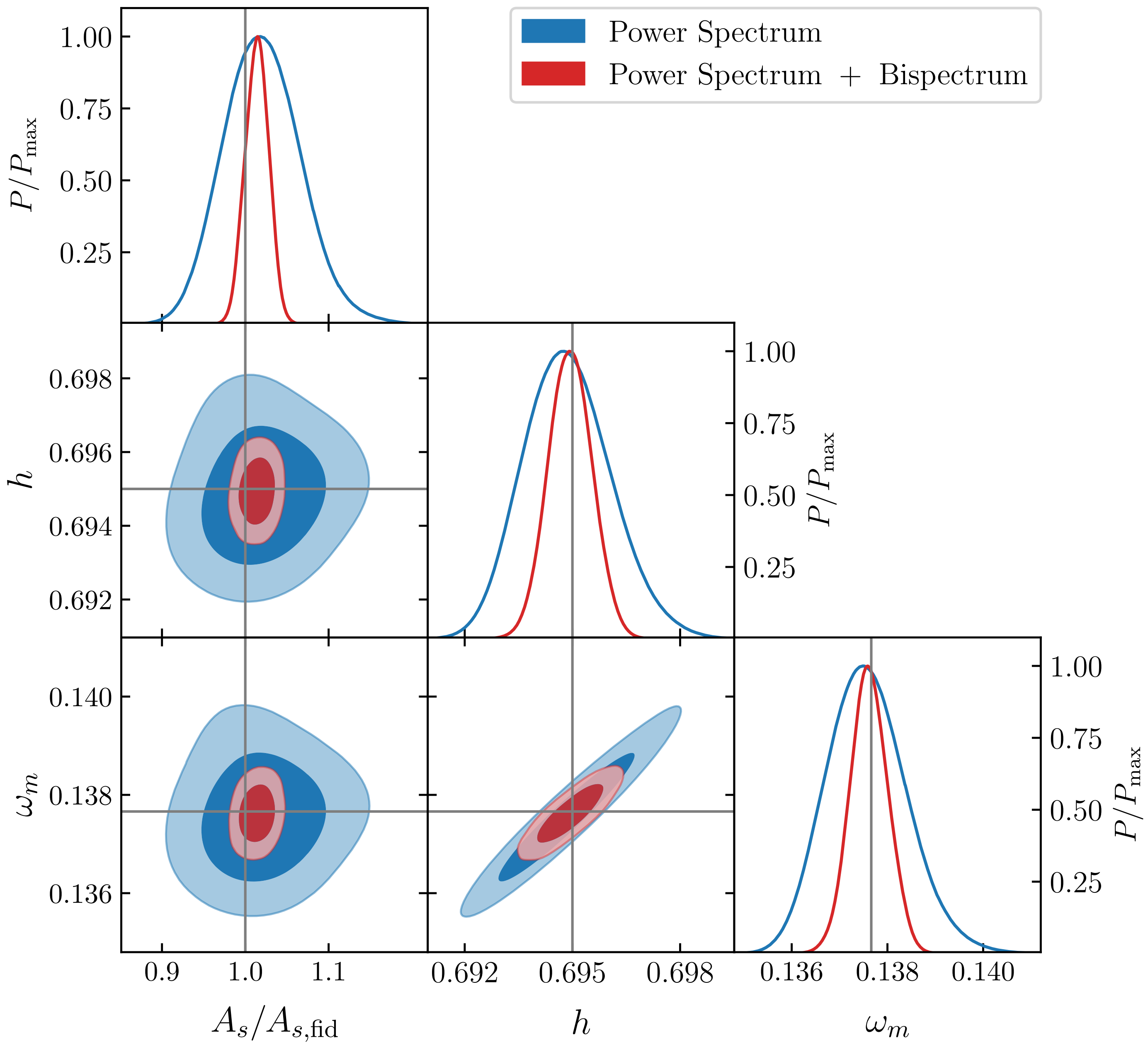

Oddo *et al.* (2021)

See also Ivanov *et al.* (2022)

The bispectrum is expected to reduce degeneracies in the power spectrum loop corrections

$$\delta_g(\boldsymbol{k}) = b_1\delta(\boldsymbol{k}) + \frac{b_2}{2}\delta^2(\boldsymbol{k}) + b_{\mathcal{G}_2}\mathcal{G}_2(\boldsymbol{k})$$

$$\downarrow$$

$$P_\ell(k) = P_\ell^{\rm tree}(k) + P_\ell^{\rm loop}(k) + P_\ell^{\rm ctr}(k)$$

Limited reach on such a large volume:
$k_{max}^B \simeq 0.09\,h\text{Mpc}^{-1}$
Significant improvement over *P*, *but in real space!*

The Model: galaxy bias at 1-loop

Test of 1-loop bispectrum
bias model in real space

HOD galaxies (CMASS, LOWZ)
& halos
$6\,\mathrm{Gpc}^3 h^{-3}$

8 parameters (tree-level B)
15 parameters (one-loop B)

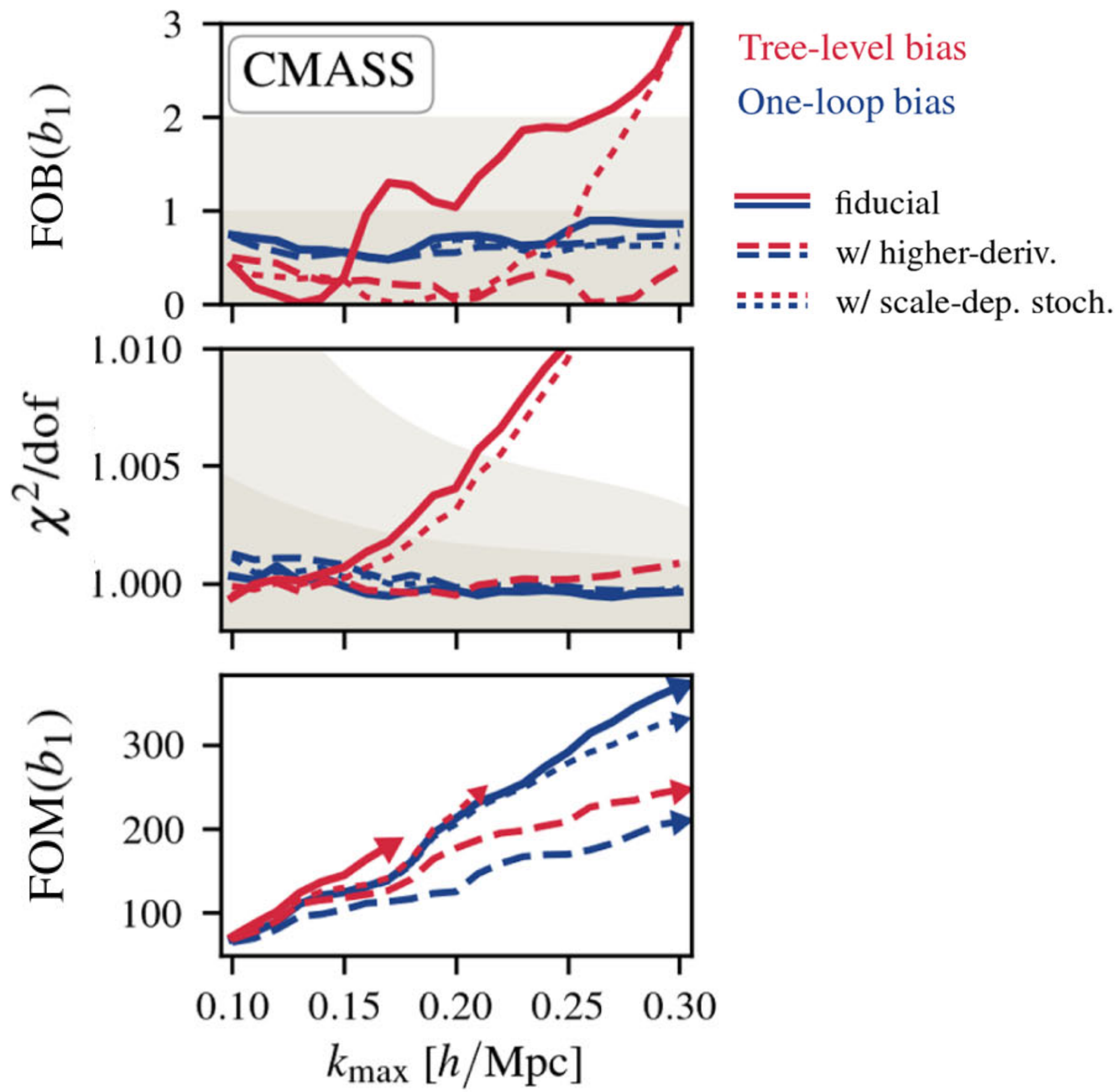

One-loop corrections greatly extend the reach of the model and its potential to constrain its parameters
(despite their larger number)

but, again, this is still real space ...

Eggemeier *et al.* (2021)

The Model: redshift-space

Galaxy density in redshift space:

$$\delta_s(\mathbf{k}) = Z_1(\mathbf{k})\delta_L(\mathbf{k}) + \int d^3q\, Z_2(\mathbf{q}, \mathbf{k}-\mathbf{q})\delta_L(\mathbf{q})\delta_L(\mathbf{k}-\mathbf{q}) + \ldots$$

$$Z_1(\mathbf{k}) = b_1 + f\,\mu^2$$

$$Z_2(\mathbf{k}_1, \mathbf{k}_2) = b_1 F_2(\mathbf{k}_1, \mathbf{k}_2) + f\mu^2 G_2(\mathbf{k}_1, \mathbf{k}_2) + \frac{f\mu k}{2}\left[\frac{\mu_1}{k_1}(b_1 + f\mu_2^2) + \frac{\mu_2}{k_2}(b_1 + f\mu_1^2)\right] + \frac{b_2}{2}$$

+ non-local bias ...

$$B_s(\mathbf{k}_1, \mathbf{k}_2, \mathbf{k}_3) = 2\, Z_1(\mathbf{k}_1)\, Z_1(\mathbf{k}_2)\, Z_2(\mathbf{k}_1, \mathbf{k}_2)\, P_L(k_1)\, P_L(k_2) + \text{perm}\,.$$

Redshift-space bispectrum

The Model: redshift-space (monopole)

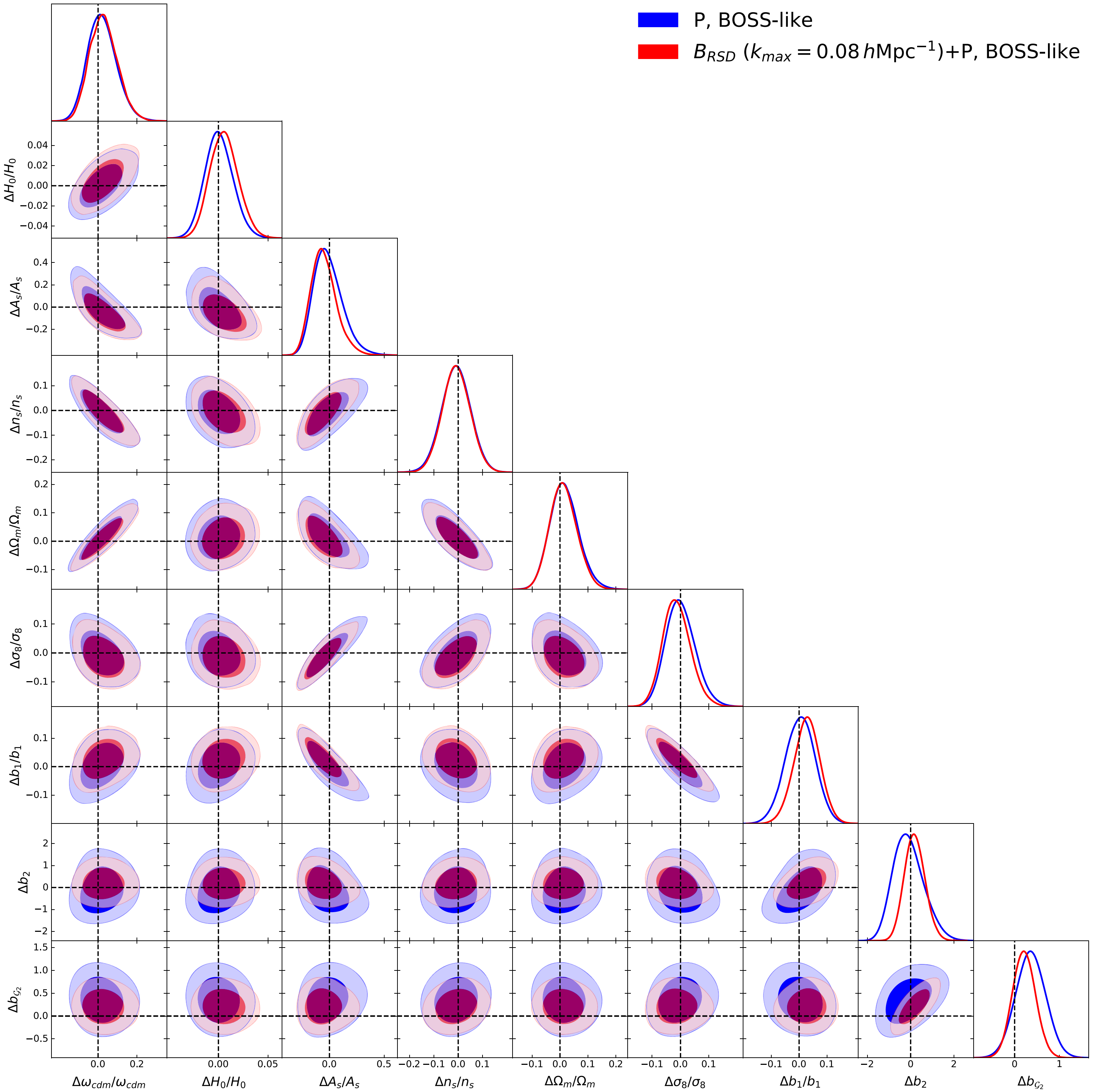

FIG. 7. Same as Fig. 5 but with the covariance rescaled by 100 to match the BOSS survey volume.

Test of tree-level bispectrum
in redshift space
EFTofLSS

BOSS-like HOD

Marginal (10%) improvement
on amplitude parameters (A_s, σ_8)
on BOSS-like volume

On full volume, $566\,h^{-3}\mathrm{Gpc}^3$:

$$\frac{\sigma_{\mathrm{P+B}}}{\sigma_{\mathrm{P}}}\{\omega_{\mathrm{cdm}}, h, n_s, A_s, \Omega_m, \sigma_8\}$$
$$= \{0.88, 0.94, 0.86, 0.95, 0.89, 0.96\},$$
$$\frac{\sigma_{\mathrm{P+B}}}{\sigma_{\mathrm{P}}}\{b_1, b_2, b_{\mathcal{G}_2}, P_{\mathrm{shot}}\}$$
$$= \{0.84, 0.18, 0.09, 0.65\}.$$

Ivanov *et al.* (2022)

Anisotropy: bispectrum multipoles

$$B_s(\mathbf{k}_1, \mathbf{k}_2, \mathbf{k}_3) = B_s(k_1, k_2, k_3, \theta_1, \phi_{12})$$

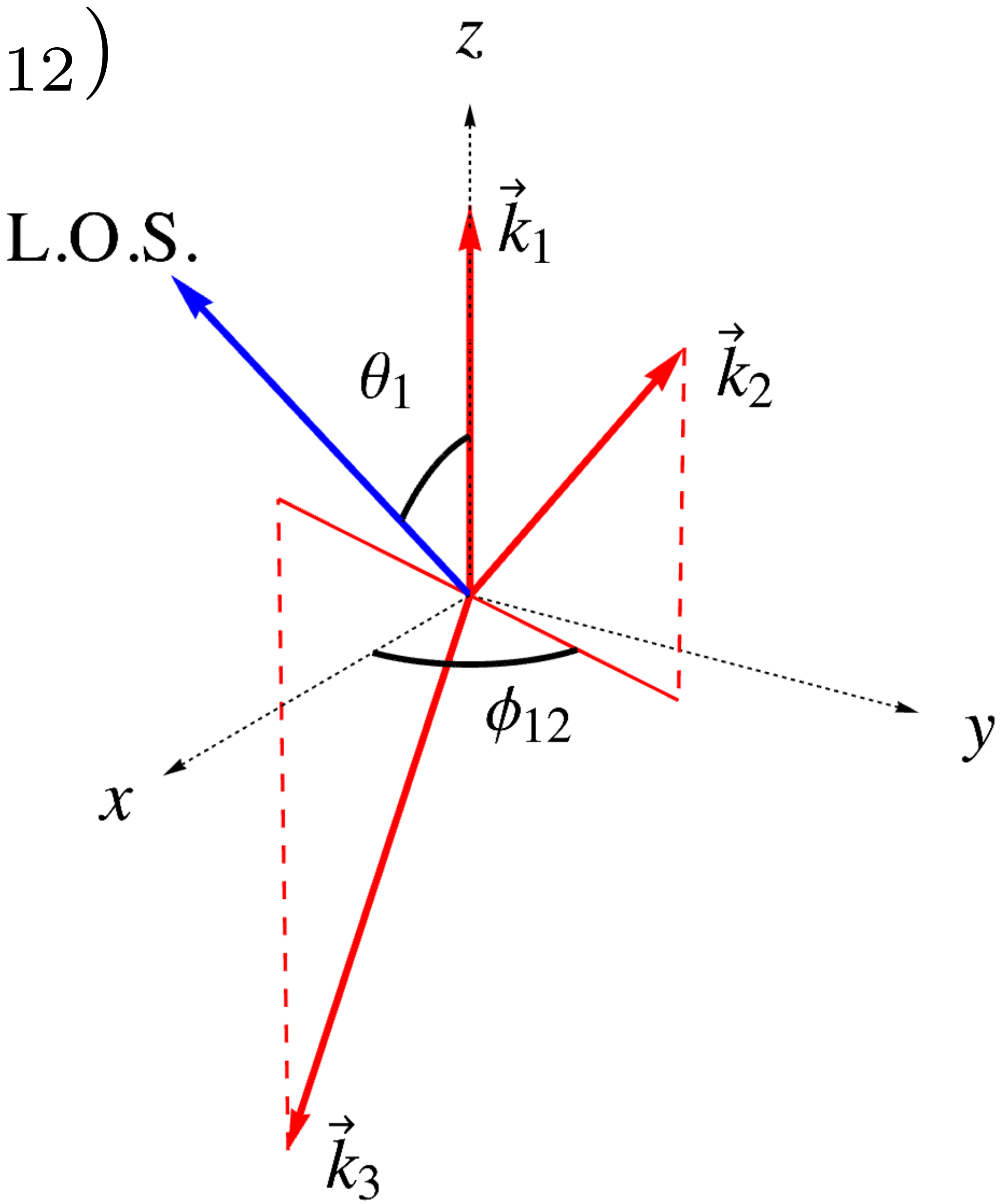

The orientation of the triangle w.r.t. the line-of-sight now matters

Different choices are possible
(see e.g. Hashimoto *et al.*, 2017, Gualdi & Verde, 2020)

We (OULE3) follow
Scoccimarro *et al.* (1999),
with the FFT-based estimator of
Scoccimarro, 2015.

$$B_s(k_1, k_2, k_3, \theta_1, \phi_{12}) = \sum_{\ell,m} B_{\ell,m}(k_1, k_2, k_3) Y_{\ell,m}(\theta_1, \phi_{12})$$

$$\mu_1 \equiv \mu \equiv \cos\theta_1$$

Anisotropy: bispectrum multipoles

Test of bispectrum multipoles

Halos
$1000\,h^{-3}\mathrm{Gpc}^3$ of cumulative volume
(300 Minerva sims
+ 10,0000 Pinocchio mocks for covariance)

bias parameters + f

Significant (but not surprising) improvement on the growth rate:

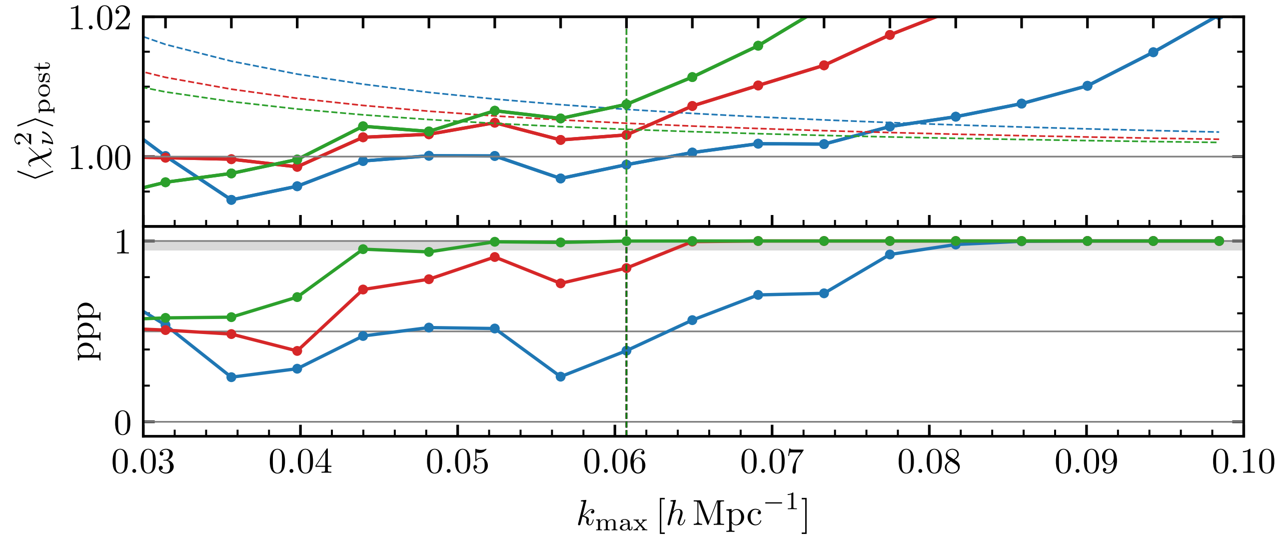

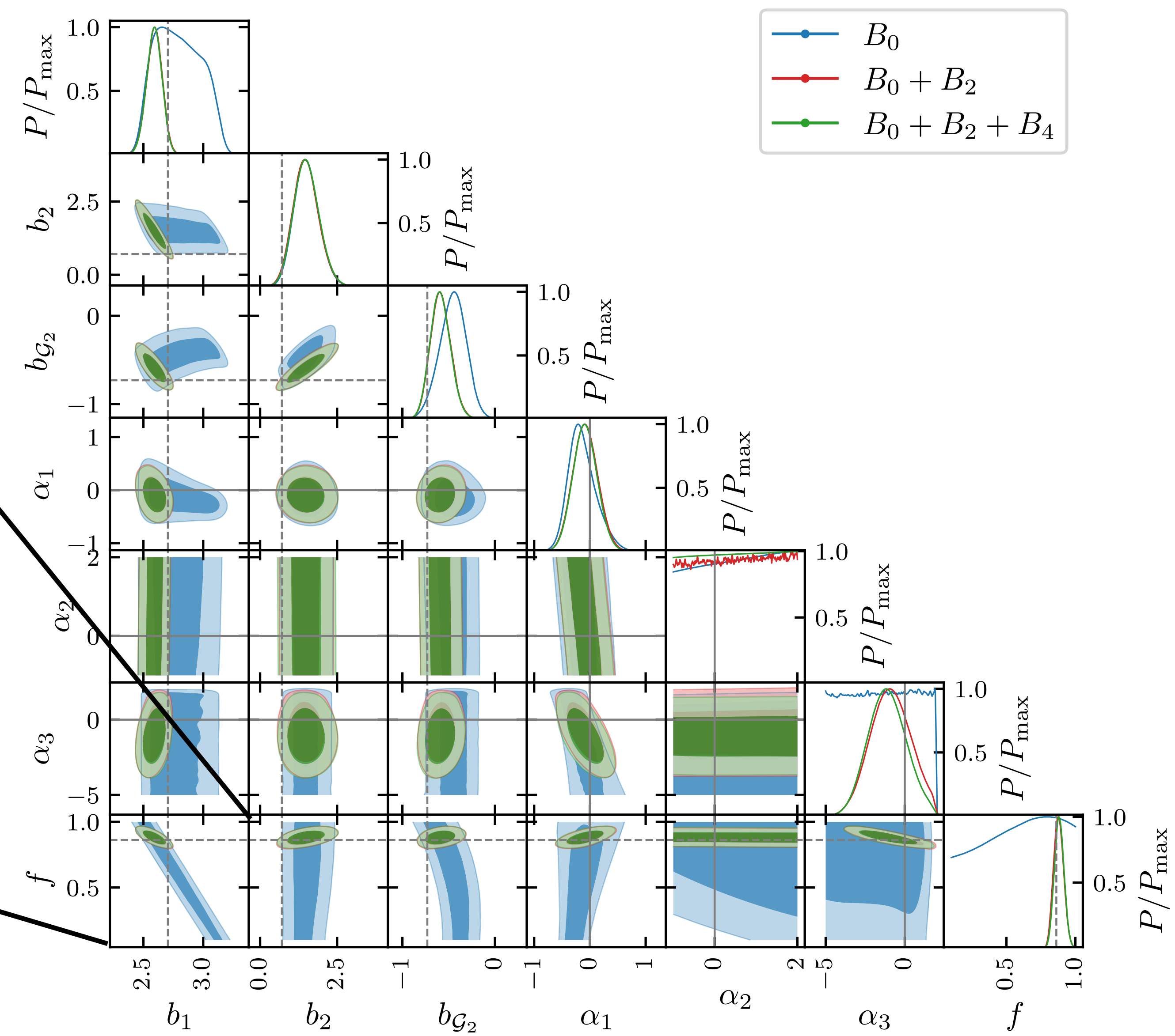

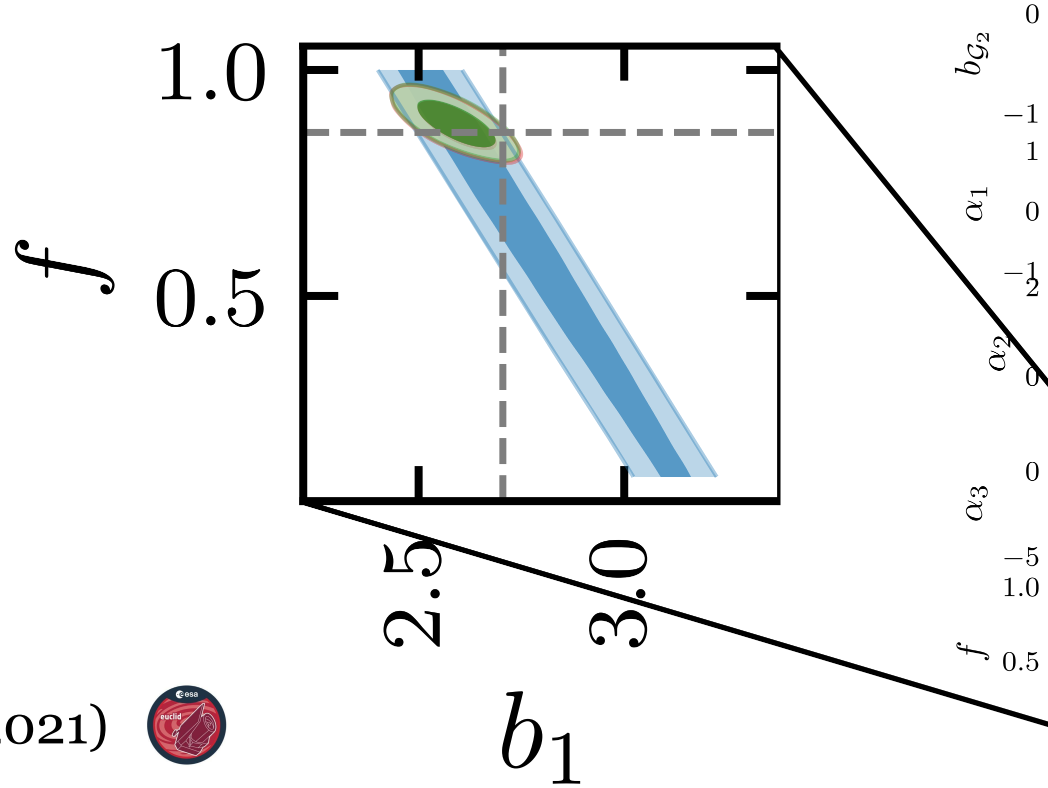

Rizzo *et al.* (2021)

See also Gualdi & Verde (2020), Gualdi *et al.* (2021), D'Amico et al. (2022)

Anisotropy: bispectrum multipoles

Test of the bispectrum model:
B_0 at 1-loop
B_2 tree-level

CMASS HOD mocks + window

Significant improvement adding B_0 at one-loop, much less adding B_2 tree-level
(but very limited number triangles in this case ...)

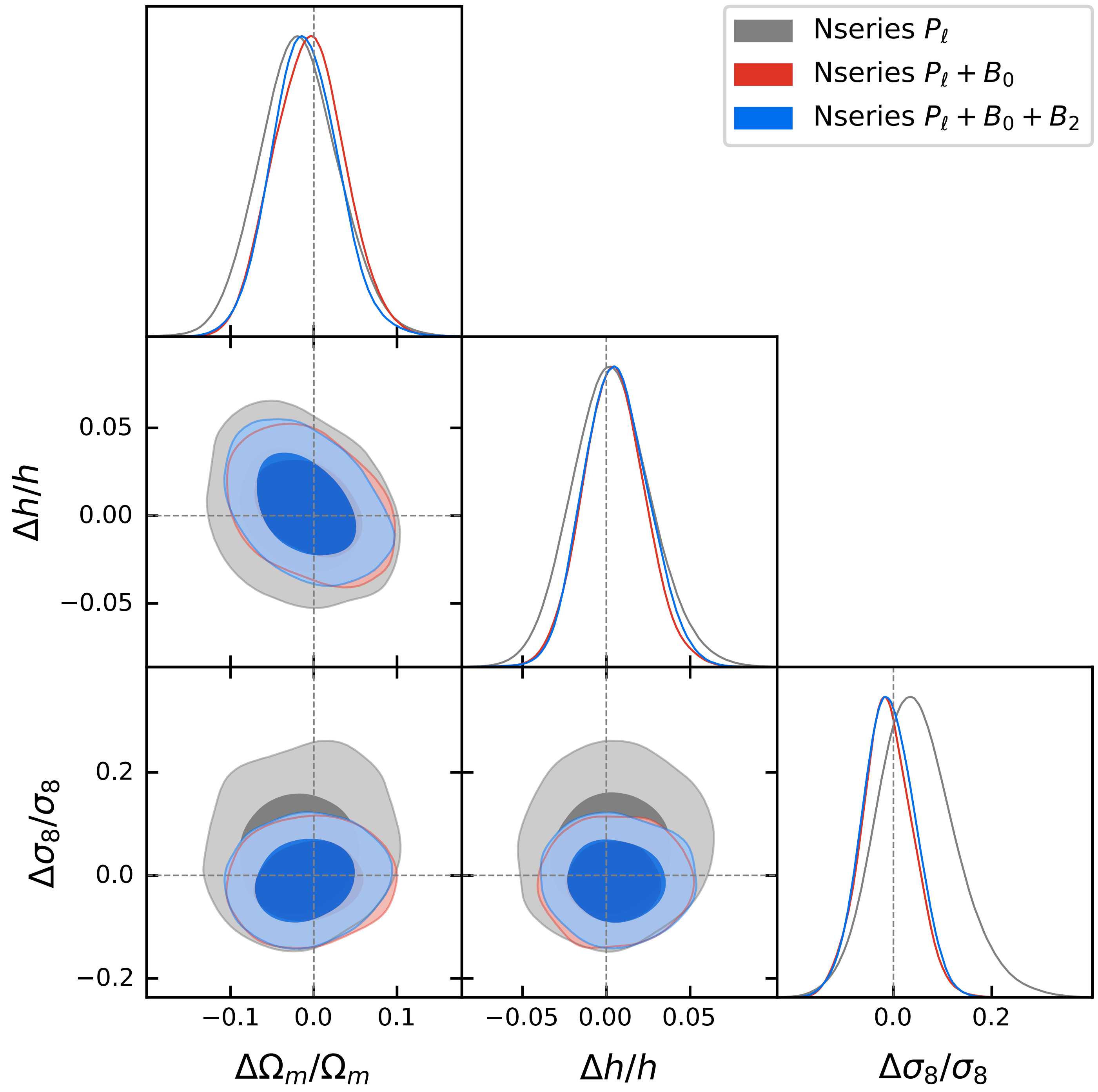

D'Amico *et al.* (2022)

Primordial Non-Gaussianity

Non-Gaussian Initial Conditions

Gaussian initial conditions:

- their **statistical properties are *completely* specified by the** two-point correlation function or the **power spectrum of the curvature perturbations:**

$$\langle \Phi_{\vec{k}_1} \Phi_{\vec{k}_2} \rangle = \delta_D(\vec{k}_1 + \vec{k}_2) P_\Phi(k_1)$$

- All **higher-order correlation functions are vanishing**

Bispectrum: $$\langle \Phi_{\vec{k}_1} \Phi_{\vec{k}_2} \Phi_{\vec{k}_3} \rangle = \delta_D(\vec{k}_1 + \vec{k}_2 + \vec{k}_3)\, B_\Phi(k_1, k_2, k_3) = 0$$

Trispectrum: $$\langle \Phi_{\vec{k}_1} \Phi_{\vec{k}_2} \Phi_{\vec{k}_3} \Phi_{\vec{k}_4} \rangle = \delta_D(\vec{k}_1 + \ldots + \vec{k}_4)\, T_\Phi(\vec{k}_1, \vec{k}_2, \vec{k}_3, \vec{k}_4) = 0$$

$\Rightarrow$ **Non-Gaussian initial conditions are characterized by an *infinite* set of functions**:

$$B_\Phi(k_1, k_2, k_3) \neq 0$$

$$T_\Phi(\vec{k}_1, \vec{k}_2, \vec{k}_3, \vec{k}_4) \neq 0$$

, etc ...

The shapes of non-Gaussianity

Most inflationary models predict a *scale-invariant* curvature bispectrum

$$B_\Phi(k,k,k) \sim P_\Phi^2(k) \sim \frac{1}{k^6}$$

What distinguish them is the *shape*

"shape" = the **dependence *of*** the curvature bispectrum predicted by a given model of inflation ***on*** the shape of the triangular configuration k_1, k_2, k_3

$$B_\Phi(k_1,k_2,k_3) = f_{NL}\frac{1}{k_1^2k_2^2k_3^2}F\left(r_2=\frac{k_2}{k_1}, r_3=\frac{k_3}{k_1}\right)$$

Models of primordial non-Gaussianity

id est, *Shapes of non Gaussianities*

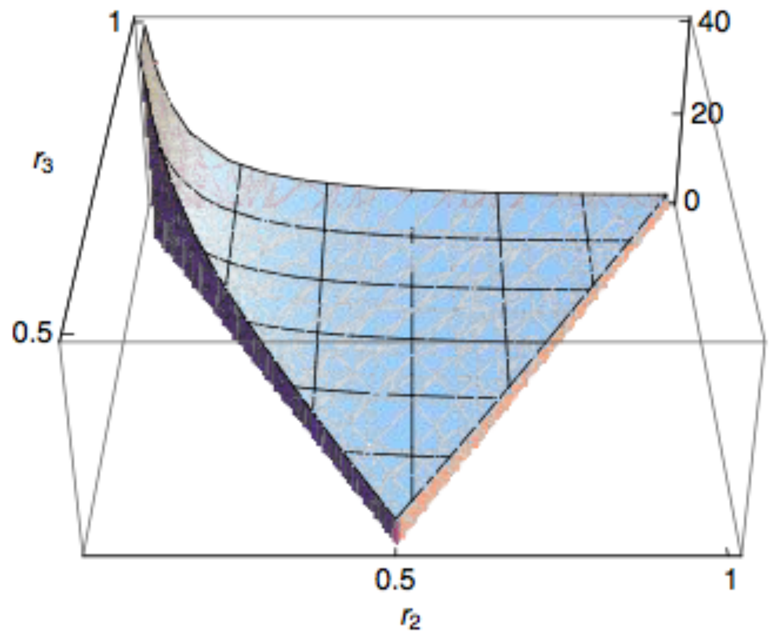

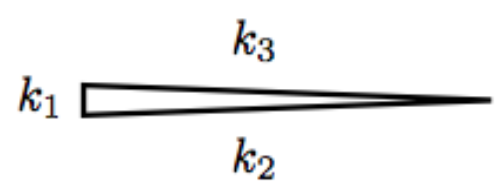

Local

Multiple fields

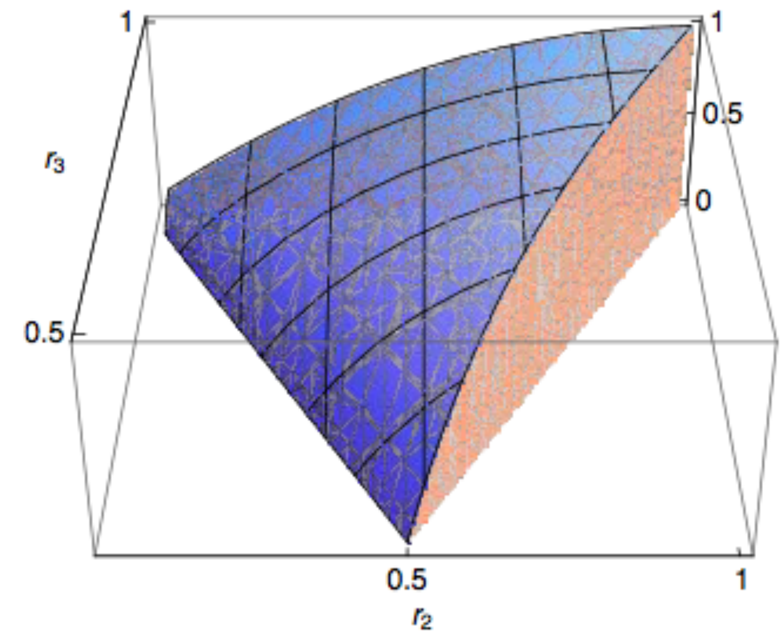

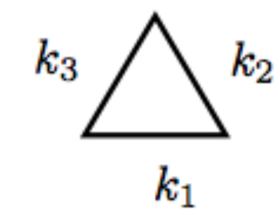

Equilateral

$(\partial\pi)^3$

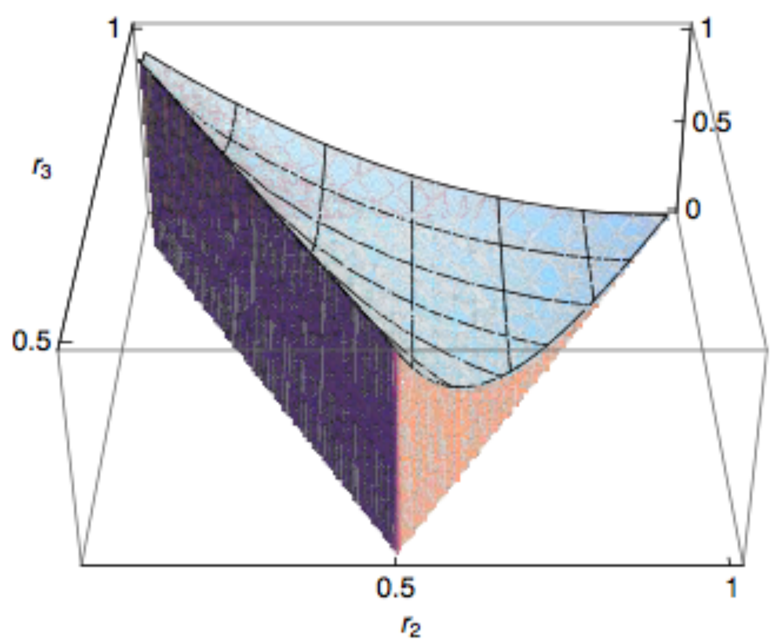

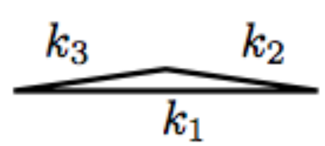

Enfolded

Modified vacuum

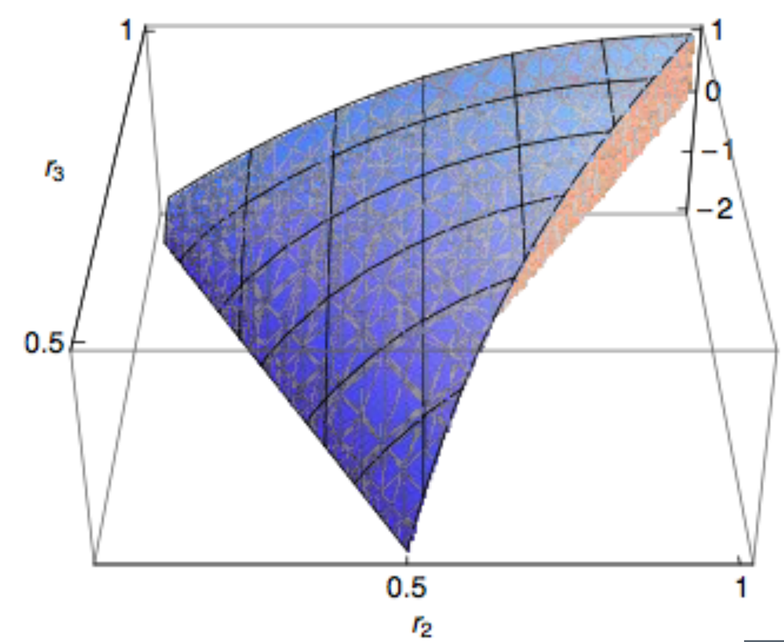

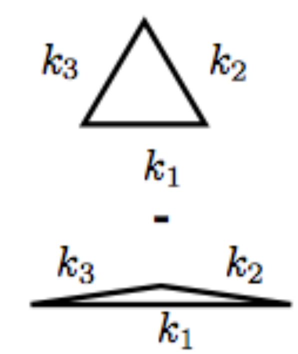

Orthogonal

$$\dot{\pi}\frac{(\partial_i\pi)^2}{a^2} + 5.4\frac{2}{3}\dot{\pi}^3$$

courtesy of G. D'Amico

Matter Power Spectrum & Bispectrum

In Perturbation Theory ...

$$P = P_0 + P_G^{loop}[P_0] + P_{NG}^{loop}[P_0, B_0]$$

matter power spectrum

Linear power spectrum

Gravity-induced contributions (depending on P_0 alone)

Additional gravity-induced contributions present *only* for NG initial conditions (B_0)

$$B = B_0 + B_G^{tree}[P_0] + B_G^{loop}[P_0] + B_{NG}^{loop}[P_0, B_0]$$

& **bispectrum**

Primordial component

The matter **bispectrum** and PNG

At large scales I can approximate the matter bispectrum with the tree-level expression on PT:

$$B(k_1,k_2,k_3) \simeq B_0 + B_G^{tree}[P_0]$$

Primordial component

Gravity-induced component

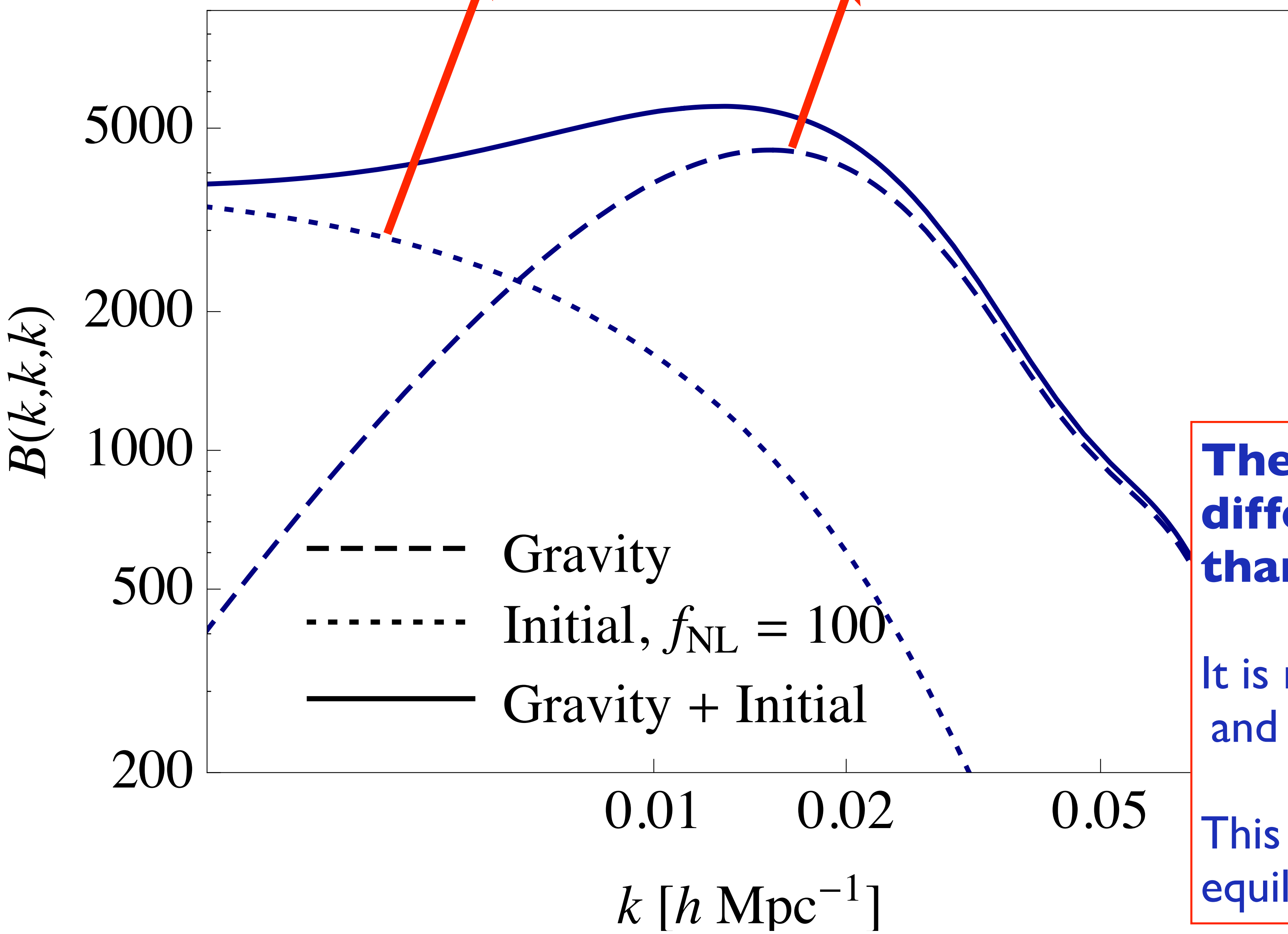

Equilateral configurations of the matter bispectrum

$$\frac{B_0(k,k,k)}{B_G^{tree}(k,k,k)} \overset{k\to 0}{\sim} \frac{f_{NL}}{D(z)k^2}$$

The primordial component has a different dependence on scale than the gravity-induced one!

It is relevant at **large scales** and **early times**

This is true for almost all models (local, equilateral, orthogonal ...)

The matter **bispectrum** and PNG

At large scales I can approximate the matter bispectrum with the tree-level expression on PT:

$$B(k_1,k_2,k_3) \simeq \underbrace{B_0}_{\text{Primordial component}} + \underbrace{B_G^{tree}[P_0]}_{\text{Gravity-induced component}}$$

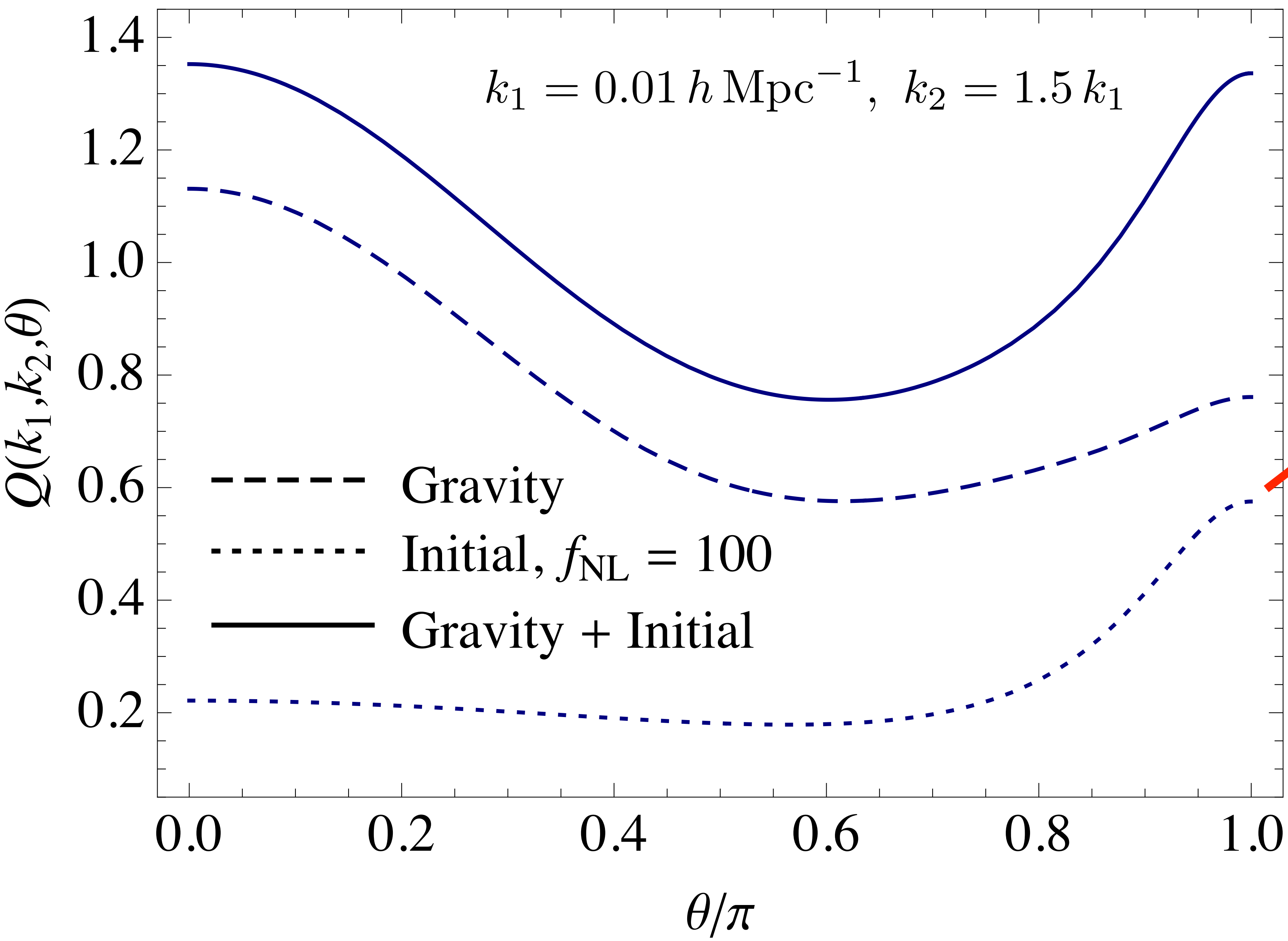

Reduced bispectrum as a function of the angle between two wavenumbers

Primordial component for **local non-Gaussianity**: large contribution in the squeezed limit!

The primordial component has a different dependence on the shape of the triangular configurations

and it is *specific* to the non-Gaussian model (local, equilateral, orthogonal ...)

The matter **bispectrum** and PNG

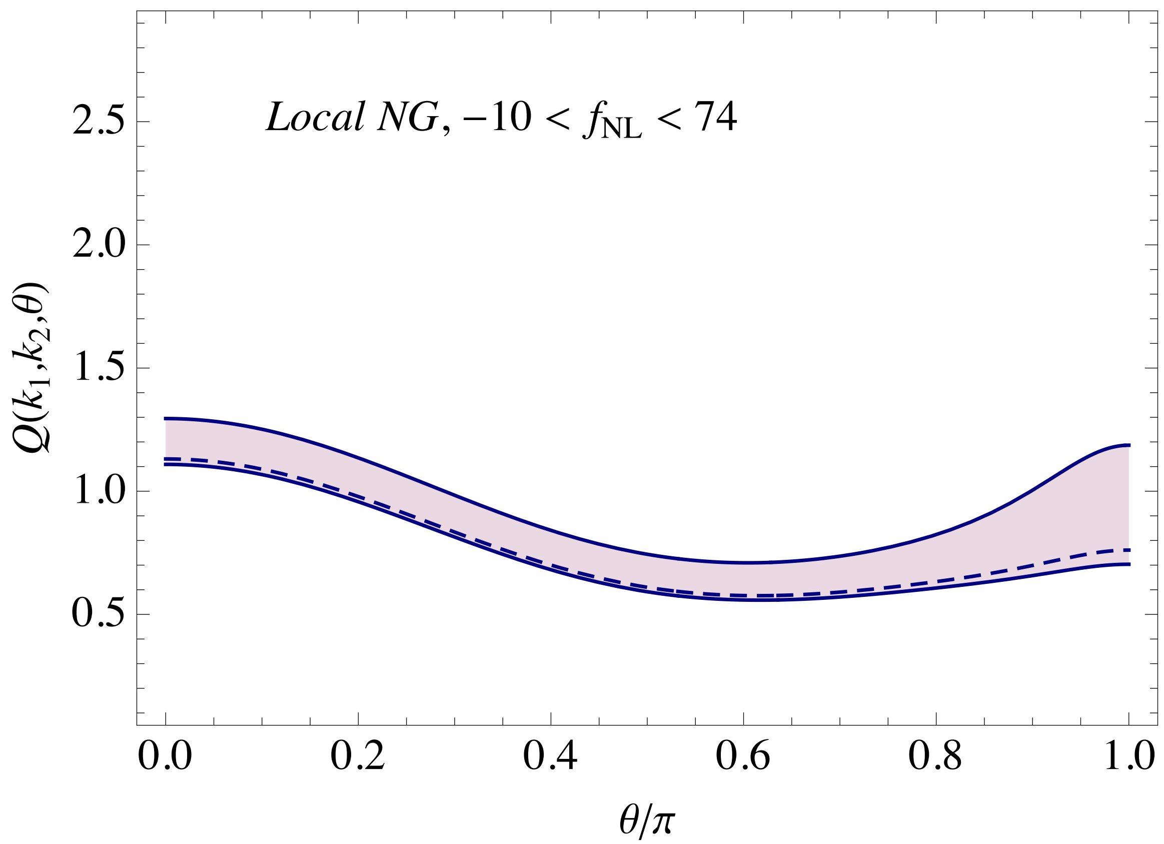

Current CMB constraints for different models of non-Gaussianity as uncertainties on the generic configurations of the matter bispectrum, $B \simeq B_0 + B_G^{tree}[P_0]$

The matter bispectrum can distinguish different non-Gaussian models

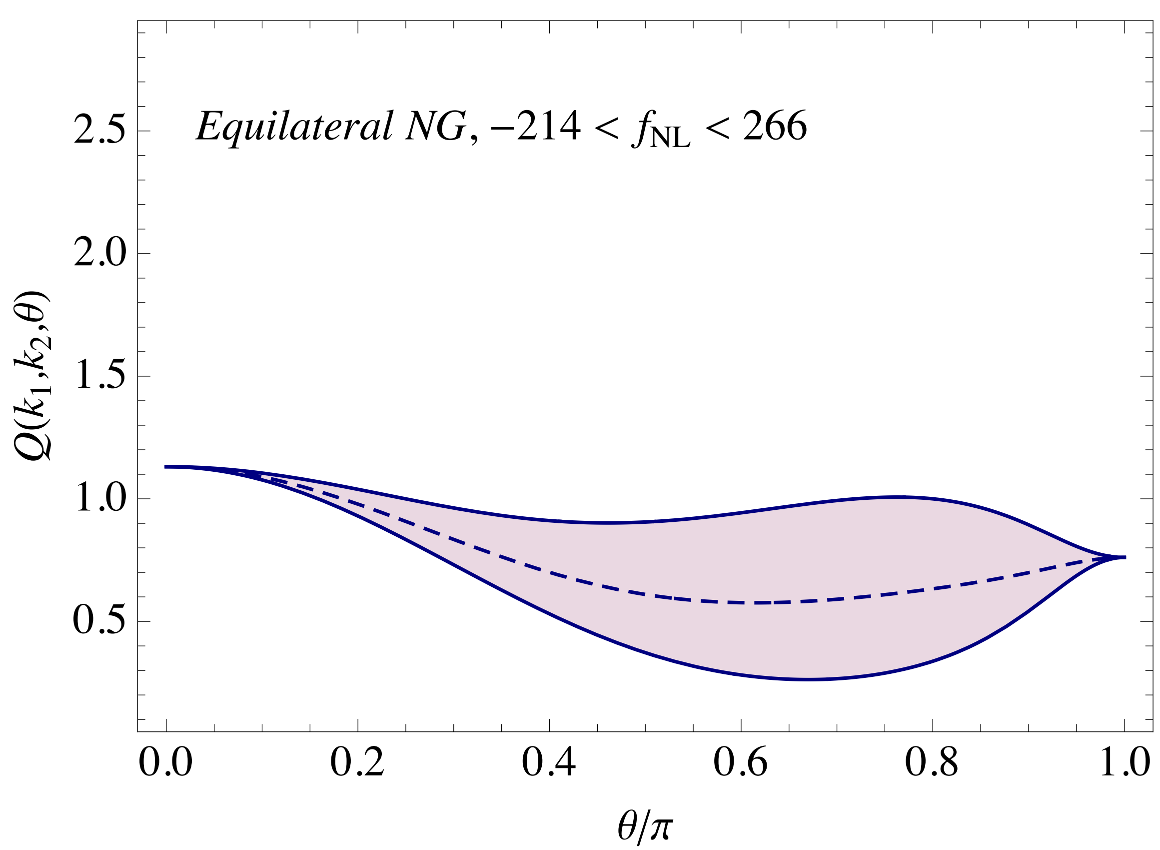

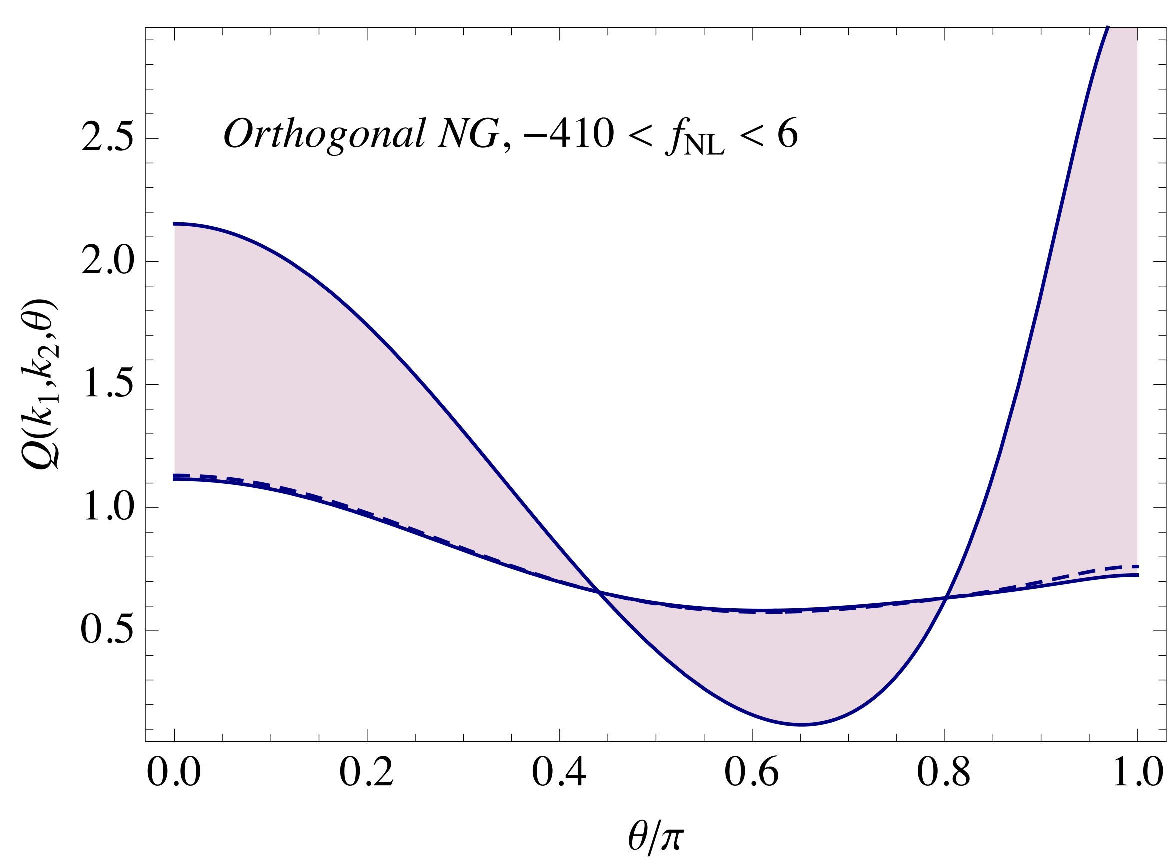

The matter **bispectrum** and PNG

In Perturbation Theory ...

$$P = P_0 + P_G^{loop}[P_0] + P_{NG}^{loop}[P_0, B_0]$$

matter power spectrum

Linear power spectrum

Gravity-induced contributions (depending on P_0 alone)

Additional gravity-induced contributions present *only* for NG initial conditions (B_0)

$$B = B_0 + B_G^{tree}[P_0] + B_G^{loop}[P_0] + B_{NG}^{loop}[P_0, B_0]$$

& **bispectrum**

Primordial component

Nonlinear corrections are *also* affected by the initial conditions!

Galaxy Bias with Local Non-Gaussian Initial Conditions

Dalal *et al.* (2008):
The bias of galaxies receives a significant *scale-dependent* correction for NG initial conditions of the *local* type

$$P_g(k) = [b_1 + \Delta b_1(f_{NL}, k)]^2\, P(k)$$

"Gaussian" bias

Scale-dependent correction due to local non-Gaussianity

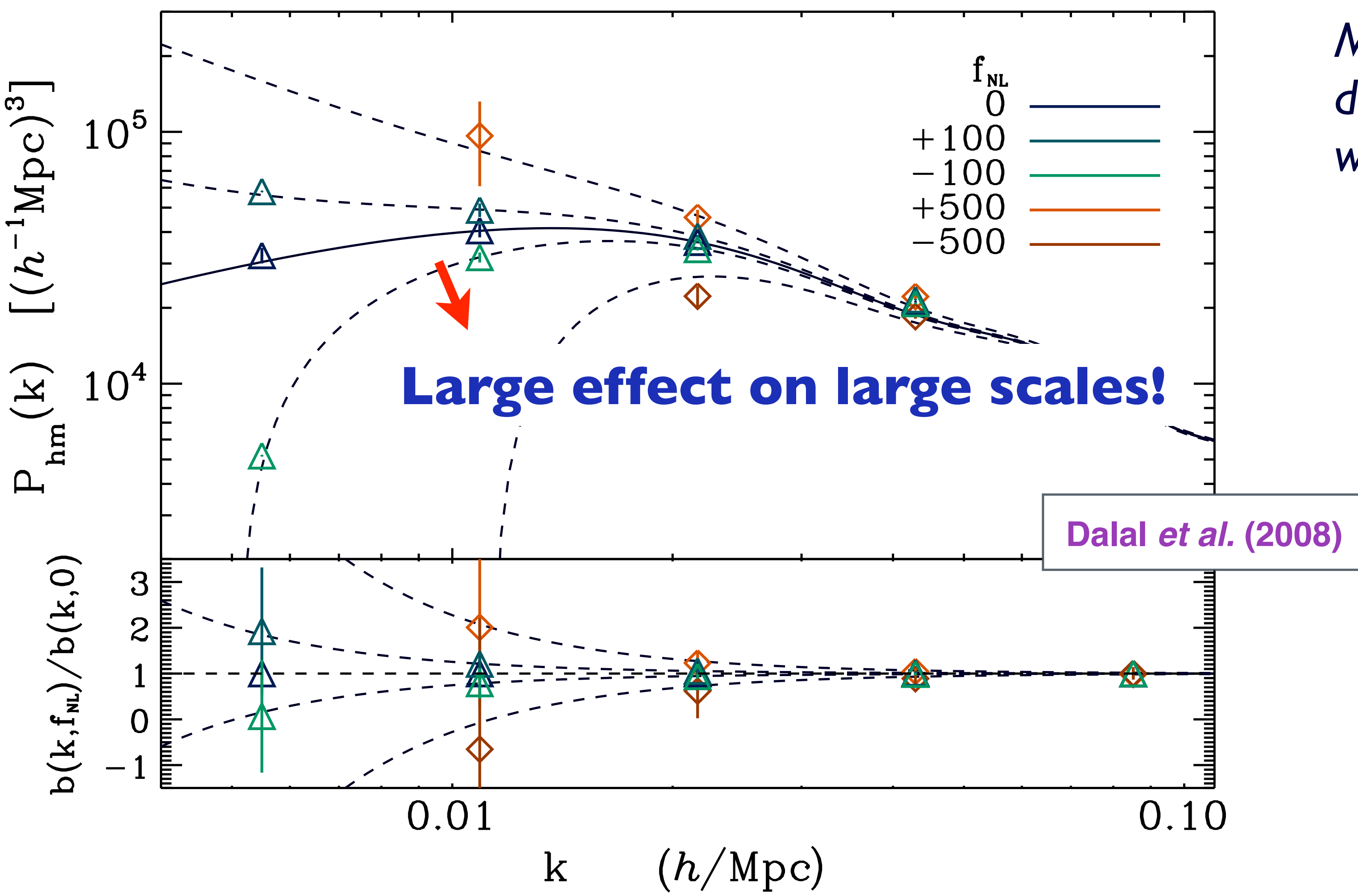

Measurements of the power spectrum of dark matter halos in N-body simulation with local NG initial conditions

$$\Delta b_{1,NG}(f_{NL}, k) \sim \frac{f_{NL}}{D(z)\, k^2}$$

Galaxy Bias with Local Non-Gaussian Initial Conditions

Dalal *et al.* (2008):

The bias of galaxies receives a significant *scale-dependent* correction for NG initial conditions of the *local* type

$$P_g(k) = [b_1 + \Delta b_1(f_{NL}, k)]^2 \, P(k)$$

"Gaussian" bias

Scale-dependent correction due to local non-Gaussianity

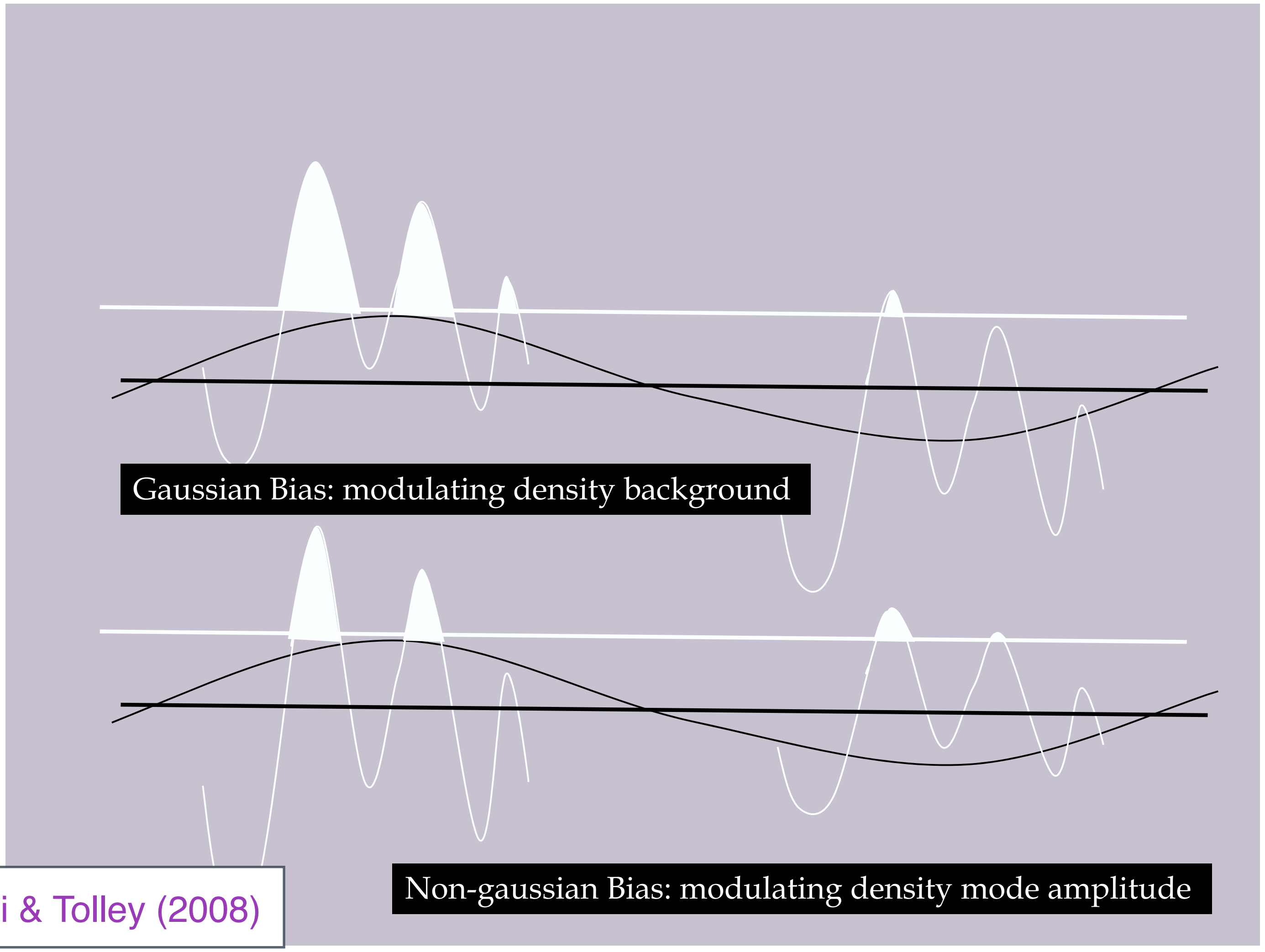

Afshordi & Tolley (2008)

Local non-Gaussianity introduces a correlation between large-scale fluctuations and the small-scales responsible for the formation (collapse) of dark matter halos (and therefore, galaxies)

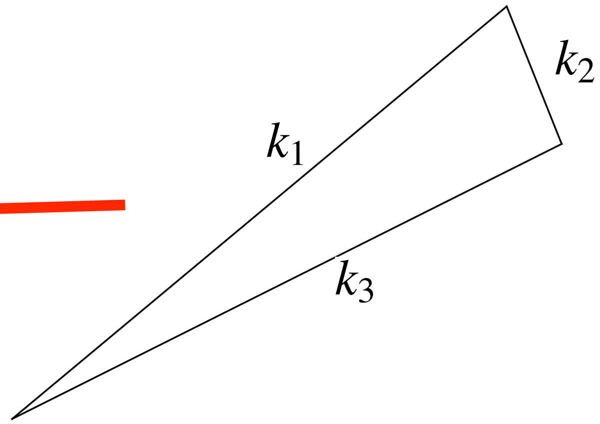

Galaxy Bias with Local Non-Gaussian Initial Conditions

The bias expansions receives several additional contributions (with new parameters)

$$\delta_g^{\rm LPNG}(\mathbf{x}) = b_\phi f_{\rm NL}\phi(\mathbf{q}) + b_{\phi\delta} f_{\rm NL}\phi(\mathbf{q})\delta(\mathbf{x}) + b_{\phi\delta^2} f_{\rm NL}\phi(\mathbf{q})\delta^2(\mathbf{x}) + b_{\phi\mathcal{G}_2} f_{\rm NL}\phi(\mathbf{q})\mathcal{G}_2(\mathbf{x}).$$

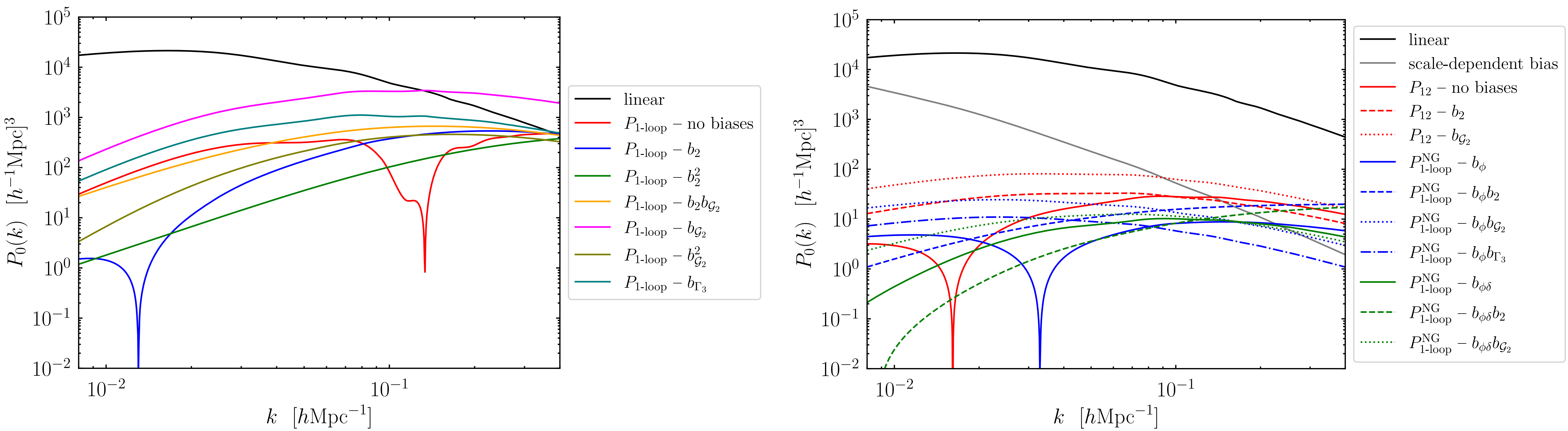

from Cabass et al. (2022)

We now have many new corrections to the power spectrum, at the linear and loop level

P+B in real space

Test of the power spectrum & bispectrum model in real space

Eos simulations, $80\,h^{-3}\,\mathrm{Gpc}^3$
Halo catalogs

Significant improvement (factor of 5) over power spectrum only

Also from the reduction of the $f_{\rm NL} - b_\phi$ degeneracy

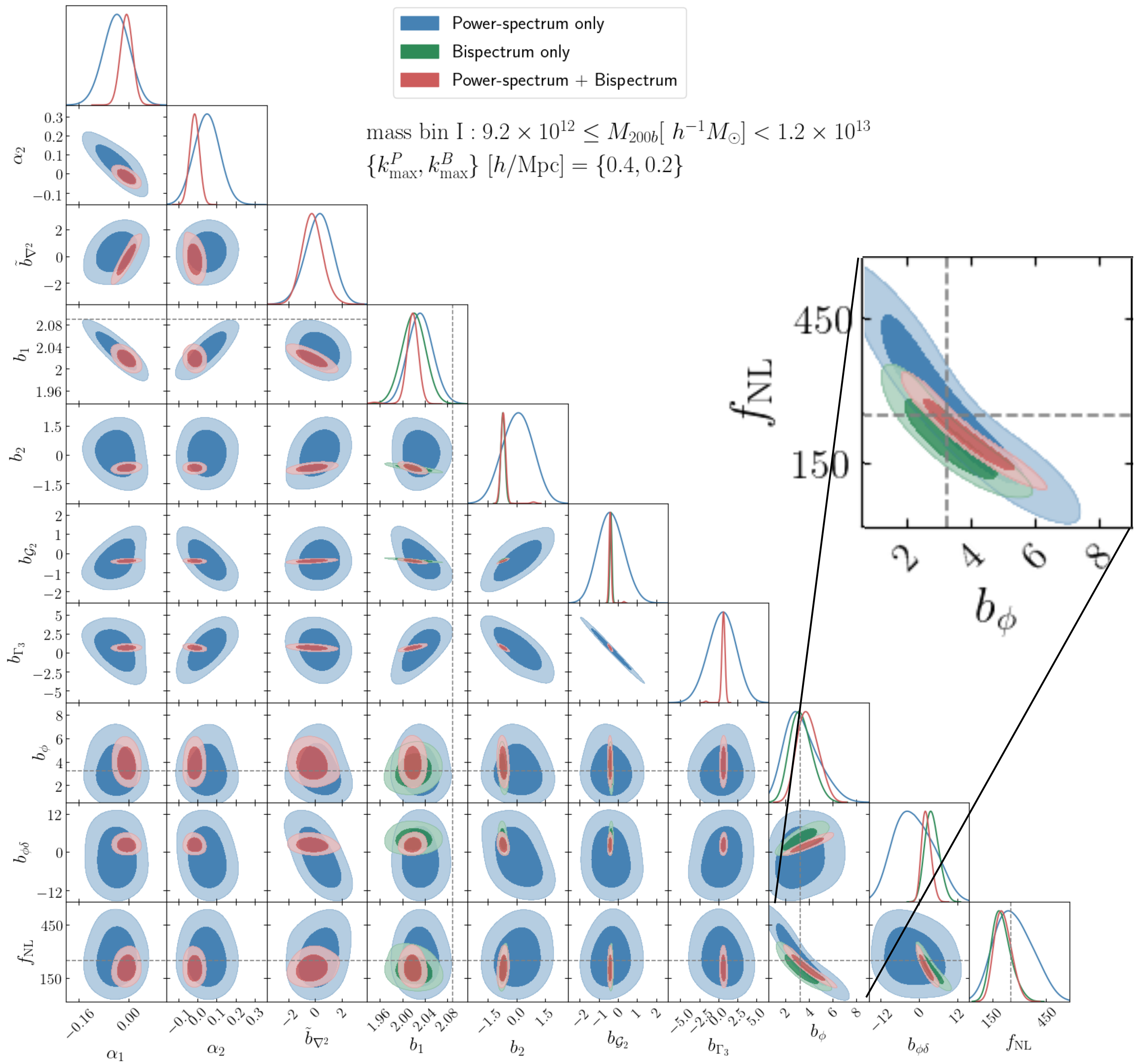

Moradinezhad *et al.* (2021)

Recent constraints on PNG

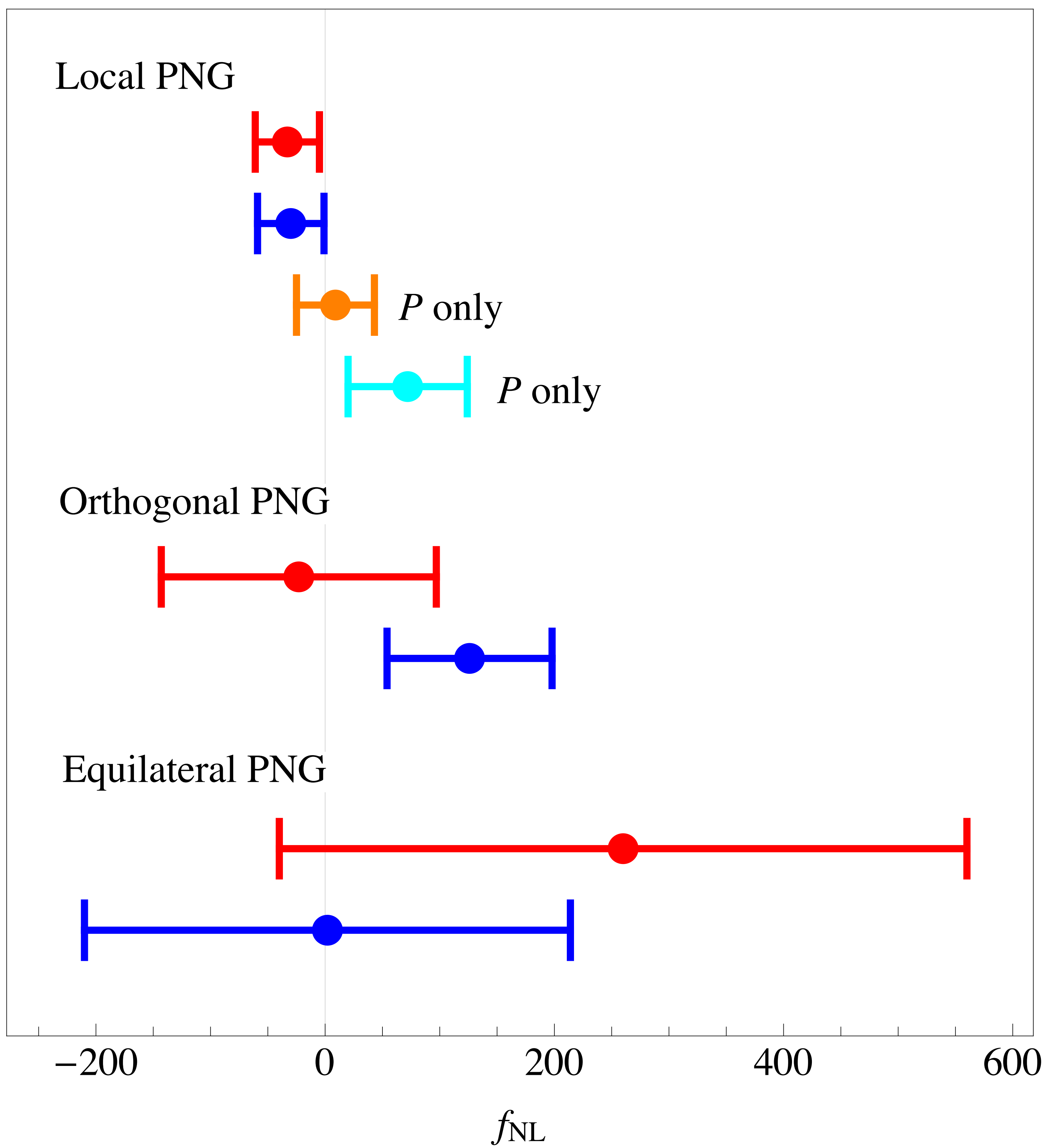

D'Amico *et al.* (2022)
Cabass *et al.* (2022A, 2022B)